Mineralogy and Occurrence of Europium-Rich Dark Monazite

GEOLOGICAL SURVEY PROFESSIONAL PAPER 1181

Mineralogy and Occurrence of Europium-Rich Dark Monazite

By SAM ROSENBLUM *and* ELWIN L. MOSIER

GEOLOGICAL SURVEY PROFESSIONAL PAPER 1181

Mineral-exploration research on Alaskan panned concentrates, resulting in recognition of a new guide to contact aureoles

UNITED STATES GOVERNMENT PRINTING OFFICE, WASHINGTON: 1983

UNITED STATES DEPARTMENT OF THE INTERIOR

JAMES G. WATT, *Secretary*

GEOLOGICAL SURVEY

Dallas L. Peck, *Director*

Library of Congress Cataloging in Publication Data
Rosenblum, Sam.
Mineralogy and occurrence of europium-rich dark monazite.
(Geological Survey Professional Paper 1181)
Bibliography: 67 p.
1. Monazite. 2. Europium. 3. Monazite—Alaska.
I. Mosier, Elwin L. II. Title. III. Series.
TN948.M7R67 1983 553.4'943 82-600301

For sale by the Distribution Branch, U.S. Geological Survey
604 South Pickett Street, Alexandria, VA 22304

CONTENTS

ILLUSTRATIONS

TABLES

MINERALOGY AND OCCURRENCE OF EUROPIUM-RICH DARK MONAZITE

By SAM ROSENBLUM and ELWIN L. MOSIER

ABSTRACT

Europium (Eu)-rich dark monazite has been found in 64 alluvial concentrates from 14 areas across Alaska between the Canadian border and the west end of the Seward Peninsula. This monazite is characterized by gray to black color, pelletlike form, high-Eu and low-thorium (Th) contents, turbidity caused by microscopic clouds of amorphous carbon and sagenitic rutile rods, and many inclusions of siltsized detrital minerals. Density (D) of Alaskan dark monazite ranges from 4.25 to 4.70, mainly due to the presence of inclusions. Otherwise, physical properties are similar to those of yellow monazite. Refractive indices, α and γ, are similar to those of yellow monazite, but interference figures are generally diffuse and show small (0°–5°) positive 2V. X-ray diffraction patterns and cell parameters are similar to those of yellow monazites. The average composition of 11 dark monazites from Alaska is (in percent): La_2O_3 13.54, Ce_2O_3 29.00, Pr_2O_3 3.34, Nd_2O_3 14.00, Sm_2O_3 1.92, Eu_2O_3 0.31, Gd_2O_3 0.98, Y_2O_3 0.47, P_2O_5 22.36, ThO_2 0.88, SiO_2 8.35, TiO_2 0.66, Al_2O_3 1.98, Fe_2O_3 1.77, CaO 0.28, MgO 0.23, H_2O 0.94=101.01. Amorphous carbon ranged from 0.22 to 1.22 percent in four samples and, in seven samples, minor elements were (in ppm): Ba 100–500, Cr 200–2,000, Cu 50, Pb 20–70, Sn 150, and U 29–260.

Comparison of average analyses of dark monazites from several countries shows generally small variations of all oxides. Major compositional differences between worldwide averages of dark and yellow monazites are (in percent): Eu_2O_3 0.36 (dark), 0.05 (yellow); ThO_2 0.84 (dark), 7.15 (yellow); and SiO_2 9.65 (dark), 1.70 (yellow); but totals for (La-to-Gd) $_2O_3$ are similar: 60.23 for 31 dark monazites, and 59.01 for 64 yellow monazites. In dark monazite, D varies directly with Ln_2O_3 (total lanthanide oxides) and inversely with SiO_2 contents.

REE (rare-earth element) distributions in dark monazites from Alaska, France, Taiwan, Zaire, and the U.S.S.R. follow the trend shown by REE distributions in yellow monazites in a graph of La/Nd vs. Σ (=La+Ce+Pr). The same data plotted on log-normal paper fall along a straight line. CNR (chondrite-normalized ratios) and SNR (shale-normalized ratios) of La through Gd in dark monazite from Alaska are remarkably similar to these ratios in dark monazites from France, Taiwan, Zaire, and Montana; but most of the patterns for dark monazites from the U.S.S.R. and Spain are dissimilar. CNR and SNR patterns for La to Gd in dark monazites differ from the patterns found for yellow monazites from igneous and metamorphic rocks, but the CNR and SNR patterns for La to Gd in dark monazites are similar to CNR and SNR patterns for La to Gd in sedimentary rocks, especially shales.

Yellow monazite has been shown to form mainly through igneous and high-grade regional metamorphic processes. Origin of dark monazite with low thorium and high europium has been attributed to several processes including precipitation from seawater, metamorphism of diagenetic rhabdophane, and as an accessory mineral in tin-bearing granites; but none of these concepts has general application.

The origin of dark monazite by igneous, high-grade regional-metamorphic, or diagenetic processes is rejected, because of the dissimilarity in the distributions of the REE in dark monazite and in yellow monazite of igneous, regional-metamorphic, or diagenetic origin. We presume that the REE distribution in dark monazite is inherited from the REE distribution in a former mineral, rock, or environment. Thus, rhabdophane cannot be the precursor mineral, nor can seawater be the source of the REE distribution found in dark monazite.

Contact metamorphism is proposed as the mode of origin of dark monazite. Geologic relations of the Alaskan occurrences of dark monazite show that the preferred source rock is weakly metamorphosed shale or phyllite intruded by biotite granite. Commonly the shale is black and phosphatic. Under low-grade regional metamorphism, dark monazite should be widespread, but our limited data indicate mainly local associations of this mineral with granitic intrusions. From these observations, the prediction was made that dark monazite poor in Th and rich in Eu should be present in baked shales of the Phosphoria Formation. A test of this hypothesis in Montana was successful in finding dark monazite in sediments of streams that drain phyllitic rocks of the Phosphoria Formation.

Dark monazite is an important source of Eu as well as other REE. Assuming that the contact-metamorphic origin of dark monazite is correct, then the presence of dark monazite indicates an area that should be prospected for metalliferous ores and phosphatic layers. The upper stability limit of about 300°C for dark monazite may be useful in geothermometry applications. Recommendations are made for mineral exploration in overseas localities, based on the occurrence of dark monazite.

INTRODUCTION

COMMERCIAL MONAZITE

The yellow monazite of commerce contains about 60 percent REE and 7 percent Th. About 45,000 t (metric tons) of yellow monazite are recovered each year, mainly from beach deposits in Australia, Malaysia, India, and Brazil. This monazite is the source of REE and Th for a number of special industrial uses. The traditional uses of REE in mantles for gas lanterns, lighter

flints, arc carbons, polishing compounds, special glasses, and ceramics continue to be important. However, since 1970 the major uses of REE are in making ductile iron and steel, and as a catalyst in refining petroleum (Jolly, 1976, p. 889). A small but important demand for high-purity REE and compounds, notably Eu and Y (yttrium) oxides for production of intense phosphors for color-television picture tubes, accounts for a considerable part of the commercial value because of high unit values of these REE. In January 1980, United Mineral and Chemical Corp. of New York listed the following prices for materials of 99.99 percent purity: Eu metal, $17.60 and $19.20/g (depending on method of preparation) in lots of 500 g, and Eu oxide, $4.00/g in lots of 5 kg (kilogram). Considering that the price of 1 ton (0.9 t) of Australian (yellow) monazite as of September 1982 (Industrial Minerals No. 180) was US$415–457, the price for a ton of monazite unusually enriched in Eu might be expected to be much higher.

PURPOSE OF PRESENT STUDY

Because of scarcity of domestic sources of europium and the high unit prices of europium and its compounds, W. C. Overstreet, U.S. Geological Survey, recommended in 1970 that concentrates from Alaska be examined for Eu-rich monazite. It was thought, because of the association of Eu-rich monazite and cassiterite in eastern Siberia and Malaysia, described by Phan (1967, p. 85) and supported by the observations of Serre-Ratsimandisa (1970, p. 160) in the Malagasy Republic, that geochemical anomalies for tin occurred in sediments which contained Eu-rich monazite. The most likely sites for Eu-rich monazite in the United States were inferred to be the vicinity of the tin deposits on the Seward Peninsula, Alaska. Also, about 1970, C. L. Sainsbury, then tin commodity specialist in the U.S. Geological Survey, informally recommended a search of Alaskan concentrates for cassiterite and other valuable minerals.

A project was activated to analyze more than 1,000 concentrates from the Alaskan Placer Concentrate File. This file, which contains about 5,000 samples, is a collection mainly of panned concentrates and sluice box concentrates made between 1895 and 1954 by many geologists of the U.S. Geological Survey. Most of the concentrates are from alluvial deposits, but some concentrates are from crushed rock. Following random selection of the samples to be analyzed, the concentrates were sieved to pass a 20-mesh screen, the magnetite was removed by hand magnet, and the fraction that sank in bromoform (D=2.87) was analyzed by semiquantitative emission spectrography for 45 elements (Overstreet and others, 1975). Of the 1,069 nonmagnetic concentrates analyzed, 9 showed detectable Eu at a lower limit of determination of 200 ppm (parts per million).

The Eu-bearing concentrates were examined mineralogically by Rosenblum to identify the mineral(s) that might contain Eu. The search was particularly addressed to dark, spherical to ellipsoidal grains that resembled the Eu-rich monazite described in the literature and with which Rosenblum was familiar from work in Taiwan (Rosenblum, 1960). This type of monazite was discovered in several Eu-bearing concentrates from the Eureka gold-tin district in the Tanana quadrangle, Alaska. The Eureka district, thus, is the discovery locality for this variety of monazite in Alaska. Handpicked grains were analyzed by X-ray diffraction and semiquantitative spectrography. The X-ray diffraction pattern proved that the mineral was monazite, and the chemistry indicated unusually low thorium and high europium contents. Similar dark spherical to ellipsoidal grains of monazite were identified by Rosenblum in other Eu-bearing concentrates from Alaska. After these discoveries, Overstreet made a rapid scan of the whole set of concentrates and picked out 120 for detailed study. Further work by Rosenblum disclosed 64 samples from 63 sites across Alaska that contained dark monazite (fig. 1). The pelletlike grains of gray to black monazite from Alaska differ from yellow, transparent to translucent, detrital monazite by the obvious dark color and micropitted surface. These physical differences were uniformly present in the material from the 63 sites, but only 11 samples contained enough dark monazite to be handpicked for spectrographic analysis by Mosier. The results of these analyses showed a remarkable consistency in the chemical composition of the Alaskan dark monazites: the abundance of Eu proved higher and that of Th lower than the tenors in typical commercial monazite.

For the purpose of this report, the term dark monazite is used to refer to the Eu-rich and Th-poor variety of monazite derived from weakly metamorphosed sedimentary rocks. It ranges in color from black to light gray and beige, and it is characterized by numerous microscopic inclusions of oxide and silicate minerals and clouds of submicrometer-sized amorphous carbon. This dark monazite is not to be confused with yellow monazites that are colored black by carbon (Ellsworth, 1932; Iimori, 1941).

The amount of Eu-rich dark monazite in the concentrates from Alaska may be too sparse for commercial exploitation at the localities where it was found, but the monazite from these localities provided unusually favorable material for study to determine the origin of this previously unrecognized mineral. Therefore, the investi-

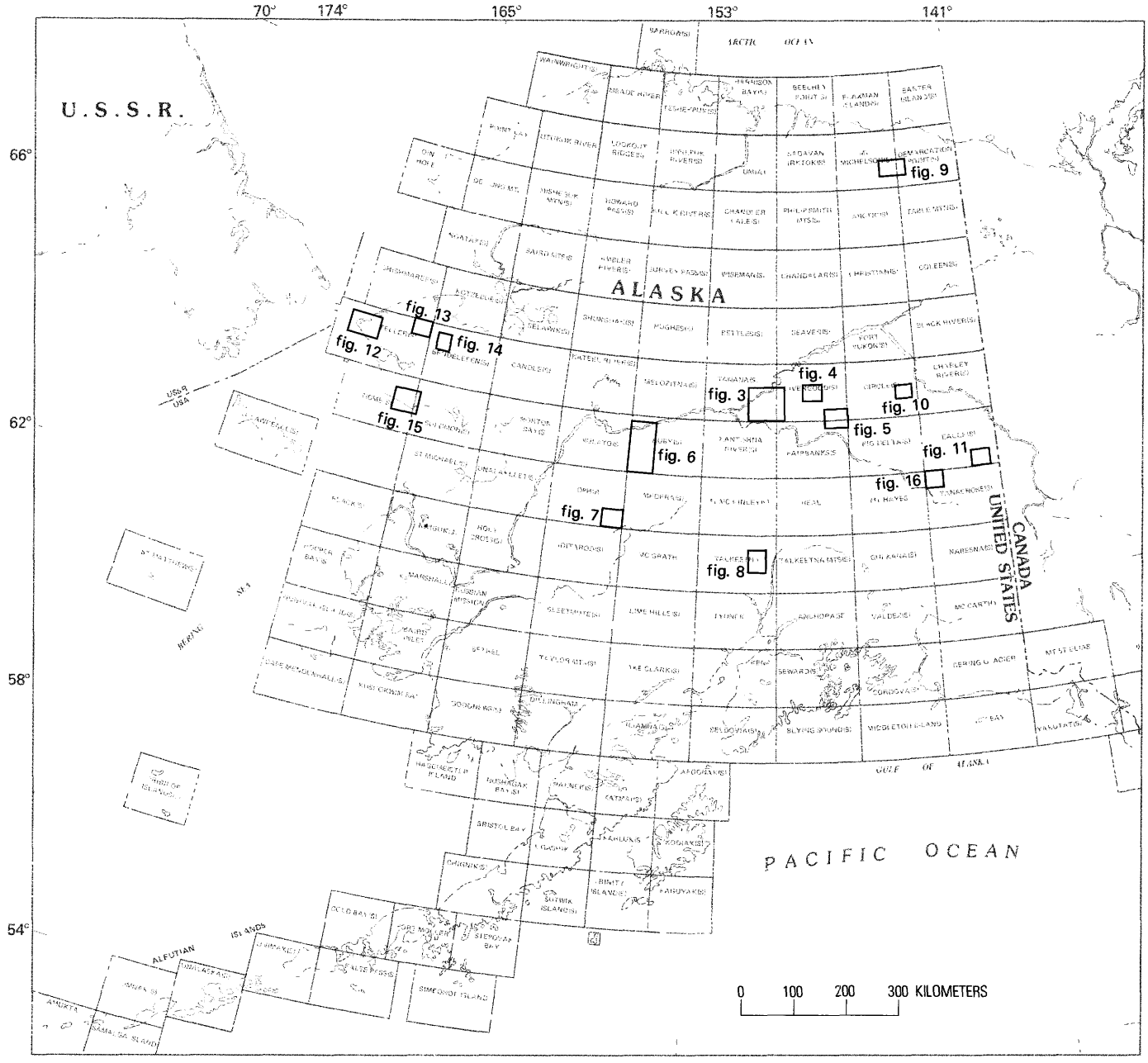

FIGURE 1.—Index map of Alaska showing areas with alluvial deposits that contain dark monazite, covered by figures 3–16 in this report.

gation leading to the present report was undertaken by Rosenblum and Mosier.

Library research soon indicated that this dark variety of monazite was indeed rare, but it had been identified in Siberia, Taiwan, France, the Malagasy Republic, Zaire, Morocco, and Gabon. In addition, dark monazite was observed in alluvial concentrates from Spain, Niger, Canada, and Bolivia (A. Parfenoff, written commun., 1977). Only the reports on dark monazite from Siberia, France, and Spain contained quantitative mineral analyses. In the present investigation, samples of dark monazite obtained from Alaska, Taiwan, Peru, Montana (U.S.A.), and Zaire were analyzed, and concentrates from Bangladesh, Pakistan, and Thailand were found to contain dark monazite. Each of these localities constitutes the discovery of dark monazite for that State or country. Undoubtedly more occurrences will be found, now that the properties and geologic setting of the mineral are known. Dark monazite is evidently much more common than the record in the literature

shows. Past failure to recognize it can be attributed to its physical appearance, which is so unlike that of commercial monazite.

The emphasis in this report is on the Alaskan dark monazite, but comparisons with other occurrences are made where data are available. Following the investigation of physical properties, chemical composition, and genesis of this poorly known mineral, brief inferences are drawn on its usefulness in mineral exploration.

HISTORY OF DARK MONAZITE INVESTIGATIONS

Eu-rich dark monazite was first reported from gold placers in the South Yenisei region, U.S.S.R. (fig. 2) by Zemel' (1936). However, no data on local geology or probable source rocks were given.

Fine-grained black monazite in the beach sands of southwestern Taiwan was reported by Huang (1958), and briefly discussed or noted by Shen, Li, and Chao (1958) and Rosenblum (1960). A summary of black monazite resources in Taiwan was presented by Ho and Lee (1963). More thorough discussions of the distribution, physical properties, composition, and possible modes of origin were given by Overstreet (1971), Chen, Li, and Wu (1973) and Matzko and Overstreet (1977); and these discussions included mineral descriptions and analyses by members of the Australian Bureau of Mineral Resources as well as by members of the U.S. Geological Survey.

About the time that dark monazite was first reported from Taiwan, gray monazite ranging in diameter from 0.7 to 7 mm and containing 0.5–0.8 percent ThO_2 was noted by Magnée (1958) in the Kivu district of Zaire. The mineral occurs in cassiterite placers, but its tenor is low and it can be recovered only as a byproduct of cassiterite mining. No other data were given on this unusual monazite, but Magnée indicated that the prospecting revealed a number of placers of yellow monazite with 3–10.1 percent ThO_2 in the same district.

Dark monazite in the northern Verkhoyan'e Range, northeastern Siberia, mentioned by Fadeev (1959) and Vinogradov, Arskiy, and Mikhailova (1960), was discussed in detail by Izrailev and Solov'eva (1975). Petrographic and mineral descriptions leave no doubt as to the identity of the mineral and the source rocks. Analyses of monazite-bearing and monazite-free rocks are given, but no quantitative analyses of the mineral are offered.

Oolitic gray monazite from the Maritime Province of Siberia, near the Sea of Japan, was discussed by Kosterin, Alekhina, and Kizura (1962). They noted its uncommon rounded form, the high content of attached water compared to common monazite, the almost complete absence of Th, and the presence of large amounts of Eu (as much as 1 percent). These characteristics suggested an unusual genesis for the gray monazite: metamorphism of sediments containing precipitated rhabdophane that is converted to gray monazite by the loss of water.

Low-thorium monazite from gold- and tin-bearing placer deposits in central Asia and the Far East, investigated by Li and Grebennikova (1962), appeared in their figures 1 to 4 to be identical to the dark monazite from Alaska. Although the genesis of this unusual variety of monazite is not clear, the writers suggested contact metasomatism involving transfer of REE from granites into the enclosing rocks. The low thorium content is attributed to thorium being less mobile than the rare-earth elements.

The westernmost occurrence of dark monazite in the U.S.S.R., found in a titanium placer of Devonian age in the central Timan Range west of the northern Urals, is thought to be of metasedimentary origin and transitional between rhabdophane and (yellow) monazite (Serdyuchenko and Kochetkov, 1974). Opaque ash-gray to brown-gray grains are isometric to tabular in shape, and analysis showed that they contained 0.2 percent Eu_2O_3 and 1.5 percent ThO_2.

Gray monazite was first reported in Bretagne, France, by Parfenoff (1963). Additional information was supplied by Guigues and Devismes (1969), and a fuller discussion, including a petrographic description of the source rocks, was given by Donnot and others (1973). Other examples of dark monazite that were cited by Donnot and others (1973, p. 15) include occurrences in Morocco and Gabon, but no details on these are given.

In southern France, Eu-rich dark monazite that resembles the Eu-bearing monazite in Bretagne was discovered in the Arize drainage near Labastide-de-Serou, on the north slope of the Pyrenees Range (Lacomme and Fontan, 1971). An analysis indicated the mineral contains 4,000 ppm Eu and only 300 ppm Th. This dark monazite is found in Pliocene terrace deposits thought to be derived from Ordovician schists upstream along the Arize River.

At Ambatofinandrahana, Malagasy Republic, oolitic gray monazite is found in low-grade metamorphosed shales and is interpreted as a recrystallization of weinschenkite and (or) rhabdophane by Altmann, Radelli, and Serre-Ratsimandisa (1970, p. 116). In another article, Serre-Ratsimandisa (1970, p. 160) indicated that the gray monazite was related to graphitic schists and contained about the same amount of Eu as the dark monazite in Zaire, 0.45–0.5 percent.

Personnel of the BRGM (Bureau de Recherches Géologiques et Minières) in France have observed dark monazite in alluvial concentrates from a number of

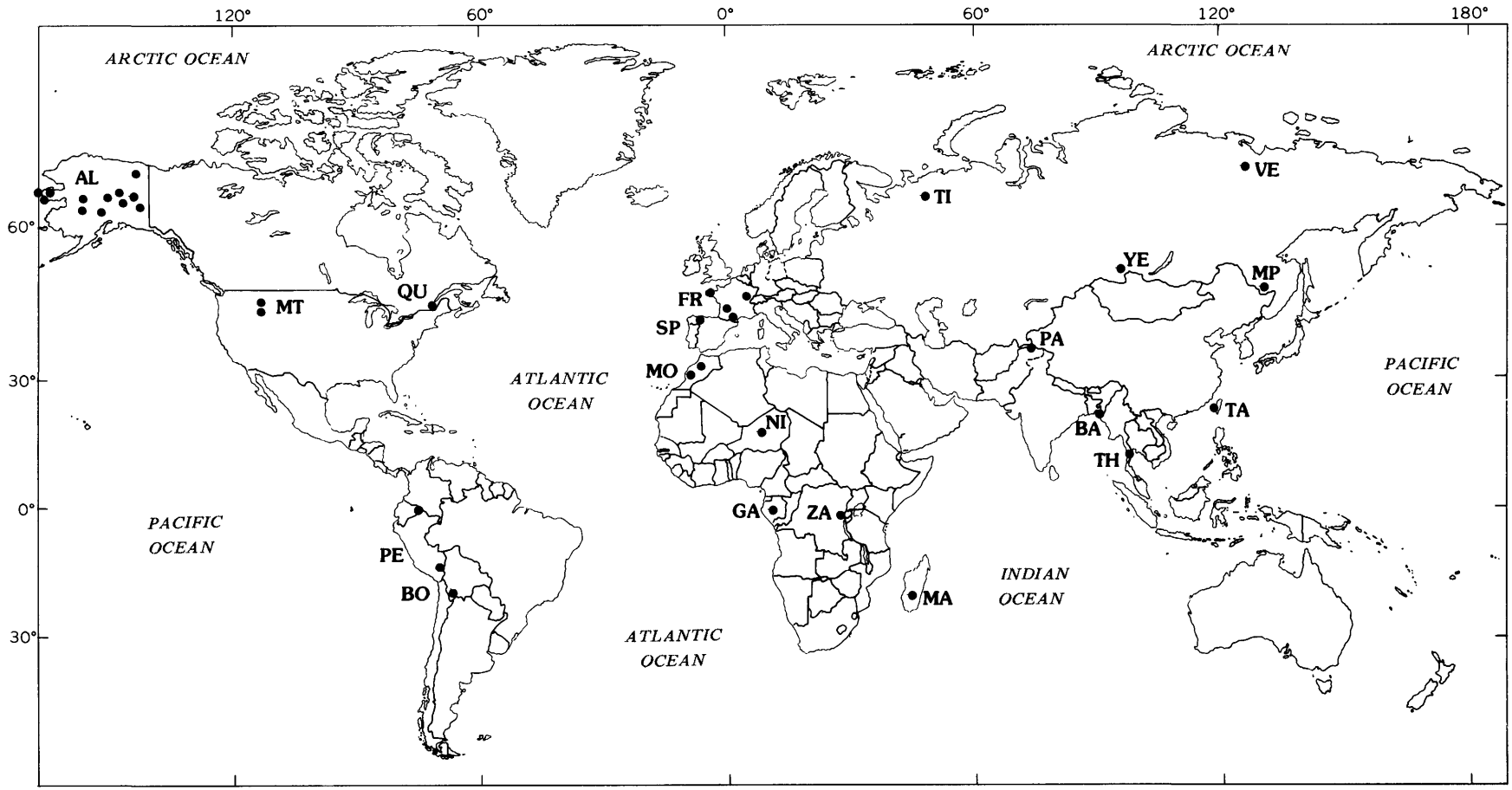

FIGURE 2.—Worldwide occurrences of dark monazite. Solid dot, area or site of dark monazite sample or samples. Localities identified in this report: AL, Alaska; MT, Montana; PE, Peru; PA Pakistan; BA, Bangladesh; TH, Thailand. Localities from the literature and other sources: FR, France; ZA, Zaire; MA, Malagasy Republic; TA, Taiwan; YE, S. Yenisei, U.S.S.R.; MP, Maritime Province, U.S.S.R.; VE, Verkhoyan'e Range, U.S.S.R.; TI, Timan Range, U.S.S.R.; MO, Morocco; SP, Spain; QU, Quebec, Canada; BO, Bolivia; NI, Nigeria (site not located); GA, Gabon (country only cited).

places in Europe, Africa, and the Americas (A. Parfenoff, written commun., 1977), as follows:

1. France: in addition to the alluvial deposits in Bretagne and on the north slope of the Pyrenees Range, occurrences are noted for the sector of Dordogne (east of Bordeaux), and for the sector of Monthureux-sur-Saône in the Vosges region.
2. Spain: a new discovery by the ADARO Society in the northwestern province of Leon and Lugo.
3. Morocco: important indications at Oulmès, and at several points in the massif of Ticlika in the High Atlas Range.
4. Niger: in the sector of Liptako.
5. Gabon: occurrences not well located.
6. Zaire: in the sectors of Rutshuru, Shaba, N'Zole, Bitso, N'Yanzale, North Kivu, and Hango.
7. Canada: in the southern region of Quebec.
8. Bolivia: in the sector of Sud Lipez.

No details were supplied by BRGM personnel on any of the foregoing occurrences; however, each is shown in figure 2 to indicate the reported worldwide distribution of this unusual variety of monazite.

A recent article on some aspects of the mineralogy of "abnormal europium-bearing monazite" in northwest Spain does not offer much information on the geologic setting (Vaquero, 1979). The sample was found in panned concentrates from slates in the vicinity of granitic stocks in the Ancares and Caurel Ranges on the east side of the Province of Lugo. The flattened ellipsoidal grains range in size from 0.125 to 4.5 mm and are mostly 0.5 to 1 mm; Th metal is 0.12 percent and Eu metal is 0.12 percent, but additional neutron activation analyses show that Th ranges from 0.08 to 0.18 percent and Eu ranges from 0.23 to 0.41 percent. Another dark-monazite locality mentioned by Vaquero (1979, p. 375) is at the batholith of Los Pedroches (tentatively located in southwest Spain), but no details are given.

A brief article on the occurrence in the Oulmès, Morocco, region noted that Eu-bearing gray monazite recovered from panned concentrates represents 500 to 1,500 g/m^3 (el Aissaoui and Devismes, 1977). Spherical or ovoid nodules of this monazite range from 0.5 to 1.4 mm in diameter, and the color is light gray to beige. Weak radioactivity indicates a low Th content, and analysis showed 0.40 percent Eu_2O_3.

ACKNOWLEDGMENTS

We are grateful to the many persons who helped with services, samples, and information used in the work reported here. Listing all the names is not practicable. However, certain individuals must be mentioned. W. C. Overstreet, U.S. Geological Survey, provided encouragement and many rewarding discussions on all aspects of the report. Dr. Michael Fleischer, U.S. Geological Survey, supplied valuable references to the Russian literature, and participated in stimulating discussions. Dr. J. J. Altmann and Dr. A. Parfenoff, BRGM, France, sent information on samples from Zaire and France, respectively. Mr. Ching Chao, Taiwan Institute of Nuclear Energy Research, supplied three samples of dark monazite from Taiwan. R. M. Chapman, U.S. Geological Survey, provided samples from Alaska and geologic data on occurrences in Alaska. J. W. Mytton, U.S. Geological Survey, assisted in field work and collection of samples in Montana. Paul M. Hopkins, mining geologist and engineer, contributed samples from northern and southeastern Peru; and William Bailey, geologist, Bangkok, Thailand, provided samples from central Thailand. Phoebe Hauff and George VanTrump, U.S. Geological Survey, aided in obtaining X-ray diffraction data and in operating a computer program for determination of cell parameters of dark and yellow monazites. Dr. P. A. Baedecker, U.S. Geological Survey, performed instrumental neutron activation analysis of five samples. J. H. Turner, U.S. Geological Survey, translated a number of Russian articles on geochemistry of minerals containing rare-earth elements. Dr. Paul H. H. Lu, U.S. Bureau of Mines, translated Chinese and Japanese articles on monazites in Taiwan and Korea.

GEOLOGY

DOMESTIC DISCOVERIES OF DARK MONAZITE

ALASKA

The geologic setting in the headwater terranes of the alluvial deposits that contain Eu-rich dark monazite is remarkably similar and consistent in Alaska as well as worldwide. The source rocks for the dark monazite are predominantly black shales or siltstones that are weakly metamorphosed. Generally, a granitic intrusive mass has thermally affected the sedimentary rocks, and the resulting metasediments have been variously referred to as slaty shales, slates, phyllites, or schists. Where the mineral has been seen in thin sections (Bretagne, France, and Verkhoyan'e Range, Eastern Siberia), the rocks are described as light-gray to black shales and siltstones. Fragments of rock enclosing dark monazite grains from one Alaskan locality indicate that the host rock is a brownish-weathering spotted phyllite and the unweathered rock may be light to medium gray in tone. The granitic rock is usually a biotite quartz monzonite, but the complete range of calcalkaline rocks,

from granite to gabbro and some ultramafic rocks, has been noted as the source of heat for the thermal metamorphism.

Dark monazite was first recognized in Alaskan panned concentrates from the Eureka, Tofty, and Rampart gold-tin districts in the southeastern part of the Tanana quadrangle, about 120 km west-northwest of Fairbanks (fig. 3). The geology covering these districts was described by Eakin (1913), Mertie (1934, 1937), Wayland (1961), Chapman, Weber, and Tabor (1971), Chapman and others (1975), and Foster and others (1973). Mertie (1937) indicated that the terrane in the headwaters of streams whose concentrates were found to carry dark monazite consists mainly of Mississippian and Cretaceous fine-clastic sedimentary rocks, in which weakly metamorphosed aureoles were present around stocks of intrusive monzonite and quartz monzonite.

The Mississippian rocks, a relatively small part of the headwater terrane, include shale, sandstone, chert, chert conglomerate, limestone, slate, phyllite, quartzite, greenstone, and several varieties of schist. Cretaceous rocks cover the major portion of the area and include argillaceous, sandy, and conglomeratic layers that show marked thermal metamorphism in the vicinity of the granitic intrusive rocks. Mertie (1937, p. 160) noted that the argillaceous rocks, particularly near the contacts, are baked and recrystallized to hornfels and related rocks: "Some are merely spotted or nodular, * * *such spots appearing under the microscope only as carbonaceous clots in a fine groundmass showing incipient recrystallization* * *."

Quaternary deposits in the area (Mertie, 1937, p. 185–194) include glacial silt, sand, and gravel; silt with considerable vegetal matter, locally called "muck" and attaining thicknesses of 30 m or more; and Holocene alluvial deposits of gravel, sand, and silt.

Heavy minerals with D greater than 2.85, from several placer deposits in the Eureka district, include apatite, augite, barite, biotite, chlorite, cinnabar, diopside, galena, garnet, gold, hornblende, hypersthene, ilmenite, limonite, magnetite, muscovite, picotite, pyrite, scheelite, sphene, tourmaline, and zircon (Waters, 1934, p. 236–238). However, no single concentrate contained all of these minerals. It is noteworthy that no other rare-earth minerals, such as yellow monazite, xenotime, or euxenite, are recorded in the Eureka district; but yellow monazite was found in the Tofty and Hot Springs districts and nioboeschynite-(Ce) was identified in the Tofty district (Waters, 1934, p. 238–242; Rosenblum and Mosier, 1975).

Recent geologic studies of the Hot Springs district (fig. 3) indicate that the Cretaceous to Jurassic sedimentary rocks include argillaceous types that are thermally altered to hornfelsic rocks around granitic stocks (Chapman and others, 1975). These rocks are generally medium to dark gray, hard, banded to laminated, and gneissic in part; and facies equivalents include albite-epidote amphibolite, amphibolite, and pyroxene hornfels.

Similar geology and heavy-mineral suites are found in most of the other districts where dark monazite appears in panned concentrates. Reconnaissance geology is shown in figures 4–16, based on the literature and on written communications from U.S. Geological Survey personnel familiar with the various localities. A summary of geologic and mineral-commodity data for all of the Alaskan dark monazite occurrences is listed in table 1 (page 22), as a ready reference and to facilitate comparisons. References cited are generally the latest ones that give the most pertinent information.

Examination of table 1 shows an almost one-to-one relation of dark monazite occurrence to source rocks of low-grade metamorphosed shaly or silty sediments with graphitic (or carbonaceous) affinities. Of 18 districts or parts of quadrangles, only in the Circle and Tanacross areas are schists cited, and the more likely slaty shale, phyllite, and graphitic siltite are not mentioned. Of 62 samples, 50 are associated with biotitic granitic intrusive masses and 12 are near biotite-poor or biotite-free granitic rocks. Horizontal distances of less than 10 km to contacts are equally represented between granitic rocks and mafic and (or) ultramafic rocks. Perhaps significantly, mafic and ultramafic rocks are not found in or near four of the districts. Among the mineral commodities, Sn and W are noted in all occurrences, Au is reported in all but the Tanacross area, Pb is reported in 12 of the districts, and REE minerals are cited in 8 districts.

MONTANA

Confronted with the geologic data of table 1, the proposal of contact metamorphism of fine-clastic sediments as an origin for Eu-rich dark monazite seemed inescapable. To test this proposal, a region with unmetamorphosed phosphatic black shales that were intruded by granitic rocks was sought in which to collect panned concentrates to examine for dark monazite among the heavy minerals. Three districts in Montana were sampled where the Permian Phosphoria Formation was close to intrusive granitic contacts, and dark monazite was discovered in all three districts. In 43 panned concentrates taken from sites downstream from the contacts, dark monazite was present in 12 samples that indicated nine separate source areas: three in the sector northeast of Philipsburg, five in the area north of Wise River, and one in Rock Creek, north of Dillon, Mont.

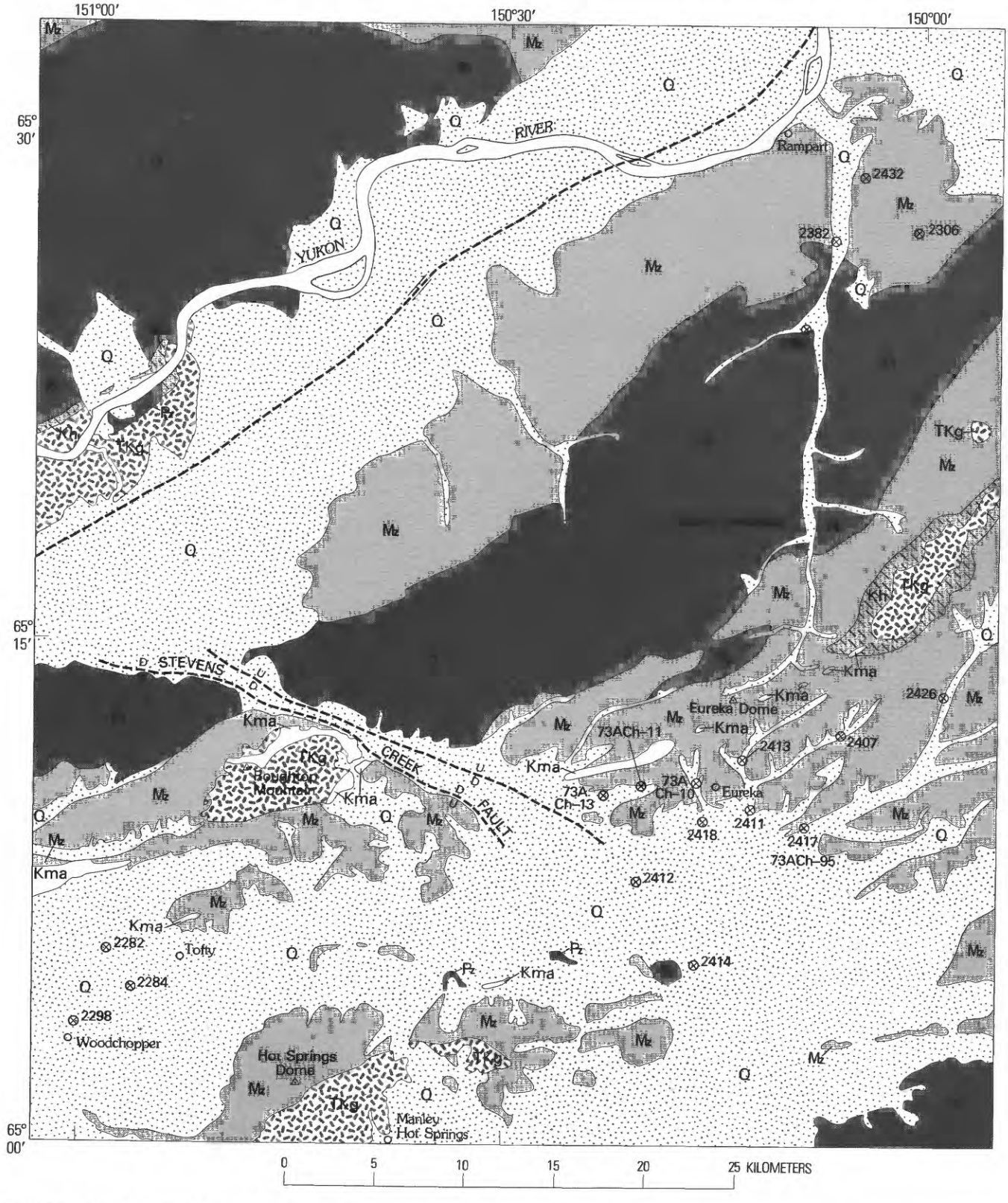

FIGURE 3.—Geologic sketch map of the southeastern part of the Tanana quadrangle, Alaska. Geologic data modified from Chapman and others (1975).

EXPLANATION

Q — UNCONSOLIDATED SEDIMENTARY DEPOSITS (QUATERNARY)—Alluvium, fan deposits, colluvium, terrace deposits, till, loess, and landslide debris

TKg — GRANITIC INTRUSIVE ROCKS (TERTIARY TO CRETACEOUS)—Range in composition from biotite granite to granodiorite

Kma — MAFIC ROCKS (CRETACEOUS)—Gabbro, diorite, serpentinite with some diabase, and mafic volcaniclastic rocks

Kh — HORNFELS (CRETACEOUS)—Mainly sedimentary rocks surrounding the granitic intrusive rocks, shown where easily differentiated and mappable

Mz — SEDIMENTARY ROCKS (MESOZOIC)—Sandstone, conglomerate, siltstone, slaty shale, graywacke, and lignite; include some Tertiary rocks

SEDIMENTARY ROCKS (PALEOZOIC)—Slaty shale, siltstone, graywacke, sandstone, conglomerate, limestone, and chert, and metamorphosed equivalents of these rocks

CONTACT

D / U — FAULT—Dashed where inferred; arrows and letters indicate direction of movement; U, upthrown side, D, downthrown side

⊗2426 SITE OF PANNED STREAM CONCENTRATE WITH DARK MONAZITE

Where shaly members of the Phosphoria Formation were intruded by granitic rocks, they were converted to hornfelses and phyllites, but outcrops of these rocks are sparse in the heavily wooded and glacial-debris-covered region. Dark spots in phyllitic rocks proved to be carbonaceous clots that are apparently similar to those observed in baked argillaceous rocks in the Rampart and Hot Springs districts, Alaska (Mertie, 1937, p. 160). Mertie indicated marked thermal metamorphism in the vicinity of the granitic intrusions. In Montana, the heavy cover precludes rapid and accurate measurement of the widths of contact aureoles, but judging from the sparse outcrops these zones are estimated to be 2–4 km wide. Dark monazite has not been identified in thin sections of rocks from the three districts where it is present in stream deposits.

FOREIGN LOCALITIES

The literature indicates dark monazite at one or more localities in the U.S.S.R., Taiwan, the Malagasy Republic, Zaire, France, Gabon, and Morocco. Personnel of BRGM (France) have reported dark monazite from additional localities in France, Spain, Niger, Canada, and Bolivia (fig. 2). To these reported foreign localities, this investigation has added discoveries of dark monazite in Bangladesh, Pakistan, Thailand, and Peru. The most complete descriptions of the geologic setting, mineralogy, and the composition of dark monazite from the foreign localities are given in the literature for deposits in France and the U.S.S.R.

FRANCE

The source rocks of dark monazite in Bretagne, France, are gray or black schists of Precambrian to middle Paleozoic age. Granitic rocks in the region are assigned Precambrian and late Paleozoic ages. The rocks richest in this monazite are Early Ordovician schists that have been affected by regional metamorphism at temperatures that do not exceed 300°C (Donnot and others, 1973, p. 11). Petrographic studies show that the dark monazite occurs as 0.1- to 1.8-mm-long nodules that lie with long axes inclined greater than 45° to the plane of schistosity. These nodules are surrounded by light aureoles of micaceous minerals (mica, chlorite, clay) that make up the rock; the aureoles are about 0.5 mm wide and display radial-fibrous structure. Thin sections cut perpendicular to the schistosity show that the micaceous minerals in the aureoles may form two symmetric cones diametrically opposed and their axes lie in the plane of schistosity. The monazite nodules are dispersed in the rock and the tenor in dark monazite ranges from 50 to 200 grams per ton, which represents 30–120 nodules per dm^3 (cubic decimeter) of rock. Placer deposits derived from the monazite-bearing rocks contain from 1 to 4 kg of dark monazite per cubic meter. Analyses presented by Donnot and others (1973, p. 14) showed 0.5 percent Eu_2O_3 in two samples and about the same amount in three others, but neither ThO_2 nor water was reported. Totals for the five analyses range from 91.2 to 97.2 percent; thus, the balance in each may represent ThO_2 and water. Origin of the dark monazite by low-grade metamorphism of authigenic rhabdophane in marine silts was proposed.

The brief communication that announced the presence of dark monazite in southern France near Labastide-de-Serou gave few details on the occurrence (Lacomme and Fontan, 1971). The Arize River, whose sand deposits contained Eu-rich dark monazite, traverses Cambrian to Silurian schists (or shales) as well as gneiss with aplitic veins, pegmatoids, and granitoids. The mineral was thought to be derived from Ordovician schists, in which it is apparently well rounded and of sedimentary origin. Detrital grains are beige to light gray and are opaque. Associated minerals include pyrite, anatase, ilmenite, leucoxene, garnets, staurolite, cassiterite, gold, and scheelite. Dark monazite averages

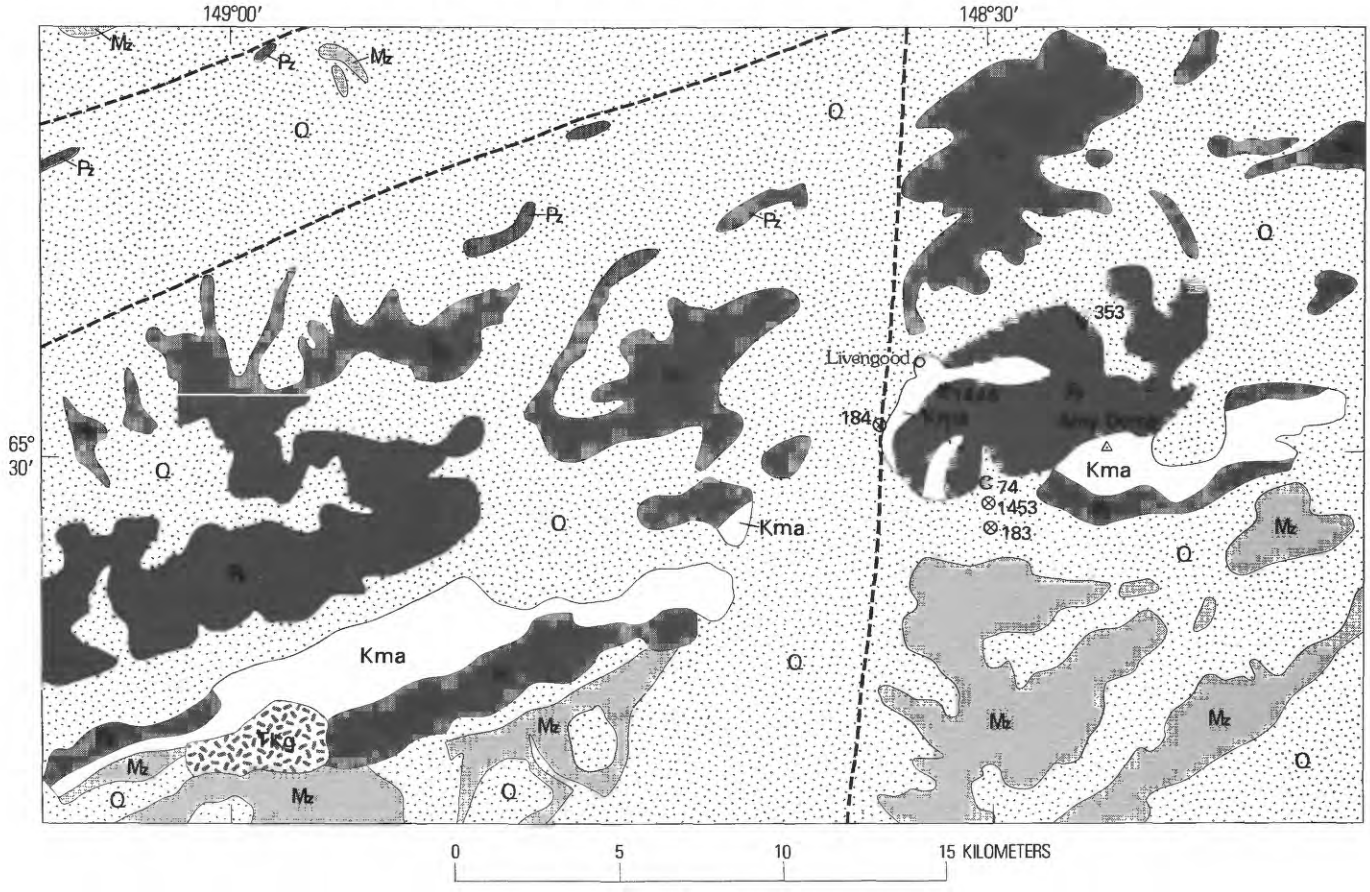

EXPLANATION

Q — UNCONSOLIDATED SEDIMENTARY DEPOSITS (QUATERNARY)—Alluvium, fan deposits, colluvium, terrace deposits, till, loess, and landslide debris

Tkg — GRANITIC INTRUSIVE ROCKS (TERTIARY TO CRETACEOUS)—Range in composition from biotite granite to granodiorite

Kma — MAFIC ROCKS (CRETACEOUS)—Diorite, gabbro, diabase, basalt, and metamorphic equivalents; and serpentinite

Mz — SEDIMENTARY ROCKS (MESOZOIC)—Shale, siltstone, sandstone, graywacke, conglomerate, some greenstone, limestone, chert; hornfelses in contact aureoles around granitic rocks; probably Cretaceous, possibly Jurassic

Pz — SEDIMENTARY ROCKS (PALEOZOIC)—Shale, siltstone, sandstone, graywacke, conglomerate, quartzite, slate, phyllite, some chert, limestone, dolomite, and argillite

CONTACT

FAULT—Dashed where inferred

⊗183 SITE OF PANNED STREAM CONCENTRATE WITH DARK MONAZITE

FIGURE 4.—Geologic sketch map of the Livengood district in the central part of the Livengood quadrangle, Alaska. Geologic data modified from Chapman, Weber, and Tabor (1971).

about 3.5 percent of the heavy minerals in a panned concentrate. A spectrographic analysis gave (in ppm): 300 Th, 5,000 Ce, 700 Sm, 1,000 Y, and 4,000 Eu; as well as several percent La.

Inspection of a geologic map of the headwater region of the Arize River confirmed the sedimentary and plutonic rocks cited above, and Paleozoic granitic rocks are identified as biotite granites (Goguel, 1968). In addition, the headwater region includes crystalline rocks such as schists and migmatites.

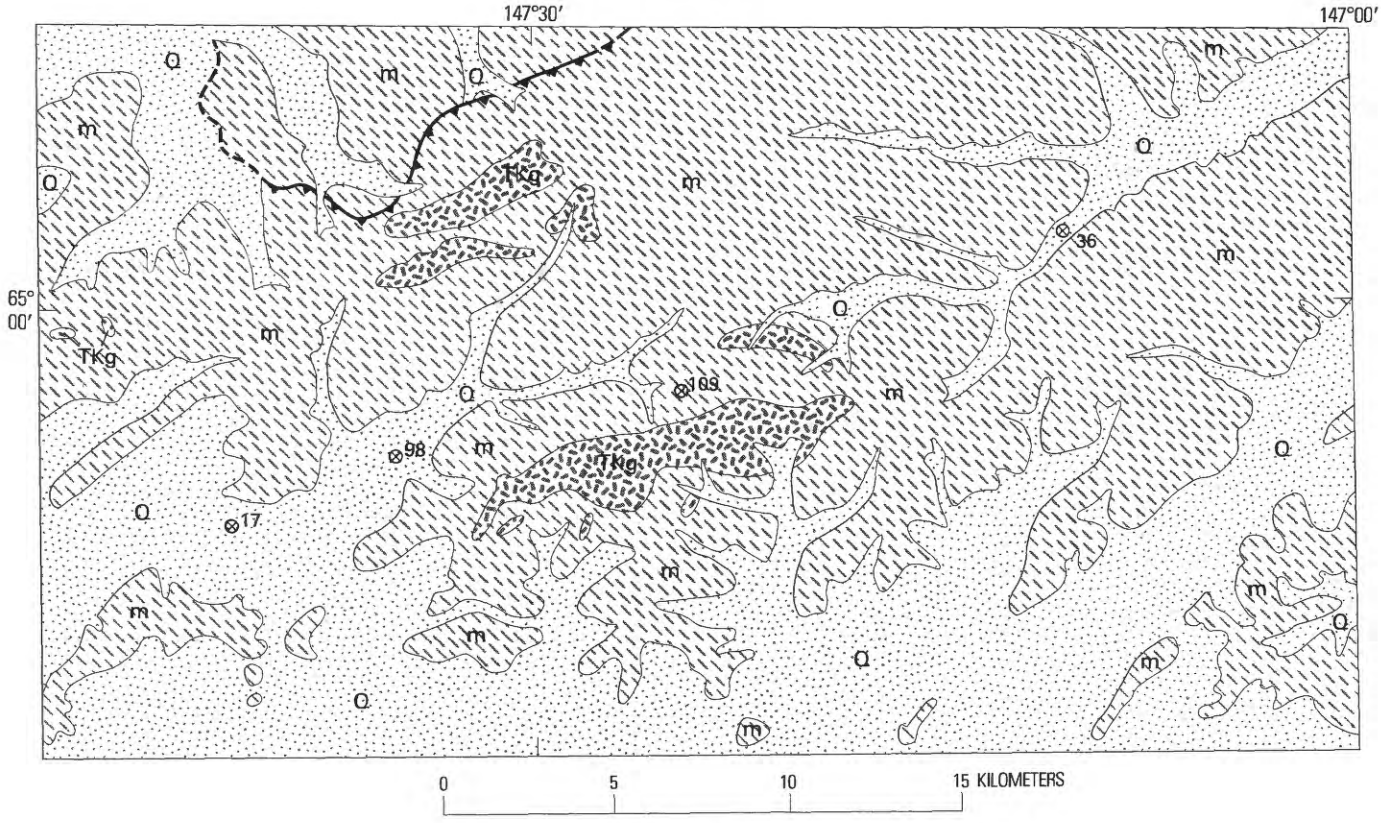

FIGURE 5.—Geologic sketch map of the Fairbanks district, northeast Fairbanks and southeast Livengood quadrangles, Alaska. Geologic data modified from Chapman, Weber, and Tabor (1971); and Péwé, Wahrhaftig, and Weber (1966).

U.S.S.R.

In a gold-placer concentrate from the South Yenisei area in south-central Siberia, Eu-rich dark-gray monazite was found to be more abundant than a light-brown variety of monazite (Zemel', 1936). A mixture of the two varieties proportional to their contents in the concentrate showed 0.26 percent ThO_2 and 0.8 percent Eu_2O_3. The density of the mixture was 4.57, but the density of the dark-gray monazite alone was not given. Zemel' did not discuss the source rocks of the placer deposit, but examination of geologic map of the region showed sedimentary rocks ranging from Precambrian to Mesozoic in age and granitic rocks of Paleozoic age (Nalivkin, 1965).

In the Maritime Province of eastern Siberia, cassiterite placers containing Eu-rich gray monazite lie on micaceous-phyllitic, quartz-micaceous, and argillo-micaceous schists that have been cut by granitic rocks of various ages (Kosterin and others, 1962). Crushed samples of micaceous schists as well as common sericite coatings on detrital grains of gray monazite prove the

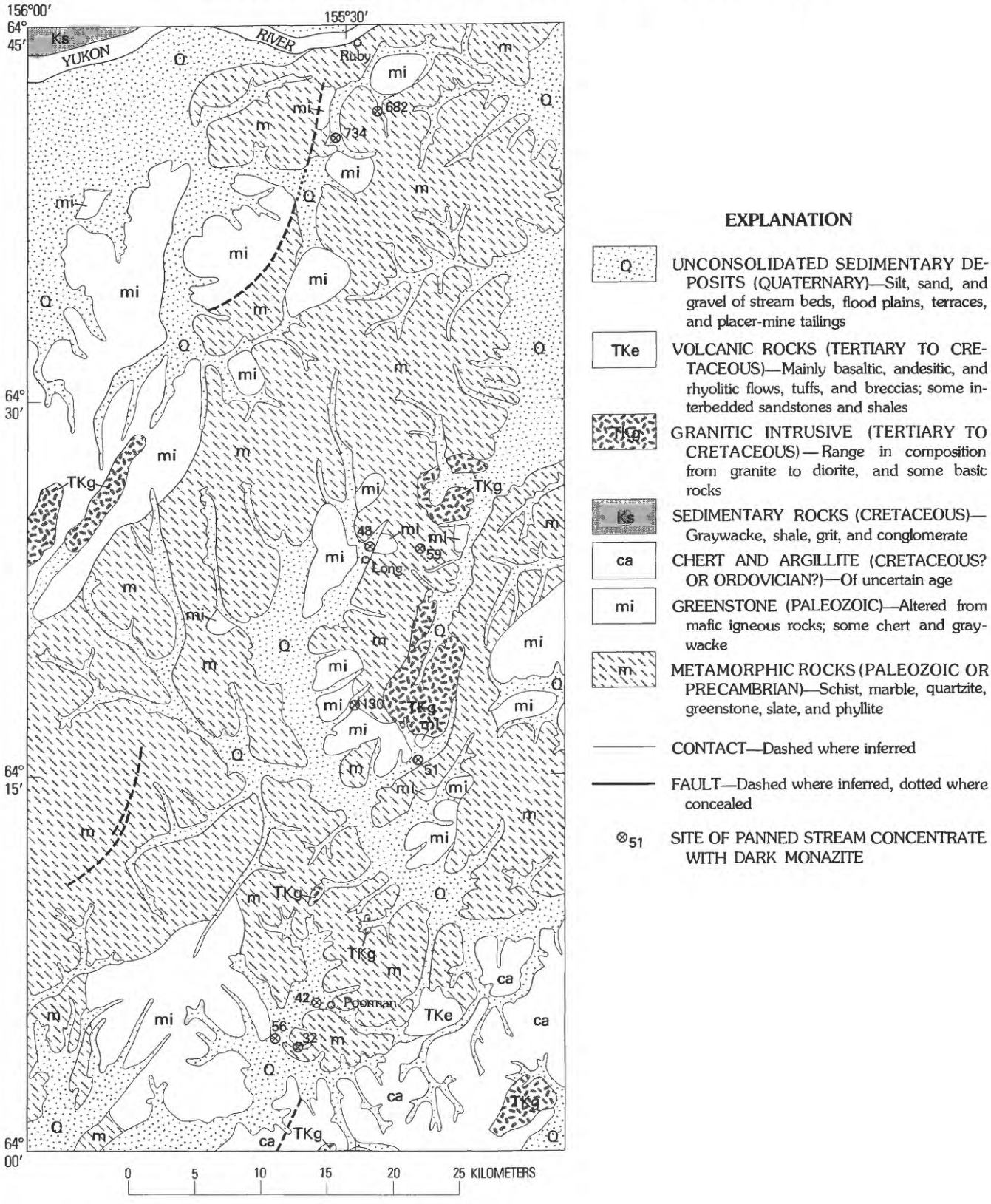

FIGURE 6.—Geologic sketch map of the Ruby-Poorman area in western Ruby quadrangle, Alaska. Geologic data modified from Cass (1959) and R. M. Chapman (written commun., 1975).

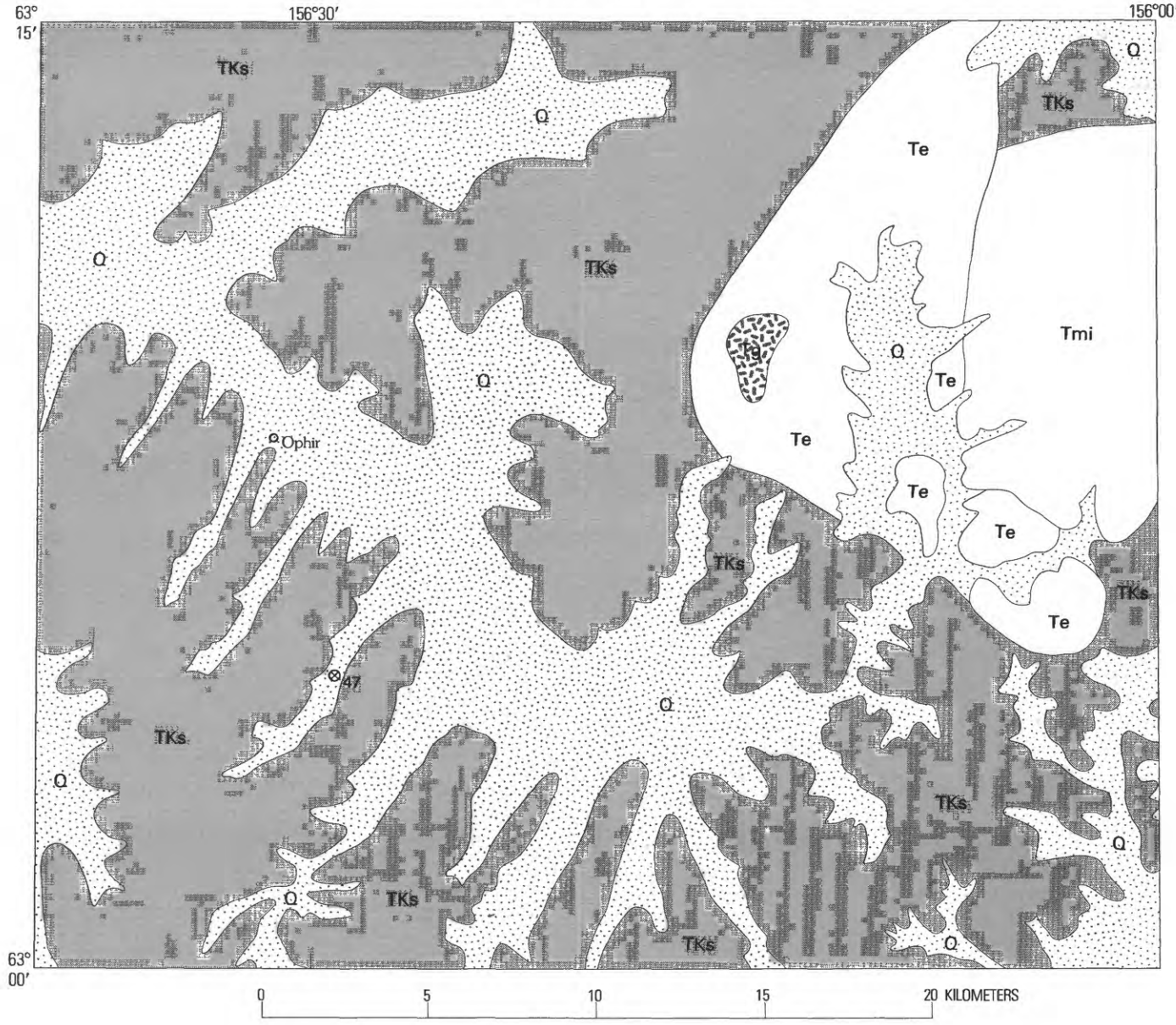

EXPLANATION

- Q — UNCONSOLIDATED SEDIMENTARY DEPOSITS (QUATERNARY)—Silt, sand, gravel, rubble, and morainal material
- Tg — GRANITIC INTRUSIVE ROCKS (TERTIARY)—Mainly quartz monzonite
- Tmi — MAFIC INTRUSIVE ROCKS (TERTIARY)—Pyroxene diorite, gabbro, diabase, and pyroxenite; some pyroxene andesite and basalt
- Te — VOLCANIC ROCKS (TERTIARY)—Mainly andesite and basalt flows and tuffs, with some interbedded sandstone and shale
- TKs — SEDIMENTARY ROCKS (TERTIARY TO CRETACEOUS)—Mainly sandstone, shale, grit, conglomerate, and some slate and quartzite
- CONTACT
- ⊗47 — SITE OF PANNED STREAM CONCENTRATE WITH DARK MONAZITE

FIGURE 7.—Geologic sketch map of the Ophir district, southeastern part of the Ophir quadrangle, Alaska. Geologic data modified from Mertie and Harrington (1924).

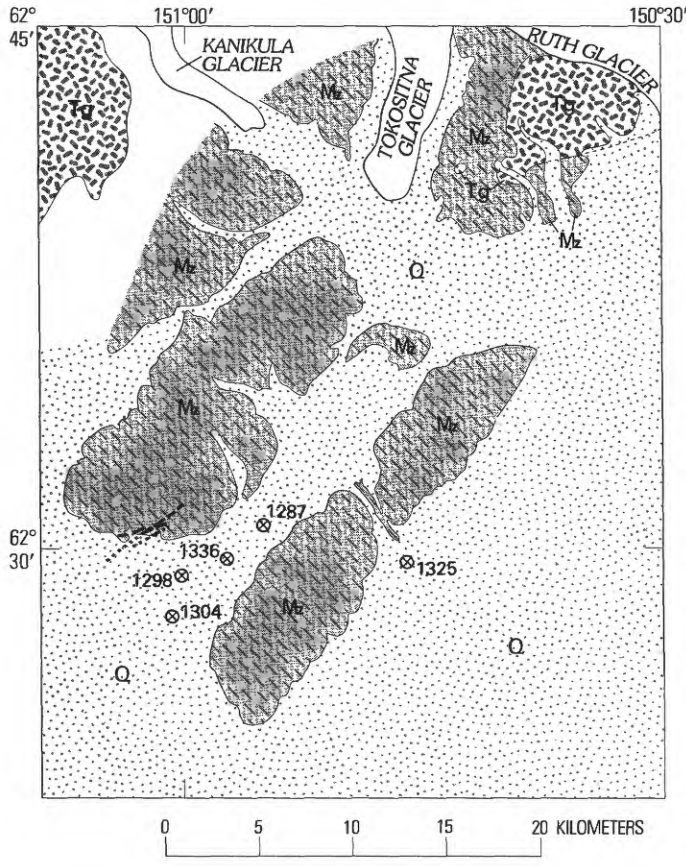

FIGURE 8.—Geologic sketch map of the Yentna district, east-central Talkeetna quadrangle, Alaska. Geologic data modified from Hawley and Clark (1973); and Clark and Cobb (1970).

source rocks of these grains to be the schists. A geologic map of the region shows sedimentary rocks ranging from Precambrian to Mesozoic in age, and granitic rocks of Precambrian, middle to late Paleozoic, and Cretaceous ages (Nalivkin, 1965).

In the northern Verkhoyan'e Range of northeastern Siberia, source rocks for dark monazite are upper Paleozoic and Lower Triassic shale, silty shales, and clayey siltstones (Izrailev and Solov'eva, 1975). Dark grains of monazite were identified in more than 100 of 720 thin sections of silt-clay rocks, but they were not found in any of the thin sections of sandstone or coarse siltstone. The dark monazite grains are unevenly distributed in the shaly rocks—no more than five grains in a thin section—and the grains do not form aggregates. Shales with dark monazite consist of chlorite and hydrous mica and contain 10–50 percent clasts of quartz, feldspar, and rock fragments. Authigenic carbonate minerals make up as much as 25 percent of the rock. Small lenses and chains of carbonaceous material are present, and the content of organic material is 1.83–2.23 percent. Spectrographic analysis of the dark monazite indicated considerable quantities of Ce, La, Y, P, Ca, Th, Si, Fe, and Ti. Numerous inclusions in the dark monazite consist of mica, quartz, and locally an unidentified opaque mineral, possibly ilmenite. Organic carbon is absent despite its presence in the surrounding rock. The dark monazite is considered to be authigenic, as indicated by inclusions of quartz grains similar to those in the host rock, by clastic quartz grains that straddle the boundary between the dark monazite grains and the enclosing rock, by the commonly observed gradation from grain to surrounding rock, by the lightening in color at the contacts with the surrounding rock, and the authigenesis of other minerals. Monazite grains in fault zones are larger, more numerous, and have sharper boundaries than grains in undisturbed rocks.

Fadeev (1959) had indicated that crushed argillites and siltstones of Permian age in the northern Verkhoyan'e Range yielded black grains in the heavy-mineral fraction that resembled dark monazite from the alluvial deposits. Under the microscope, he noted that mineral aggregates which contained REE included monazite, sphene, and ilmenite. In thin sections, the monazite occurred as irregular grains as large as 0.5 mm, a transparent colorless variety that contained a large number of minute carbonaceous inclusions. For the same deposits, Vinogradov and others (1960) confirmed that dark monazite from the heavy-mineral fraction of crushed argillites, siltstones, and sandstones of Permian to Carboniferous age contain high La and Ce, low Y, as much as 1 percent Th, and traces of U. Dark monazite grains show isometric-rounded, flat-rounded, and irregular forms; color ranges from light to dark gray and greenish gray to black; the surface is rough; luster is dull; and the density ranges from 4.42 for dark-gray grains to 4.075 for medium-gray grains. The lowest index of refraction is near 1.780; birefringence is high; and the interference figure is biaxial positive. Associated minerals in the heavy paramagnetic fraction of the detrital concentrates include limonite, garnet, ilmenite,

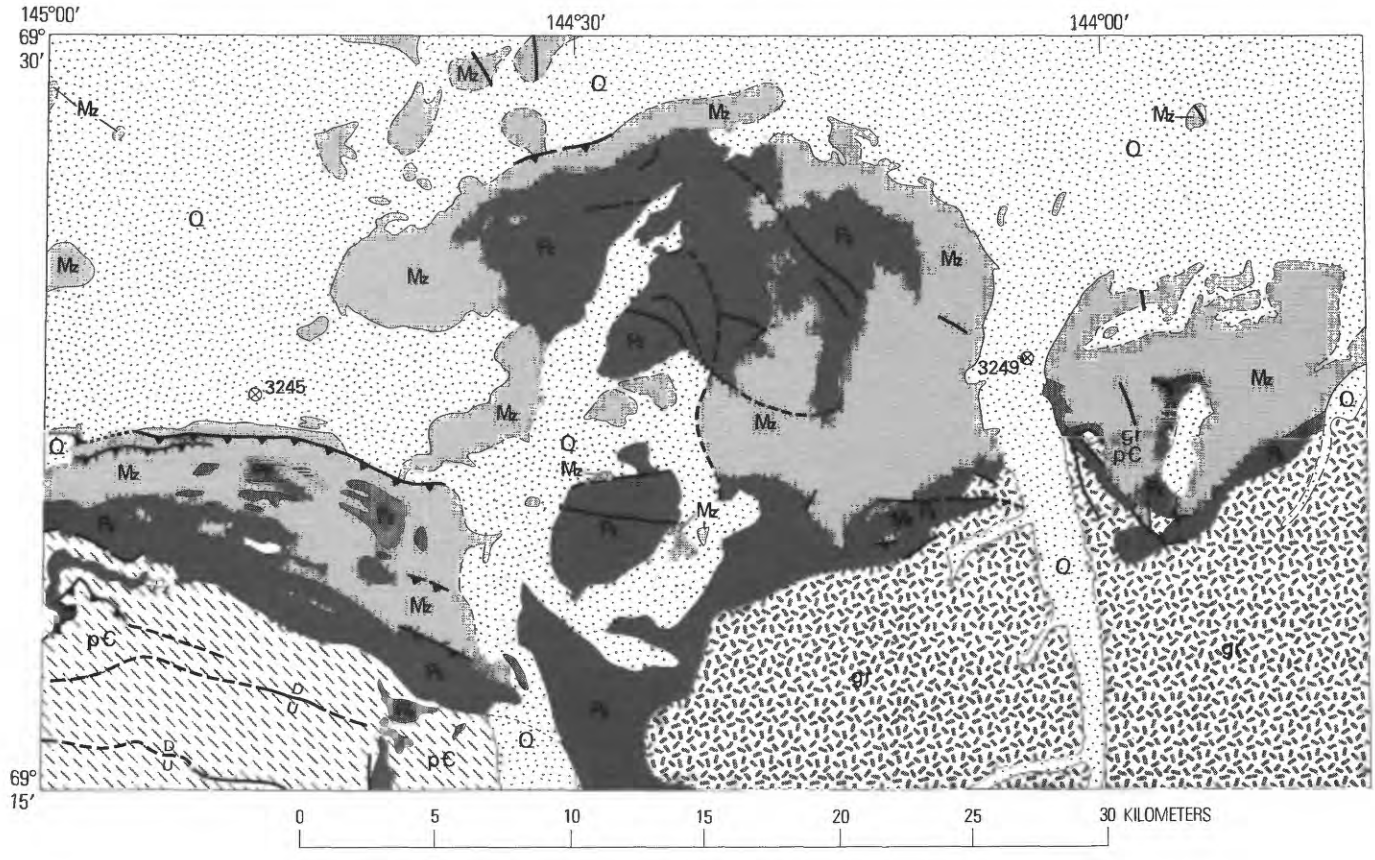

EXPLANATION

Q — UNCONSOLIDATED SEDIMENTARY DEPOSITS (QUATERNARY)—Alluvium, colluvium, and glacial deposits

gr — GRANITIC INTRUSIVE ROCKS (UNCERTAIN AGE)—Micaceous quartz monzonite and granite

Mz — SEDIMENTARY ROCKS (CRETACEOUS TO TRIASSIC)—Mainly shale, siltstone, sandstone, and conglomerate; locally calcareous or dolomitic; phosphatic nodules common

Pz — SEDIMENTARY ROCKS (LATE TO EARLY PALEOZOIC)—Mainly limestone, dolomite, chert, shale, siltstone, sandstone, conglomerate, some phyllite, and local anthracite coal

pC — METAMORPHIC ROCKS (PRECAMBRIAN)—Quartz wacke, phyllite, argillite, chert, quartz grit, and some volcanic rocks

CONTACT—Dashed where inferred; dotted where concealed

D / U — FAULT—Dashed where inferred, dotted where concealed, sawteeth on upper plate of thrust; U, upthrown side, D, downthrown side

⊗3245 — SITE OF PANNED STREAM CONCENTRATE WITH DARK MONAZITE

FIGURE 9.—Geologic map of the Mount Michelson area, eastern Mount Michelson and western Demarcation Point quadrangles, Alaska. Geologic data modified from Reiser and others (1971, 1974).

and martite; and less abundant chromite, tourmaline, pyroxene, chlorite, leucoxene, yellow monazite, siderite, sphene, marcasite, chalcopyrite, epidote, amphibole, hematite, staurolite, olivine, and spinel. Associated nonmagnetic minerals include zircon, rutile, anatase, apatite, barite, pyrite, kyanite, andalusite, sillimanite, and less commonly, sphalerite, cassiterite, gold, scheelite, and corundum.

Inspection of a geologic map of the northern Verkhoyan'e Range disclosed that in addition to the Permian to Triassic sedimentary rocks there are scattered areas of Cretaceous acid igneous rocks including granite, granodiorite, and quartz diorite, and Paleozoic and Mesozoic and basic igneous rocks including diorite, gabbro, and norite (Nalivkin, 1965).

In the Devonian and underlying (late Precambrian) rocks of the Central Timan province, a relatively high concentration of two varieties of accessory monazite was noted (Serdyuchenko and Kochetkov, 1974). One is obviously Eu-rich dark monazite; the other is a

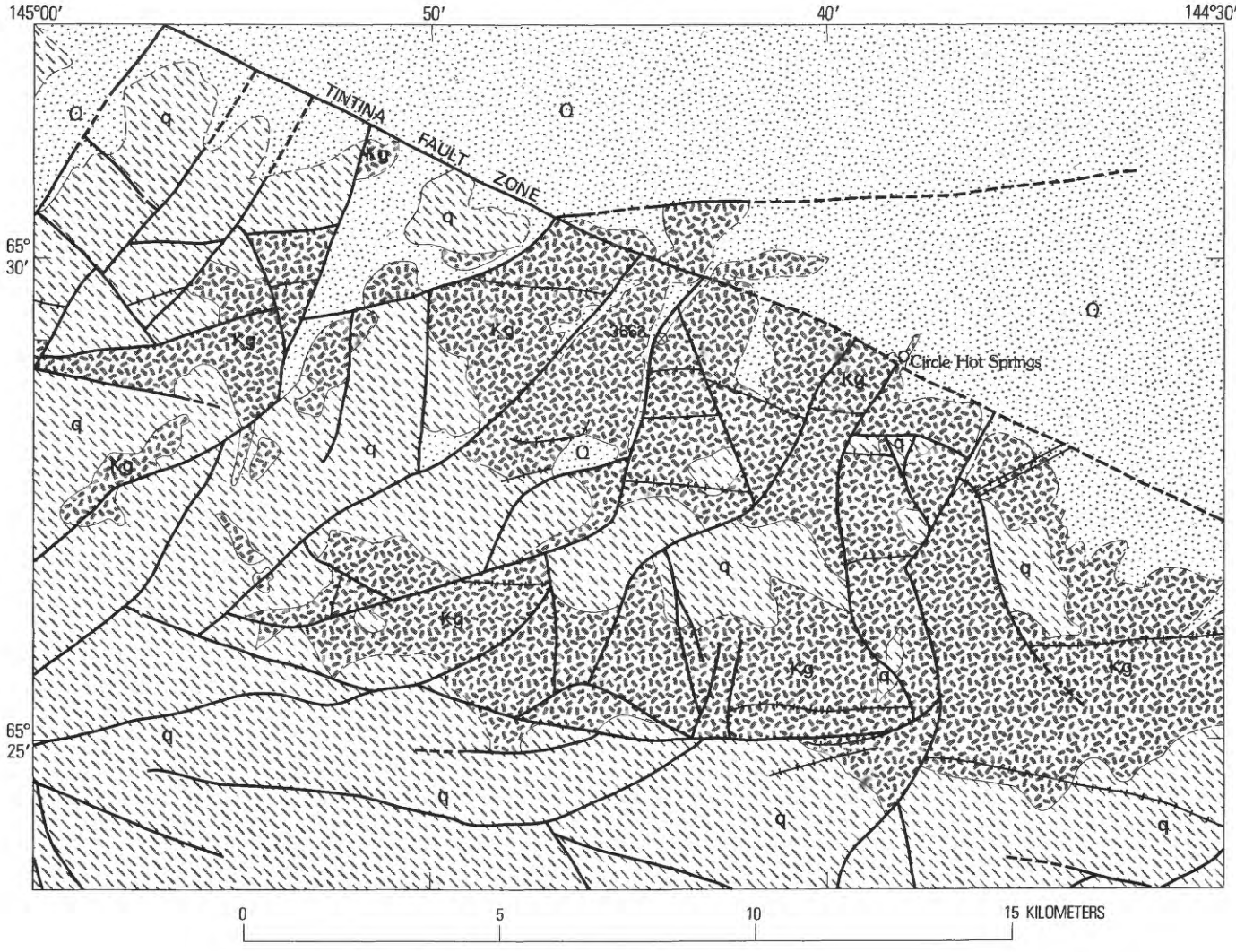

FIGURE 10.—Geologic sketch map of the Circle Hot Springs area, Circle quadrangle, Alaska. Geologic data modified from W. E. Davies (written commun., 1979) and Davies (1972).

yellowish-gray variety that contains 10.6 percent ThO_2; Eu is not reported, and the density is 5.7. Eu-rich dark monazite occurs with metamorphic leucoxene in Precambrian schist and micaceous quartzite, but the much greater rounding of the monazite compared with grains of leucoxene suggested that the dark monazite was supplied to these sediments from more remote metasedimentary rocks of the greenschist facies. In turn, the Precambrian schists were eroded and the dark monazite was again deposited in Devonian sediments. A geologic map of the region shows Proterozoic and Paleozoic sedimentary rocks underlying the Timan Ridge; the only igneous rocks are several small masses of Proterozoic granite at the north end of the ridge (Nalivkin, 1965).

For the low-thorium monazite from gold- and tin-bearing placer deposits in central Asia and the Far

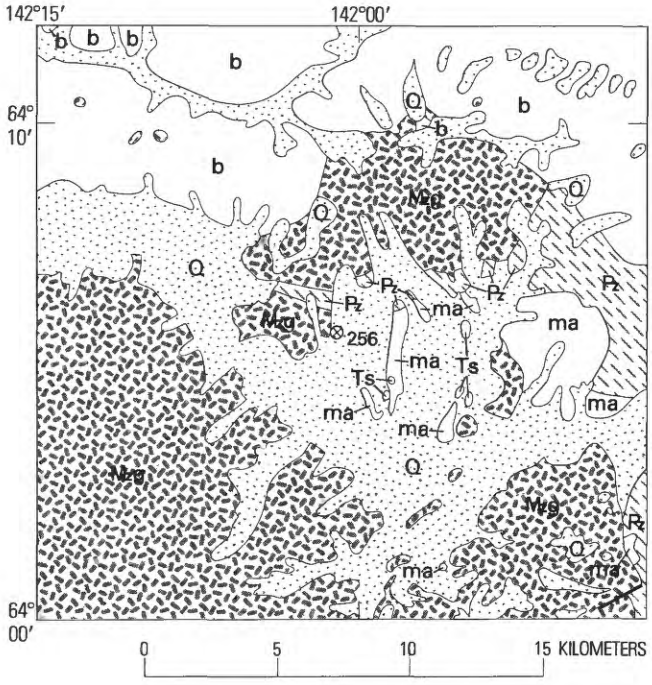

EXPLANATION

Q	UNCONSOLIDATED SEDIMENTARY DEPOSITS (QUATERNARY)—Alluvium, colluvium, and terrace deposits
Ts	SEDIMENTARY ROCKS (LATE TO EARLY TERTIARY)—Tuffaceous, ferruginous, and conglomeratic sandstones, shale and tuffaceous shale, and lignitic coal
Mg	GRANITIC INTRUSIVE ROCKS (MESOZOIC)—Mainly granodiorite; some granite to diorite
ma	MAFIC ROCKS (TERTIARY TO PALEOZOIC)—Mainly greenstone, gabbro, greenschist, serpentinite, and basalt; some quartzite, chert, and phyllite
Pz	METAMORPHIC ROCKS (PROBABLY PALEOZOIC)—Mainly quartz-mica schist and greenschist; also include graphite, chlorite, and calcareous schists, quartzite, marble, phyllite, and greenstone
b	METAMORPHIC ROCKS (PALEOZOIC OR PRECAMBRIAN)—Mainly biotite gneiss and amphibolite; include schist, quartzite, marble, and feldspathic gneiss
———	CONTACT
———	FAULT
⊗256	SITE OF PANNED STREAM CONCENTRATE WITH DARK MONAZITE

FIGURE 11.—Geologic sketch map of the southeastern part of the Eagle quadrangle, Alaska. Geologic data modified from Foster (1976).

East, Li and Grebennikova (1962) did not indicate the source rocks but did supply descriptive material. The dark monazite grains are flat-ellipsoidal to spherical, opaque, dark gray, and more rarely light gray and light brown. Sizes reach 4 mm; optical and X-ray properties are similar to those of yellow monazite; and density ranges from 4.3 to 4.6 and averages 4.5. A large number of irregularly distributed inclusions consist of quartz, mica, and an organic substance. Qualitative spectral analysis indicated (in percent): 10–19 Ce, La, and P; 1–9 Y and Si; 0.1–0.9 Ca; and traces of Be and Mg; but the Eu content is not given.

MALAGASY REPUBLIC

Oolitic dark monazite has been found in low-grade metamorphic shales in the Ambatofinandrahana district in the central part of the Malagasy Republic (Altmann and others, 1970, p. 115). Dark monazite with about 0.50 percent Eu has also been related to graphitic schists in the same area (Serre-Ratsimandisa, 1970, p. 160). An association of Eu and Sn is stressed because of the coexistence of dark monazite and cassiterite in the Malagasy Republic and in the Kivu district of Zaire, but no other data are given. A geologic map of the Malagasy Republic shows that metasedimentary rocks in the Ambatofinandrahana district include gneisses, mica schists, migmatites, marbles, and quartzites; and igneous rocks younger than the metamorphic complex include granite and gabbro (Besaire, 1969).

ZAIRE

In the Kivu district of eastern Zaire, dark monazite occurs in a contact metamorphic zone around a cassiterite-bearing granite, but the metasedimentary rocks are not identified (J. J. Altmann, written commun., 1970). Magnée (1958, p. 471) indicated that the tenor of dark monazite in the cassiterite placers is less than 5 kg/m^3, but Serre-Ratsimandisa (1970, p. 160) noted that thousands of tons of Eu-bearing monazite are localized in a halo around deposits of cassiterite. A geologic map of Zaire (Lepersonne, 1974) shows Precambrian carbonates, shales (in part graphitic), sandstones, conglomerates, quartzites, and argillic-micaceous metasedimentary rocks in this area. The sedimentary rocks include interlayered calcareous sandstones, shales, coaly layers, claystones, and conglomerates of the Lukuga series of late Carboniferous to Permian age. Igneous rocks in the area include micaceous granite and syenite of unspecified age, and basalts and trachytes of Pliocene to Holocene age. In the vicinity of granitic intrusives, some Precambrian rocks take on the metamorphic characters of mica schists, micaceous quartzites, amphibolites, and injection gneisses.

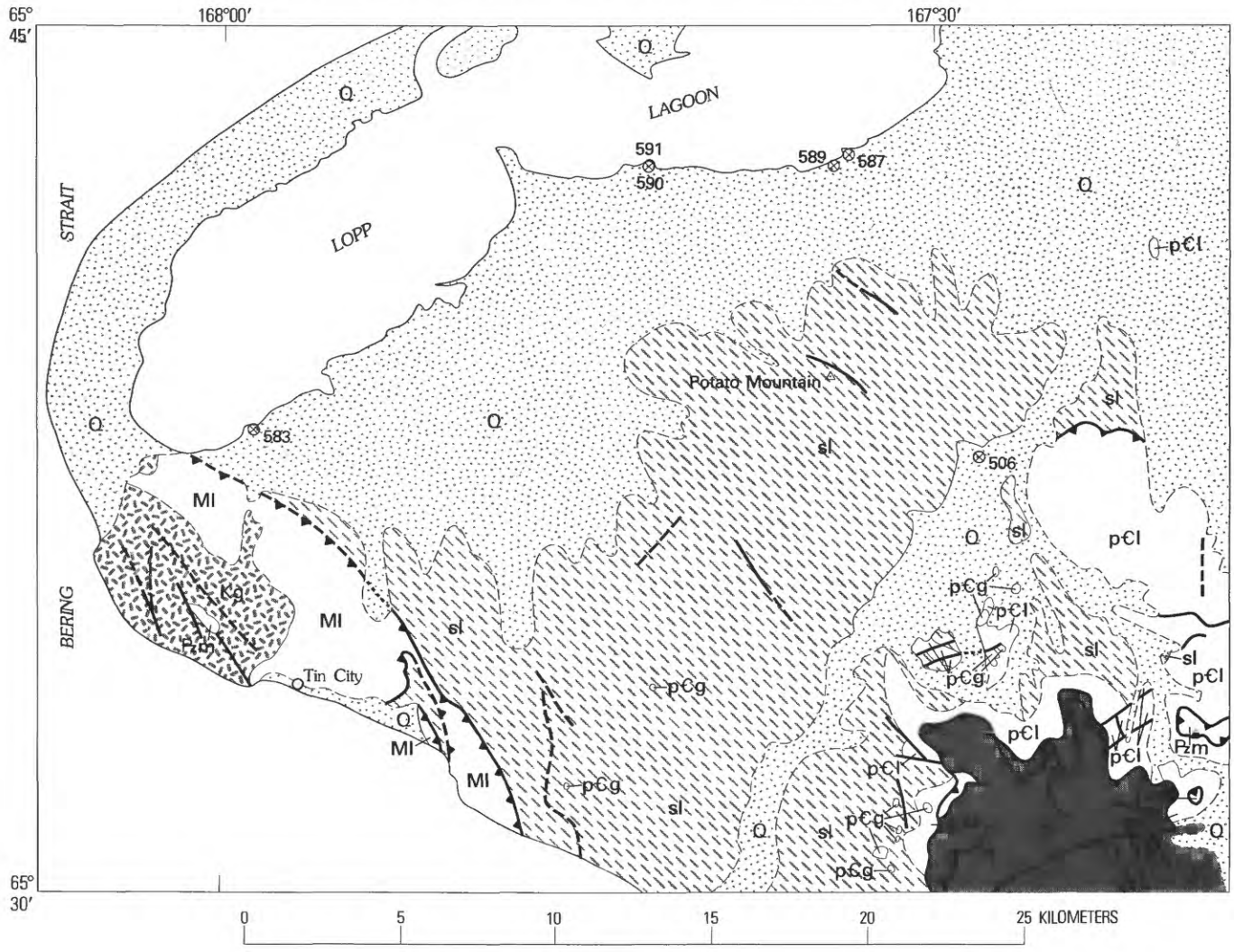

EXPLANATION

- Q — UNCONSOLIDATED SEDIMENTARY DEPOSITS (QUATERNARY)—Alluvium, tundra, silt, loess, and morainal deposits
- Kg — GRANITIC INTRUSIVE ROCKS (CRETACEOUS)—Mainly biotite granite
- MI — SEDIMENTARY ROCKS (MISSISSIPPIAN)—Limestone, dolomitic limestone, and shale
- SEDIMENTARY ROCKS (ORDOVICIAN)—Mainly limestone and dolomitic limestone, argillaceous, silty, carbonaceous, and local shale and chert nodules
- Pzm — MARBLE (PALEOZOIC)
- pC l — SEDIMENTARY ROCKS (PRECAMBRIAN)—Mostly limestone, dolomitic, argillaceous, and thin-bedded
- pC g — MAFIC ROCKS (PRECAMBRIAN)—Gabbro, diabase, and altered equivalents
- sl — METAMORPHIC ROCKS (PRECAMBRIAN)—Mainly black slate of the York region, and slightly to moderately metamorphosed graphitic siltite, slate, graywacke, and calcareous siltite
- CONTACT—Dashed where inferred
- FAULT—Dashed where inferred, dotted where concealed; sawteeth on upper plate of thrust
- ⊗506 — SITE OF PANNED STREAM OR BEACH-SAND CONCENTRATE WITH DARK MONAZITE

FIGURE 12.—Geologic sketch map of the western part of Teller quadrangle, Alaska. Geologic data modified from Sainsbury (1972).

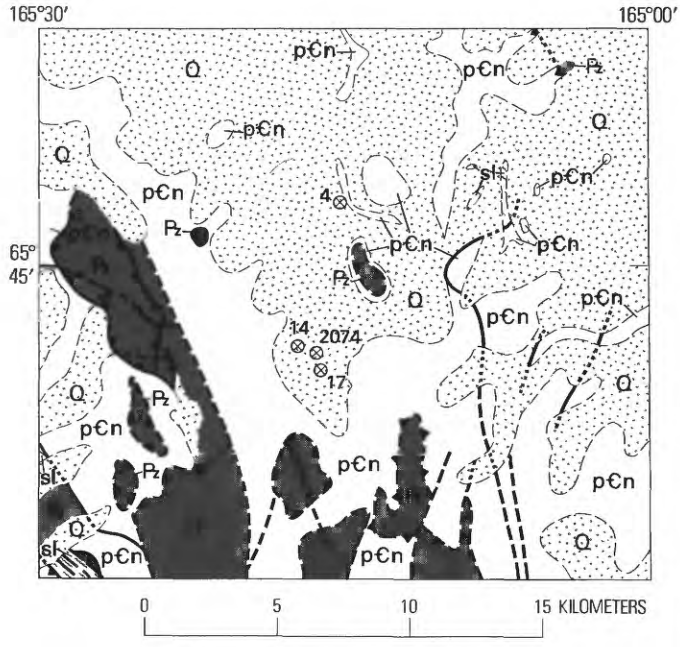

EXPLANATION

Q — UNCONSOLIDATED SEDIMENTARY DEPOSITS (QUATERNARY)—Mostly tundra

SEDIMENTARY ROCKS (PALEOZOIC)—Mainly limestone and marble, intensely deformed

sl — METAMORPHIC ROCKS (PRECAMBRIAN)—Mainly black slate of the York region, and slightly to moderately metamorphosed graphitic siltite, slate, graywacke, and calcareous siltite

p€n — NOME GROUP (PRECAMBRIAN)—Mainly chloritic schist, marble schist, chlorite-epidote-amphibole schist, locally graphitic; and retrograde blueschist

CONTACT—Dashed where inferred

FAULT—Dashed where inferred, dotted where concealed; sawteeth on upper plate of thrust

⊗17 SITE OF PANNED STREAM CONCENTRATE WITH DARK MONAZITE

FIGURE 13.—Geologic sketch map of the northeastern part of Teller quadrangle, Alaska. Geologic data modified from Sainsbury (1972); and Marsh and others (1972).

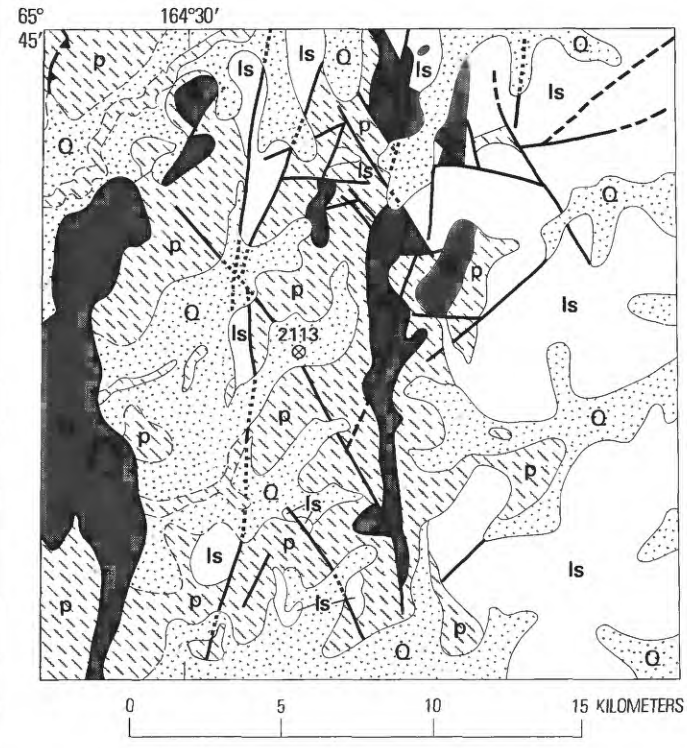

EXPLANATION

Q — UNCONSOLIDATED SEDIMENTARY DEPOSITS (QUATERNARY)—Alluvium, colluvium, terrace deposits, and tundra

SEDIMENTARY ROCKS (PALEOZOIC)—Mainly marble with variable amounts of limestone and dolomite

ls — SEDIMENTARY ROCKS (PRECAMBRIAN?)—Mainly thin bedded, schistose, argillaceous, and dolomitic limestone, locally greatly deformed

p — METAMORPHIC ROCKS (PRECAMBRIAN)—Mainly graphitic phyllite of the York region, greatly deformed near thrust faults

CONTACT—Dashed where inferred

FAULT—Dashed where inferred, dotted where concealed, sawteeth on upper plate of thrust

⊗2113 SITE OF PANNED STREAM CONCENTRATE WITH DARK MONAZITE

FIGURE 14.—Geologic sketch map of the northwestern part of the Bendeleben quadrangle, Alaska. Geologic data modified from Sainsbury (1974).

TAIWAN

Dark monazite occurs in offshore bars and along the beaches of southwestern Taiwan (fig. 17), but the source of these detrital grains has not been identified (Ho and Lee, 1963, p. 436; Soong, 1970, p. 10; Matzko and Overstreet, 1977, p. 23). Among other possible modes of origin, Overstreet, Warr, and White (1971, p. 36) mentioned metasedimentary and contact-metamorphic processes, and suggested (p. 72) that dark monazite

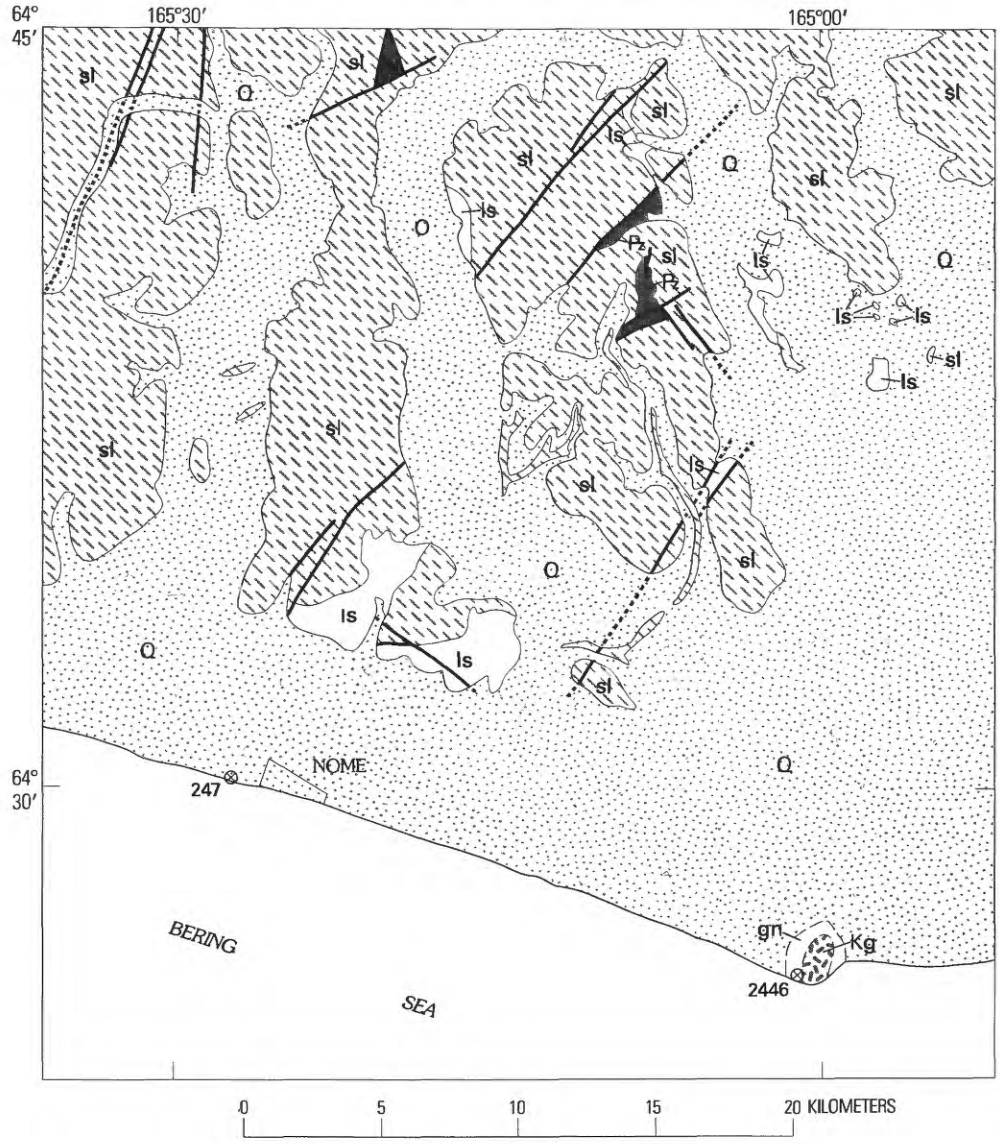

EXPLANATION

Q — UNCONSOLIDATED SEDIMENTARY DEPOSITS (QUATERNARY)—Alluvium, colluvium, morainal deposits, and fan deposits

Kg — GRANITIC INTRUSIVE ROCKS (CRETACEOUS)—Mainly biotite granite, gneissic, cataclastic, coarse-grained to porphyritic

Pz — SEDIMENTARY ROCKS (PALEOZOIC)—Mostly marble, locally schistose, chloritic, siliceous, micaceous, or graphitic; with local relict bedding, chert nodules, and fossils

sl — METAMORPHIC ROCKS (PRECAMBRIAN)—Mostly slate of the York region, including graphitic siltite, phyllite, calcareous graywacke, gray marble, and green schists with chlorite, albite, epidote, amphibole, graphite, plagioclase, and quartz

gn — METAMORPHIC ROCKS (PRECAMBRIAN)—Paragneiss with quartz, biotite, graphite, plagioclase, garnet, and local sillimanite; may be high-rank equivalent of slate of the York region

ls — METAMORPHIC ROCKS (AGE UNKNOWN)—Mostly schistose limestone and marble; isolated exposures which cannot be assigned but which probably belong to one of the known units

CONTACT—Dashed where inferred

FAULT—Dotted where concealed

⊗247 SITE OF PANNED STREAM CONCENTRATE WITH DARK MONAZITE

FIGURE 15.—Geologic sketch map of the Nome area, eastern Nome and western Solomon quadrangles, Alaska. Geologic data modified from Sainsbury, Hummel, and Hudson (1972); and Sainsbury, Hudson, and others (1972).

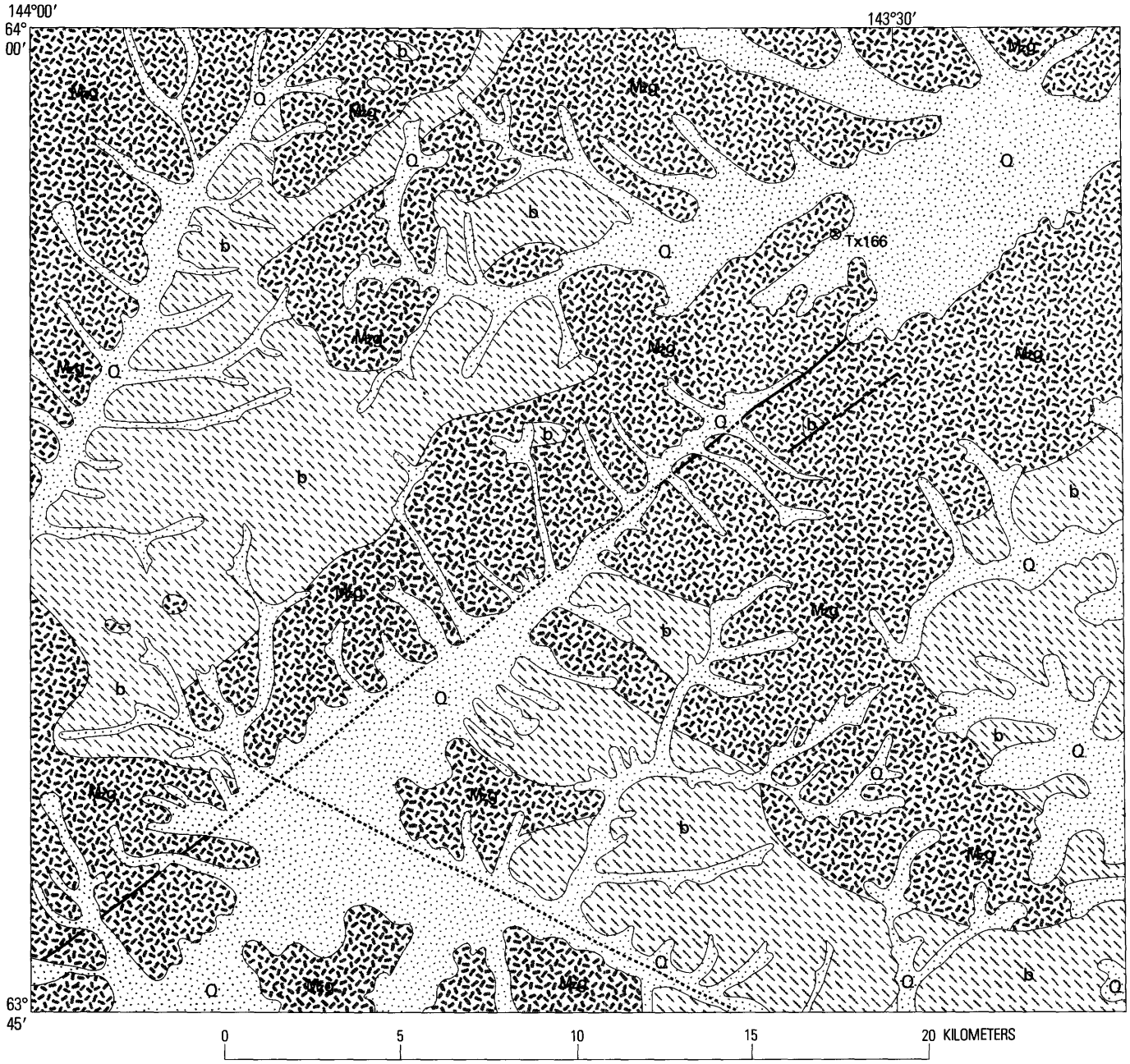

EXPLANATION

Q — UNCONSOLIDATED DEPOSITS (QUATERNARY)—Alluvium, colluvium, peat, and eolian deposits

Mzg — GRANITIC INTRUSIVES (MESOZOIC)—Granitic rocks ranging from granite to diorite, mostly biotite and biotite-hornblende granodiorite

CONTACT

FAULT—Dashed where inferred, dotted where concealed

b — METAMORPHIC ROCKS (PALEOZOIC TO PRECAMBRIAN)—Quartz-biotite gneiss and schist, quartz-hornblende gneiss, quartz-feldspar-biotite gneiss, augen gneiss, quartz-muscovite-garnet gneiss, and quartzite; many rocks highly garnetiferous

⊗Tx166 SITE OF PANNED STREAM CONCENTRATE WITH DARK MONAZITE

FIGURE 16.—Geologic sketch map of the northwestern part of the Tanacross quadrangle, Alaska. Geologic data modified from Foster (1970).

TABLE 1.—*Alaskan dark monazite provenance, distance to igneous contacts, and associated mineral commodities*

Fig.	Quadrangle	District (or part)	Number of samples	Headwater terrane[1]	References	Distance (km) to granitic contact	Distance (km) to mafic/ultramafic rock	Mineral commodities[2]	References
3	Tanana	Tofty	3	(Pz, Mz) slaty shale, siltstone, graywacke; (K) gabbro, diorite, serpentinite; (K-T) granitic stocks, hornfelsed contact zones.	Mertie, 1934, 1937; Chapman, Weber, and Tabor, 1971; Foster and others, 1973	9-13	3-7	Ag, Au, Bi	Cobb, 1972a.
	--do--	Rampart	4			10-15	17-25	Cr, Cu, FM, Hg,	
	--do--	Eureka	11			3-17	1-15	Mn, Ni, Pb, REE,	
	Livengood	Eureka	1					Sb, Sn, W,	
4	Livengood	Livengood	6	(Pz, Mz) chert, slaty shale, argillite, siltstone; (K?) mafic rocks, serpentinite; (K-T) granitic stocks.	Chapman, Weber, and Tabor, 1971	18-30	0-2	Ag, Au, Cr, FM, Hg, Ni, REE, Sb. Sn, W.	Cobb, 1972b.
5	Livengood	Fairbanks	1	(pC-Pz) quartzites, schists, phyllites, marbles, amphibolites; (K-T) granitic stock.	Chapman, Weber, and Tabor, 1971; Pewe Wahrhaftig, and Weber, 1966	0-3	>10[3]	Ag, Au, Bi, Cr, FM, Hg, Mo, Ni REE, Sb, Sn, W.	Cobb, 1972c.
	Fairbanks	Fairbanks	3						
6	Ruby	Ruby	2	(pC-Pz) schist, marble, quartzite greenstone, slate, phyllite; (Pz) altered mafic igneous rocks; (K) graywacke, shale, grit conglomerate; (K) granitic stocks; (K-T) basalt-rhyolite flows.	Cass, 1959; R. M. Chapman, (written comm., 1975).	25	0-2	Ag, Au, FM, Pb, Pt, REE, Sn, W.	Cobb, 1972d.
	--do--	Long	4			1-2	0-2		
	--do--	Poorman	3			7-10	0-5		
7	Ophir	Ophir	1	(K) slate; (T) mafic and granitic stocks.	Mertie and Harrington, 1924.	15-25	20	Au, Bi, Hg, Sb, Sn, W.	Mertie, 1936.
								Au, Hg, W.	Cobb, 1972e.
8	Talkeetna	Yentna	5	(Mz) argillite, phyllite, siltite, graywacke, conglomerate; (T) granitic batholith.	Hawley and Clark, 1973; Clark and Cobb, 1970.	18-25	72-80	Au, Cu, FM, Pb Pt, Sn, W.	Clark and Cobb, 1972.
								Au, As, Cr, Cu FM, Pb, Pt, REE, Sb, Sn, Ti, W.	Hawley and Clark, 1973.
9	Mount Michelson	(East-central)	2	(pC) argillite, phyllite, schist, wacke, chert; (Pz, Mz) clastic and carbonate layers; granitic batholith, stocks of uncertain age.	Reiser and others, 1971, 1974.	3-19	12-18	Au, Sn.	Cobb, 1972f.
10	Circle	Circle Hot Springs	1	(pC-Pz) quartzite, schists, marble, phyllite, greenstone; (K) quartz monzonite; terrane much faulted.	Davies, 1972; written commun., 1976	0	---[4]	Au, Bi, Cu, FM Hg, Pb, REE, Sn, W, Zn.	Cobb, 1972g.
11	Eagle	Fortymile	1	(pC-Pz?) schists, quartzite, phyllite, marble, greenstone; (Pz, T) mafic rocks, (Mz-T) granodiorite batholith; (T) sandstone, shale, coal.	Foster, 1976.	0	2	Ag, Au, Cu, FM, Hg, Pb, REE, Sn. W.	Cobb, 1972h.
12	Teller	York	6	(pC) gabbro, diabase, limestone, slate, siltite; (Pz) limestones; (K) biotite granite	Sainsbury, 1972.	1-22	4	Ag, Au, Be, Cr, Cu, FM, Mo, Nb Pb, REE, Sb, Sn, Ta, W, Zn.	Cobb and Sainsbury, 1972.
13	Teller	(Northeast)	4	(pC) schists, siltite, slate, graywacke; (Pz) limestone	Sainsbury, 1972.	25-29	---	Au, Cu, Pb, Sn, W.	Cobb and Sainsbury 1972.
14	Bendeleben	(Northwest)	1	(pC) slate, limestone; (Pz) marble, limestone, dolomite	Sainsbury, 1974.	20	---	Ag, Au, Cu, Pb, Sn, W.	Cobb, 1972i.
15	Nome	Nome	2	(pC) paragneiss, slate, siltite, phyllite, graywacke, marble schists; (Pz) marble; (K) biotite granite.	Sainsbury, Hummel, and Hudson, 1972; Sainsbury Hudson, and others, 1972.	0-25	0-35	Ag, Au, Bi, Cr, Cu, Mo, Pb, Sb, Sn, W, Zn.	Cobb, 1972j,k.
16	Tanacross	(Northwest)	1	(pC-Pz) gneisses, schist, quartzite; (Mz) biotite-hornblende granodiorite.	Foster, 1970.	0	---	Be, Bi, Cu, Pb, Sn, W.	Tripp and others, 1976.

[1] pC, Precambrian; Pz, Paleozoic; Mz, Mesozoic, K, Cretaceous; T, Tertiary.
[2] FM, fissionable materials, REE, rare-earth elements.
[3] >, greater than.
[4] Leaders (---), not known.

FURTHER SAMPLE AREA DESCRIPTION

1. Reconnaissance geology in the Ruby quadrangle (fig. 6) by Mertie and Harrington (1924, pl. 3) indicated a small soda-rhyolite stock of Tertiary age just west of Poorman. The bedrock in Solomon Creek, about 3 km south of Poorman, is slate tending toward phyllite, and the gold-bearing gravel consisted of 50-90 percent vein quartz (Mertie, 1936, p. 164-165). Minerals associated with gold in the streams near Poorman include arsenopyrite, barite, cassiterite, magnetite, and pyrite.

2. In the Ophir district (fig. 7) reconnaissance geology by Mertie and Harrington (1924) and Mertie (1936) shows the headwater terrane of Little Creek, about 10 km south of Ophir, to be mainly slate. In adjacent areas the country rock is cut by dikes of dacite, andesite, and related rocks. Gold is the only other heavy mineral indicated in the Little Creek placers that contain dark monazite, but other placers in the region contain bismuth, cassiterite, cinnabar, galena, scheelite, and stibnite (Mertie, 1936, p. 143).

3. Reconnaissance geology in the Circle Hot Springs area (fig. 10) by Davies (1972; written commun., 1979) shows that the complexly faulted metasedimentary and granitic terrane is bounded on the north by the Tintina Fault, a major crustal break that is a right-lateral wrench fault and trends southeastward for hundreds of kilometers into northwestern Canada. The grade of regional metamorphism in the area is low (Davies, 1972, p. 212). The site of a sample with dark monazite is in Ketchem Creek downstream from Holdem Creek, about 5 km west of Circle Hot Springs. Although the site is entirely within granitic terrane, the headwaters drain metasedimentary fault blocks to the south and southwest.

4. In the northeastern part of the Teller quadrangle (fig. 13), three of the sample sites shown are for samples collected in the 1960's and supplied by C. L. Sainsbury; thus, they are not part of the Alaska Concentrate File. No intrusive rocks are mapped in the area, and the nearest ones seem too far to be significant: 25–29 km northeastward to the biotite granite at Serpentine Hot Springs (Sainsbury, 1974, p. 15), and about 47 km northwestward to the biotite granite at Ear Mountain (Sainsbury, 1972).

5. In the Nome area (fig. 15), other than the small biotite granite mass at Cape Nome 18 km to the east of Nome, the nearest calc-alkaline intrusive rocks are stocks ranging in composition from biotite granite to granodiorite and a granitic batholith 18–25 km to the north and northwest of the map area. Small stocks of gabbro and metagabbro are exposed within 10 km of the northern border of the area, and these seem most likely to have affected the headwater terrane of the streams that probably carried the dark monazite toward their present beach-sand sites.

6. In the Tanacross quadrangle (fig. 16), the headwater terrane of the stream deposit with dark monazite (collected in 1975) appears to be entirely biotitic granitic rocks. However, the dark monazite grains are both tiny and sparse and may represent a second or third cycle of deposition. The source rocks for this sample may be a long way off or, perhaps, eroded away.

7. Noteworthy among heavy minerals in concentrates that contained dark monazite were abundant yellow monazite in samples from the Tanana, Ruby, Mount Michelson, and Talkeetna quadrangles, and abundant phosphate aggregates of microcrystalline texture in samples from the Talkeetna quadrangle.

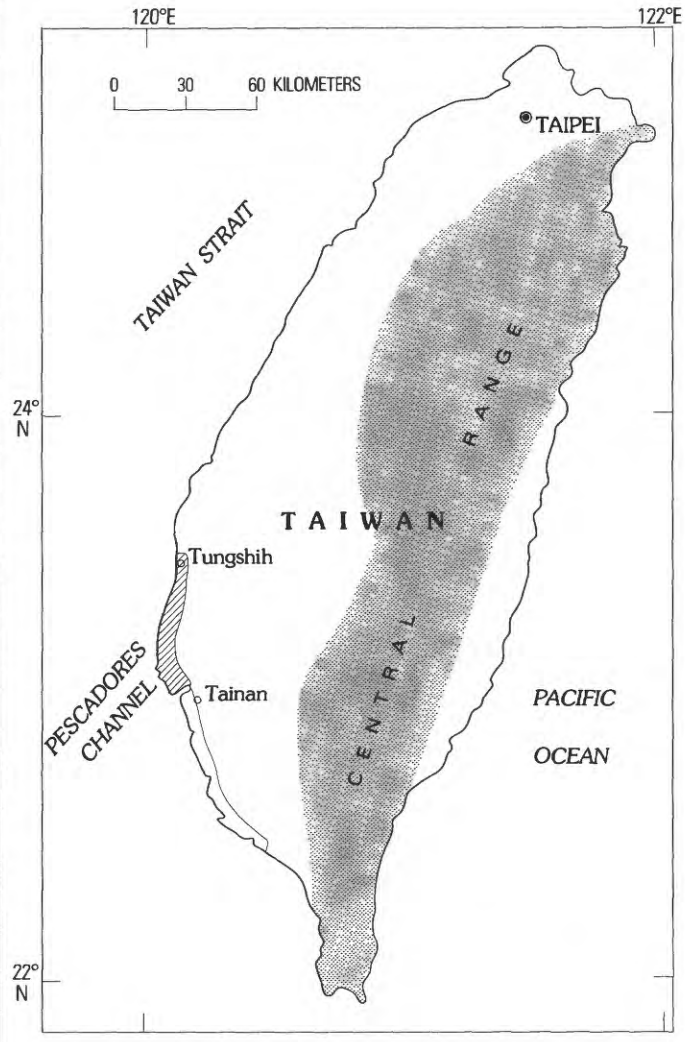

FIGURE 17.—Index map showing location of the area (line pattern) of the principal monazite placers on Taiwan. Data from Chen (1953) and Huang (1958).

might be sought in dark slate, phyllite, and mica schist in the Central Range of the island (fig. 17). The latest geologic map of Taiwan (Ministry of Economic Affairs, 1974) shows that such rocks are drained by streams that empty into Taiwan Strait north and south of the richest deposits of dark monazite. Four major streams that enter Taiwan Strait in the dark monazite area drain Miocene to Pleistocene sandstones, shales, mudstones, and some limestone. The nearest mapped intrusive rock is an elongate sill-like mass of mafic to ultramafic rocks (Ho, 1975, p. 113) on the eastern slope of the Central Range that comes within 10 km of the headwaters of streams flowing westward to the dark monazite deposits. The relatively small area of dark monazite concentration along the southwestern coast apparently precludes a second-cycle deposition with the primary

source being on the mainland of China. Rather, the source of these grains is most likely a small area in the present terrane of Taiwan that is being drained by the four main streams between Tungshih and Tainan.

PAKISTAN

A heavy-sand concentrate taken from the Hunza River about 1 km from its confluence with the Gilgit River in northern Pakistan was found to contain dark monazite. A geologic map of the area (Bakr and Jackson, 1964) shows the headwater terrane to be mostly late Paleozoic and early Mesozoic volcanic, sedimentary, and metasedimentary rocks interlayered with large elongate units described as granite, gneiss, and schist; some metasedimentary rocks of possible Precambrian age; and intrusions of granodiorite, granite, syenite, and diorite of probable early Tertiary age. The nearest mafic intrusions shown are 140–180 km southeast, out of the Hunza River drainage.

BANGLADESH

Dark monazite was identified in three concentrates prepared from beach sand collected near Cox's Bazar, Bangladesh, and two similar samples from Kutubdia Island about 32 and 54 km north of Cox's Bazar (Schmidt and Asad, 1962, 1963). The terrane east of the beach consists mainly of Miocene sandstone, shale, and siltstone; but no igneous rocks are shown as far as the border with Burma. A more likely source of the dark monazite is the mouth of the Ganges-Brahmaputra River system about 150 km northwest of Cox's Bazar. Fine sand discharged from the common mouth of these large rivers probably is carried across the head of the Bay of Bengal and deposits along the eastern beaches. The areas drained by these streams include a multitude of sedimentary, metamorphic, and igneous rocks of the southern Himalayan Mountain Range.

According to Walter Danilchik (oral commun., 1979), the Irrawaddy River, about 650 km south of Cox's Bazar, is the most likely source of the dark monazite, for the longshore current along the Bangladesh coast is northward. The Irrawaddy River, like the Ganges-Brahmaputra system, drains metamorphic, sedimentary, and igneous rocks ranging in age from Precambrian to Recent. Another source might be the Kaladan River, whose mouth is about 200 km south of Cox's Bazar. However, the Kaladan River is a relatively short stream and drains only Tertiary rocks (Krishnan, 1956).

OTHER LOCALITIES

Other foreign localities, mentioned in the section on history, lack adequate location of sample sites to permit detailed statements on the geologic settings of the dark monazite. These include localities in Spain, Morocco, Canada, Peru, Bolivia, Niger, and Gabon. However, inspection of the Becerreá (Spain) 1:50,000 scale geologic map and information booklet indicated that the Aqüeira Formation cited as the source of dark monazite by Vaquero (1979, p. 375) consists of Ordovician clayey, silty, and sandy strata that were affected by low-grade regional metamorphism and by contact metamorphism (Marcos and others, 1980). The contact-metamorphic zone around the two-mica Ancares Granite attains a width of 5 km on the north side of this late Paleozoic intrusive mass, which lies in the southeast corner of the Becerreá sheet.

In the Oulmès, Morocco, area, the source of Eu-rich gray monazite is without doubt in the shales or other sedimentary rocks in the contact-metamorphic aureole around the granite of Oulmès (el Aissaoui and Devismes, 1977). The source rocks are Ordovician in age, but the mineral may also occur in Silurian, Devonian, and lower Carboniferous rocks. Other heavy minerals that accompany gray monazite include cassiterite, scheelite, wolframite, pyrite, gold, yellow monazite, ilmenite, garnet, barite, zircon, rutile, anatase, and less commonly, cerussite and pyromorphite. Gray monazite is found 20 and 50 km downstream from source rocks in two areas.

A geologic map of southern Quebec, Canada, showed Devonian and older sedimentary rocks intruded by Devonian and Cretaceous granite and mafic rocks at the head of the St. Lawrence Seaway (Laurin, 1969). This terrane could be the source of alluvial concentrates that contain dark monazite (A. Parfenoff, written commun., 1977). In southern Bolivia, lower Paleozoic sedimentary rocks and Mesozoic intrusive rocks were indicated by Ahlfeld and Branisa (1960). In southeastern Peru, Paleozoic sedimentary rocks including shales and siltstones are intruded by Jurassic to Cretaceous calc-alkaline stocks in the headwaters of Rio Huari Huari (Instituto de Geología y Minería, 1975). Panned concentrates containing considerable gray monazite were collected from Spanish gold placers near Communidad, about 150 km NNE. of Lago Titicaca; and abundant weathered pyrite accompanied the monazite pellets. Northern Peru is mostly covered by alluvium of the Amazon Basin. However, the major tributaries crossing this area derive their sediments from southern Ecuador, where the terrane includes Paleozoic to Quaternary sedimentary rocks intruded by Mesozoic granitic porphyries (Ballén, 1969).

MINERALOGY

PHYSICAL PROPERTIES

Typical detrital grains of Eu-rich dark monazite from Alaska are small dark pellets with a distinctive matte surface (fig. 18). They appear identical to alluvial dark monazite else where in the world. Terms like "nodules," "oolites," "pellets," and "small flat lentils," and adjectives including "rounded," "oval," "ellipsoidal," and "discoidal" have been used to describe the form. Because differences in size and internal structures among the grains transcend the terms "oolite," and "pellet" (Gary and others, 1972, p. 484, 524), the terms used in this report are ones required by internal as well as external features. The physical properties of Alaskan dark monazite are listed in table 2, where the properties are compared with those for detrital grains of dark monazite from other areas as well as with the properties of yellow monazite.

COLOR

The color of Alaskan dark monazite is generally dark gray inclining to black, but medium- to light-gray and buff-gray varieties are noted. The lighter toned grains are translucent to opaque; the dark grains are uniformly opaque. Although the luster is generally dull to subresinous, that of micropitted surfaces tends toward silky and pearly in some grains. The mineral crushes easily to a light-gray powder. Crushed grains in refractive-index liquids are opaque in the thick centers, but the thinner edges are transparent enough to yield optical data. The color of dark monazite is clearly due to numerous, mainly submicrometer-sized inclusions of two types. One is amorphous carbon; the other is a transparent microacicular and columnar mineral distributed randomly as a fine sagenitic mesh and tentatively identified as rutile. In addition, slightly larger occasional grains of opaline silica, apatite and (or) tourmaline, micas, and epidote (?) were noted. The darker grains apparently contain greater amounts of carbon, and the lighter toned grains are translucent due to the scatter of light by the sagenitic mesh of rutile.

Vaquero (1979, p. 378) attributed gray tones to different amounts of powdery graphite; and brown, reddish, and yellowish tones were due to oxidation of inclusions of iron-bearing minerals or to the presence of abundant rutile.

Overstreet, Warr, and White (1971, p. 18, 29–33) summarized the findings of others on the black pigment of dark monazite from Taiwan and cited numerous inclusions of ilmenite(?), rutile(?), leucoxene, quartz, microcrystalline quartz, dustlike alteration products(?), limonite or goethite, epidote(?), opaque products of weathering(?), greigite(?), and amorphous carbon (0.23 percent). Also, for Taiwanese material, Matzko and Overstreet (1977, p. 12) cited the microcrystalline character of the monazite as a possible cause of the dark color.

In other occurrences of dark monazite, Ellsworth (1932, p. 22–23) found the color of a black monazite from pegmatite in Canada was due to carbon and estimated no more than a few hundredths of a percent. Also, Iimori (1941, p. 1052) indicated that on heating dark monazite from a Korean gold placer to 800°C for a long period, the color disappeared and the residue turned reddish. This result points to carbon as the major coloring agent, but Iimori suggested the black color may be due to the composition of the rare earths. Recent analyses of this black monazite from Iimori's collection indeed showed that it contained 0.20 percent carbon (analyst: T. G. Ging, U.S. Geological Survey). An association of carbonaceous material with monazite in a metasedimentary sequence is cited by Huebschman (1973). Dark, slightly metamorphosed siltstone in rocks of the Precambrian Belt Supergroup of Idaho, Montana, and British Columbia is colored by amorphous carbon and clusters of minute monazite grains. No mention is made of the color of the monazite, but the significance of the available carbon to an origin of the dark color seems obvious.

To confirm the occurrence of carbon in Eu-rich dark monazite, samples from Alaska, Taiwan, and Zaire were heated 3 hours at 1000°C in a muffle furnace. In each sample the dark color in the outer parts vanished and was replaced by white to light-gray or buff to pink tints. A few grains of Alaskan monazite still retained gray cores, indicating incomplete oxidation over the relatively short period of the experiment. Samples of dark monazite from Alaska submitted for carbon and hydrogen analyses gave positive results for carbon, which are presented in the section, "Chemical composition."

A small number of the dark monazite grains in Alaskan stream concentrates are subangular and mottled gray to brownish gray. These also have low Th and high Eu contents, but their relation to the dark pelletal monazite is not clear. Possibly they represent an intermediate variety between dark and yellow monazite.

FORM

The form of dark monazite from Alaska is characteristically ovoid to ellipsoidal, and most grains appear to have been flattened to a lesser or greater degree (fig. 18). In many Alaskan concentrates it is difficult to find

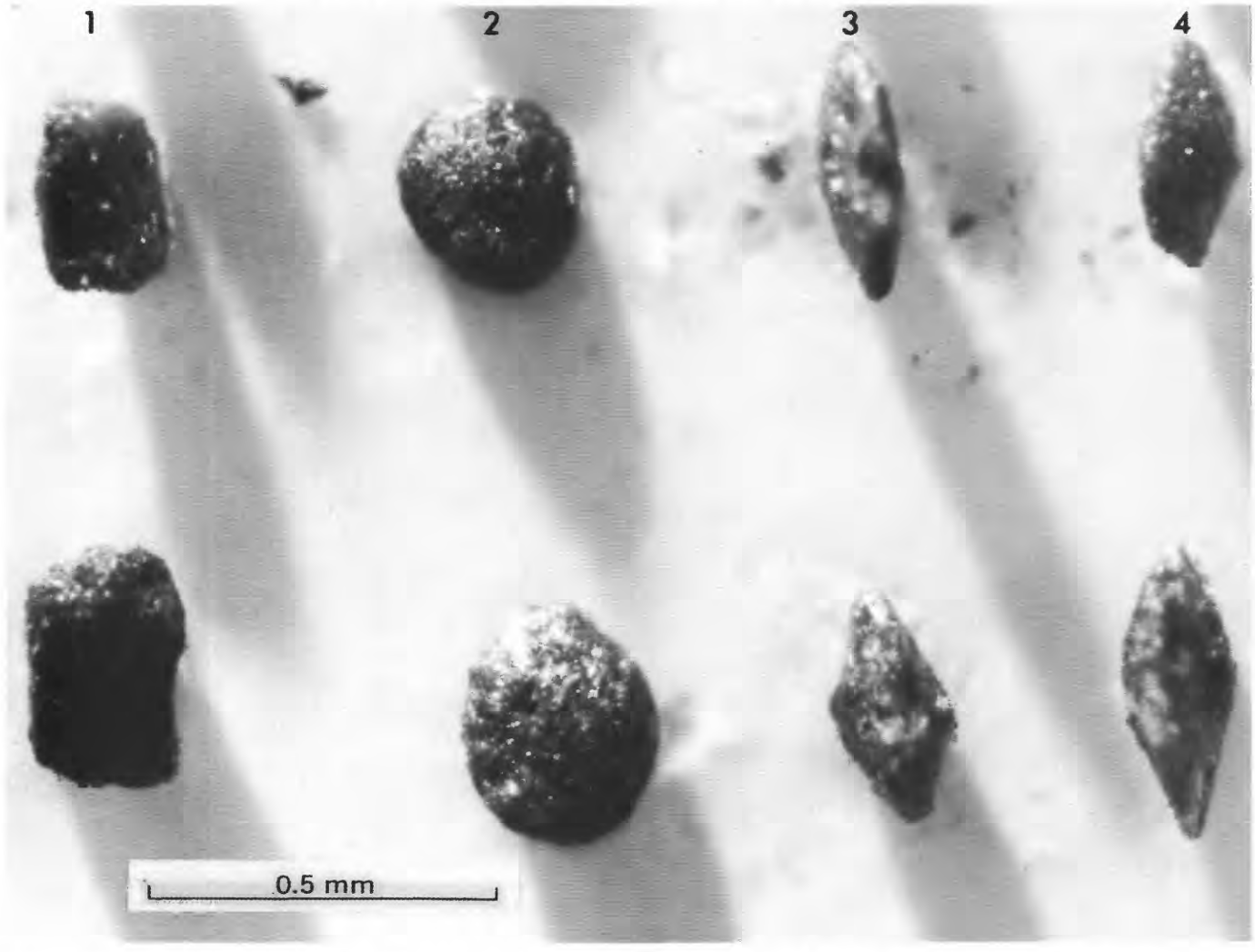

FIGURE 18.—Eu-rich dark monazite from Alaska. Typical grains are shown lying flat (col. 2) and on end (cols. 3 and 4). Rectangular grains (col. 1) are rare. Grains in columns 3 and 4 show micaceous flanges.

grains that do not have girdles or dogtooth projections of sericite and chlorite in the plane of the two greater axes. How well the pellets of dark monazite may be enclosed in micaceous selvages is shown in figure 19. These grains and those in figure 18 are from the same concentrate. A number of dark grains in figure 19 are irregular in shape, and these are interpreted to be neonucleated monazite that could not have traveled far from the source terrane. Figure 20 shows how grains of dark monazite are released from a phyllitic host rock to yield grains of typical form.

Crushed grains of Alaskan dark monazite are mainly monocrystals, but a number of fragments larger than 20 μm (micrometers) proved to be aggregates of microcrystals, or to have a cryptocrystalline aspect whereby extinction positions between crossed polarizers migrated from place to place within a grain as the microscope stage was rotated. More than half of all grains examined showed a monocrystalline aspect; perhaps one-fourth consisted of microcrystalline or cryptocrystalline aggregates. Elsewhere similar internal structures have been reported. In France, dark monazite grains show one of the following internal structures (Donnot and others, 1973, p. 12):

1. A monocrystal indented toward the center and surrounded by an irregular microcrystalline border.
2. A radial mosaic structure, with or without a microcrystalline border.
3. A polycrystalline structure with random orientation of the grains.

In Spain, a microscopic study of nodular monazite showed internal radial-fibrous structure or spherulitic texture with a central monocrystal surrounded by an irregular polycrystalline corona (Vaquero, 1979, p. 378).

Dark monazite grains from Taiwan contain two generations of monazite, the earlier forming larger particles

TABLE 2.—*Properties of dark monazite*

[Data for Alaska, Montana, Taiwan, Zaire, this report; for France, Donnot and others (1973); for U.S.S.R., Zemel' (1936), Fadeev (1959), Vinogradov and others (1960), Kosterin and others (1962), Izrailev and Soloveva (1974); for yellow monazite, Deer and others (1966), Winchell and Winchell (1951). Number in parentheses, number of samples tested. Size in millimeters; D, density; H, hardness; (Av), average; L, length; W, width; leaders (—), no measurement]

	Color	Form	Cleavage	Size			D		H	Optical		
				Av	L	W	Av	Range		N	N	(+)2V
Alaska	Black, dark to light gray.	Pelletal, some mica flanges.	1 good, fair, 1 poor.	0.3 0.	0.1-1.0	0.1-0.8	4.52 (10)	4.27-4.72	3.5	1.780	1.840	Small
Montana	Gray to black	Pelletal	1 good, 1 fair,	.4	0.2-0.7	0.1-0.5	4.35 (1)	—	3.5	1.780	1.840	Do.
Taiwan	Black to dark and light gray,	Pelletal, some mica flanges.	1 good, 1 fair, 1 poor.	.25	0.1-0.5	0.08-0.3	4.20 (3)	4.13-4.26	3.5	1.780	1.840	Do.
Zaire	Dark to light gray.	Pelletal, oolitic, some light rinds.	1 perfect, 1 good, 1 fair.	1.0	0.3-2.0	0.2-1.3	4.71 (5)	4.62-4.79	4	1.780	1.840	Do.
France	Gray	Nodular, oolitic, polycrystalline aggregates.	Imperfect	0.5-1.0	0.1-1.8	—	4.65 (5)	—	5	1.768+	1.83+	Do.
U.S.S.R	Gray to black	Rounded oolitic	(100) perfect.	.5+	—	—	4.43 (3)	4.3-4.7	4.5-5.5	1.79	1.83	Small (<20°)
Yellow Monazite.	Yellow to brown and green.	Tabular or equant to rounded.	(001) perfect, (100) distinct.	[1].2	—	—	5.15 (--)	5.0-5.3	5.0-5.5	1.790	1.844	6°-19°

and the later forming the matrix (Matzko and Overstreet, 1977, p. 7). The larger particles are about 20 μm in size in some pellets, but others are composed principally of particles 2 or 3 μm in size. No nucleus has been recognized in any of the grains. For dark monazite from the northern Verkhoyan'e Range in northeastern Siberia, Vinogradov, Arskiy, and Mikhailova (1960, p. 21) and Fadeev (1959, p. 55) indicated that the grains are fine-grained aggregates of different minerals, for the greater part undefinable.

Elsewhere the forms of dark monazite are similar to the characteristic shapes found in Alaska. The ranges of shapes, sizes, and tones of gray for dark monazite from Montana (fig. 21) are duplicated by dark monazite from Bretagne, France (Guigues and Devismes, 1969, p. 115, pl. 7); and illustrations published by Kosterin, Alekhina, and Kizura (1962, p. 24), Li and Grebennikova (1962, p. 156), and Donnot and others (1973, p. 12) show the same type of material. A number of scanning electron micrographs of the surface features of black monazite from Taiwan are presented by Matzko and Overstreet (1977, pl. I, IV, V and VI). Dark monazite grains from the Kivu district in eastern Zaire differ in part from dark monazite worldwide by having a considerable proportion of light-colored rinds (possibly due to weathering or hydrothermal alteration); and by showing grains almost concentrically overgrown by dark monazite, both generations showing light-colored rinds (fig. 22). X-ray diffraction patterns of the light-colored material from three of the five samples from Zaire showed almost identical features as in X-ray diffraction patterns for corresponding dark-colored grains.

Scanning electron micrographs of dark monazite (figs. 23–25) show the nature of the surface of different grains, and the inclusions at the surface. The flaky appearance may be due to cleavages, but the micropitting is probably due to weathering and plucking of inclusions of various sizes. All inclusions and dustlike material adhering to the surface represent minerals of the metasedimentary host rocks.

CLEAVAGE

Broken or crushed grains of dark monazite from Alaska generally show a good cleavage at high angle to the longest axis of the flattened ellipsoidal form. Less commonly a good cleavage parallel to the flat form is noted in dark monazite grains from Zaire. These cleavages have not been related to crystallographic directions with any degree of confidence. Crushed grains in refractive-index liquids generally lie on the best cleavage (001 plane, according to Winchell and Winchell (1951, p. 184), and Tröger (1952, p. 33)), and two less

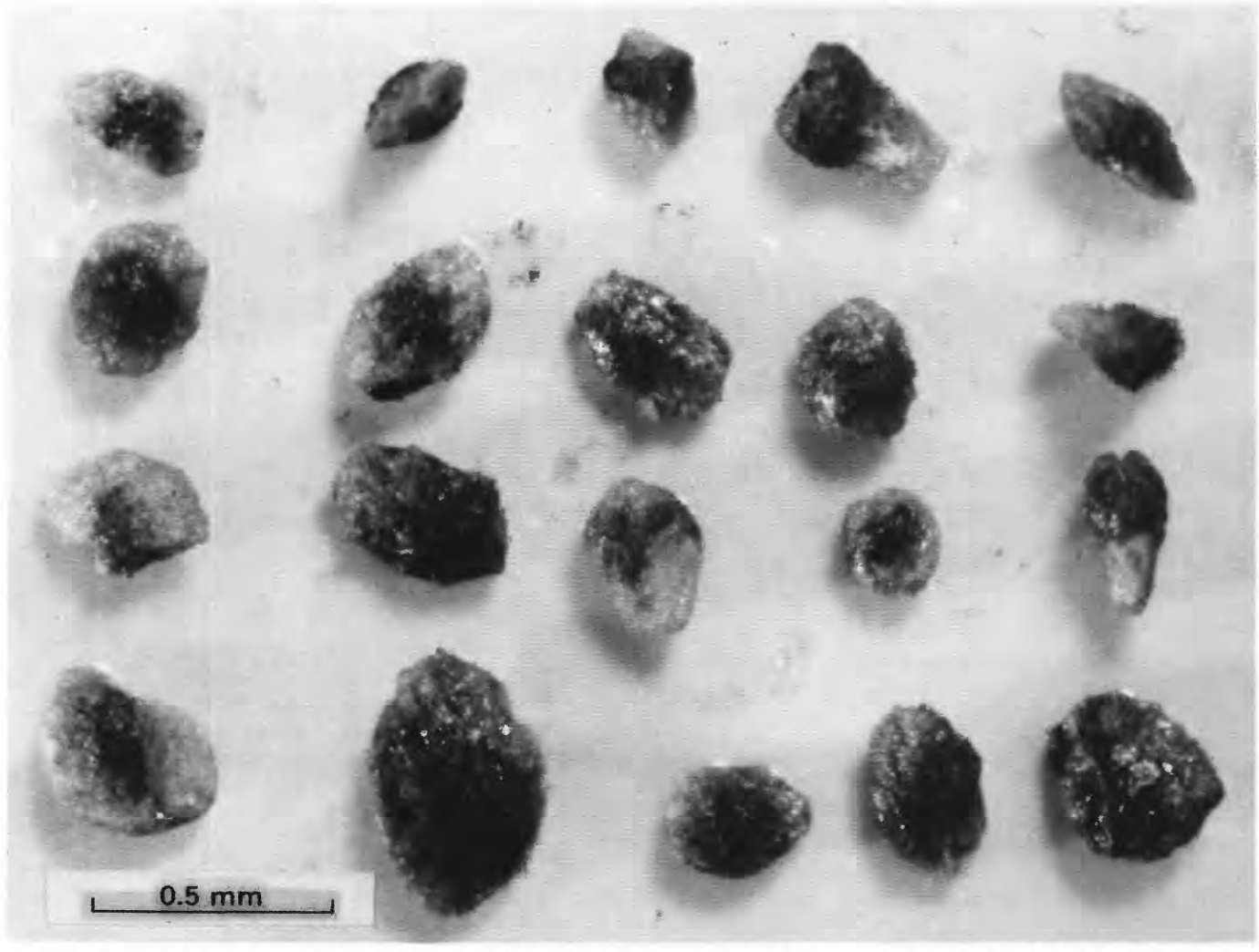

FIGURE 19.—Dark monazite grains from Alaska, showing flanges and tapered forms of attached sericite and (or) chlorite.

FIGURE 20.—Series of dark monazite grains from a single placer concentrate from western Alaska showing gradual release of grains from the phyllitic matrix.

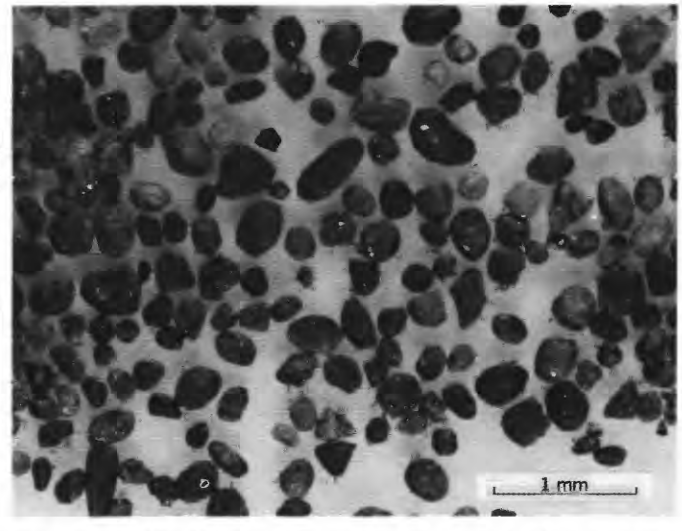

FIGURE 21.—Handpicked concentrate of Eu-rich dark monazite grains from Montana. Note range of tones from light to dark gray and diverse forms and sizes.

FIGURE 22.—Eu-rich dark monazite from Zaire. Note light-colored rinds over dark cores in broken grains, left center, and almost-concentric grains within grains, right side.

perfect cleavages tend to produce rectangular and square forms (fig. 26).

SIZE

The average size and the ranges in length and width are given in table 2 for dark monazite from Alaska and elsewhere. Despite an apparent close proximity of most of the alluvial concentrates to the source rocks, the average size of Alaskan dark monazite is near the lower end of the range of sizes reported in the literature. The average size of dark monazite in five samples from Zaire is 1 mm, but Magnée (1958, p. 471) reported the diameter reached 7 mm. At two places in the U.S.S.R., the sizes of dark monazite were reported as 0.25–0.5 mm (Kosterin and others, 1962, p. 23) and 1–1.5 mm (Zemel', 1936, p. 1969). In Spain, most grains were between 0.5 and 1 mm, but the extended range was 0.125 to 4.5 mm.

DENSITY

The density of Alaskan dark monazite grains was determined on a Berman balance using 8–35 mg of handpicked grains from 10 concentrates. Ten determinations were done for one sample from Montana, and the average of the 10 weighings is given in table 2. Six weighings of dark monazite in a sample from Bretagne, France, yielded an average considerably less than that reported by Donnot and others (1973). Density data are also shown in figure 27; obviously, this property shows a range even within one region.

As Taiwanese dark monazite was within the density range of Clerici solution at room temperature, the three samples from Taiwan were tested in this solution to learn the reaction of individual grains. Solutions that held grains in suspension were checked on a refractometer and found to range in density from 4.10 to 4.50, according to a refractive index vs. density calibration curve (Rosenblum, 1974a, p. 479).

The density of nodular monazite in Spain is reported to be 4.648 (Vaquero, 1979, p. 376).

HARDNESS

The hardness was estimated by attempting to scratch cleavage fragments of calcite (H=3.0) and fluorite (H=4.0) with grains of dark monazite. Grain fragments were carefully rubbed across the cleavage surfaces by moving the grains under a bit of cork held by tweezers. Most of the dark monazite failed to scratch fluorite, but samples from Zaire were just able to do so.

MAGNETIC SUSCEPTIBILITY

The magnetic susceptibility of dark monazite generally is identical to that of yellow monazite, and the best extraction range on the Frantz magnetic separator[1] at 15° side tilt is 0.7–0.8 A (amperes). However, some concentrates from Alaska, as well as elsewhere, had dark monazite grains that were recovered in the 0.8–1.2 A

[1]Use of brand or manufacturers' names in this report is for descriptive purposes only and does not constitute endorsement by the U.S. Geological Survey.

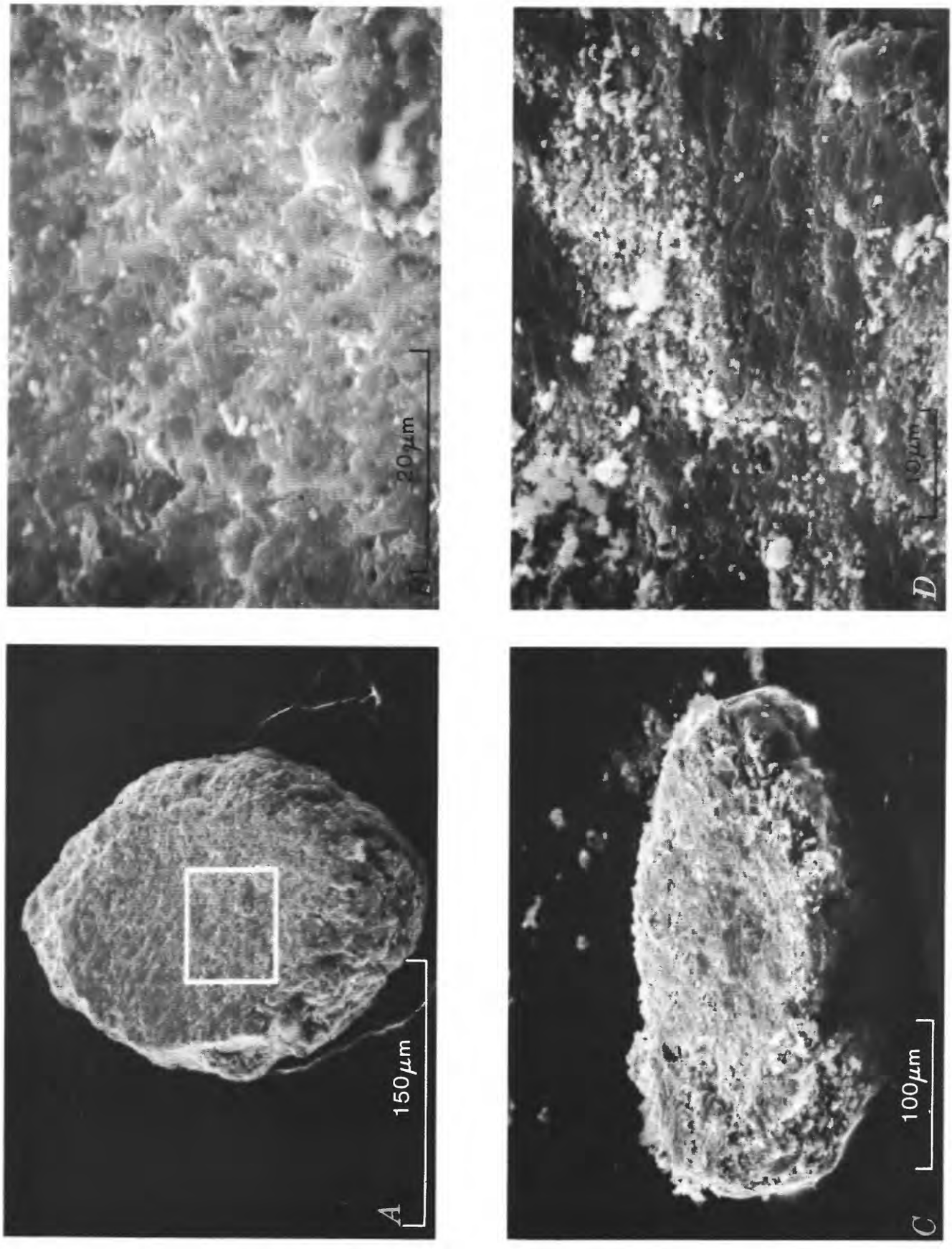

FIGURE 23.—Scanning electron micrographs of dark monazite grains. *A*, *B*, one grain from Alaska; *C*, *D*, grain from Montana. Note flaky surfaces at greater magnification (*B*, *D*). Box in *A*, area of *B*. *D* is enlargement of part of *C*.

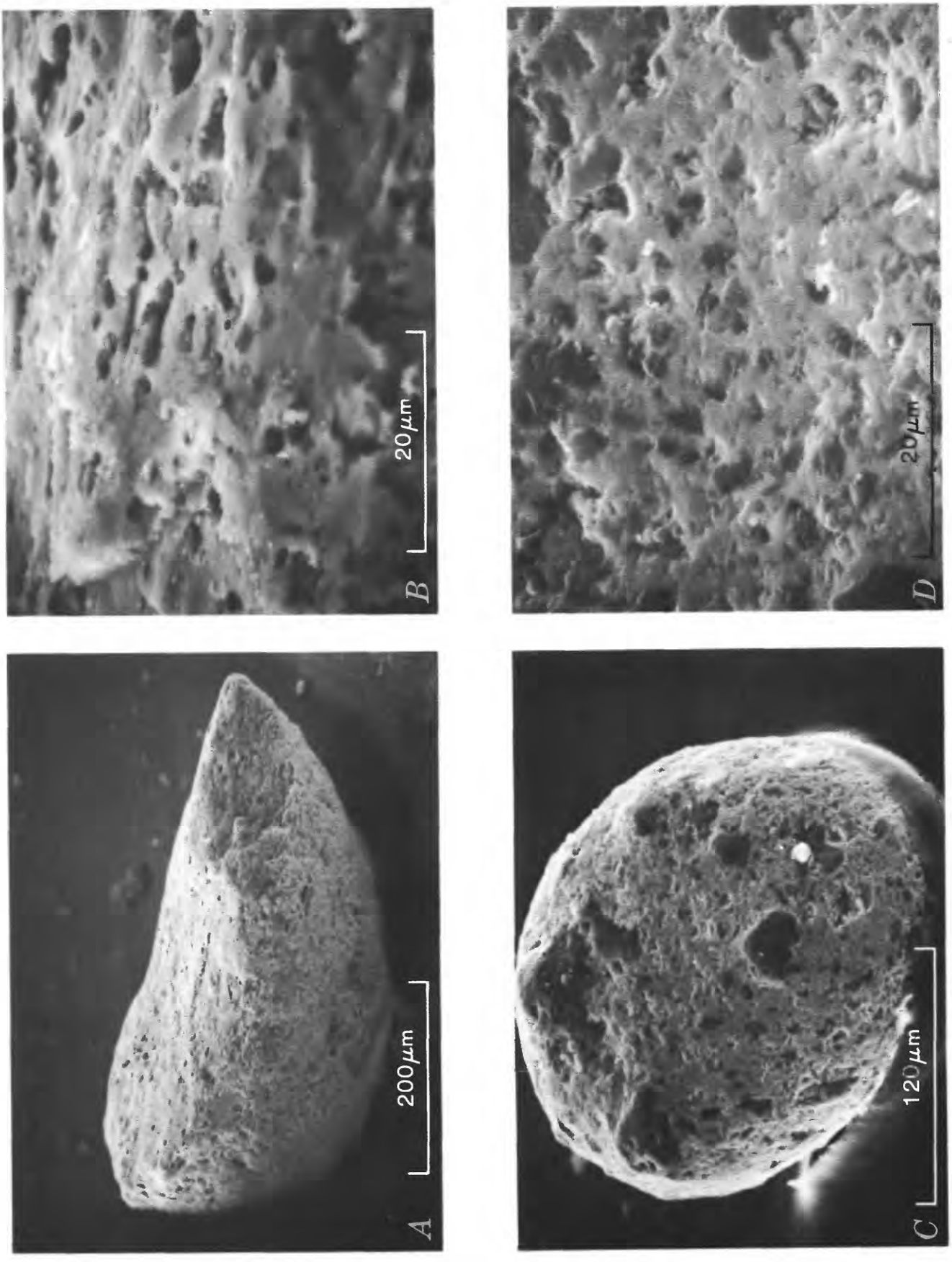

FIGURE 24.—Scanning electron micrographs of dark monazite. *A*, *B*, grain from Zaire; *C*, *D*, grain from Taiwan. Note porous surfaces at greater magnification (*B*, *D*). Dark areas in *C* and *D* are silica inclusions.

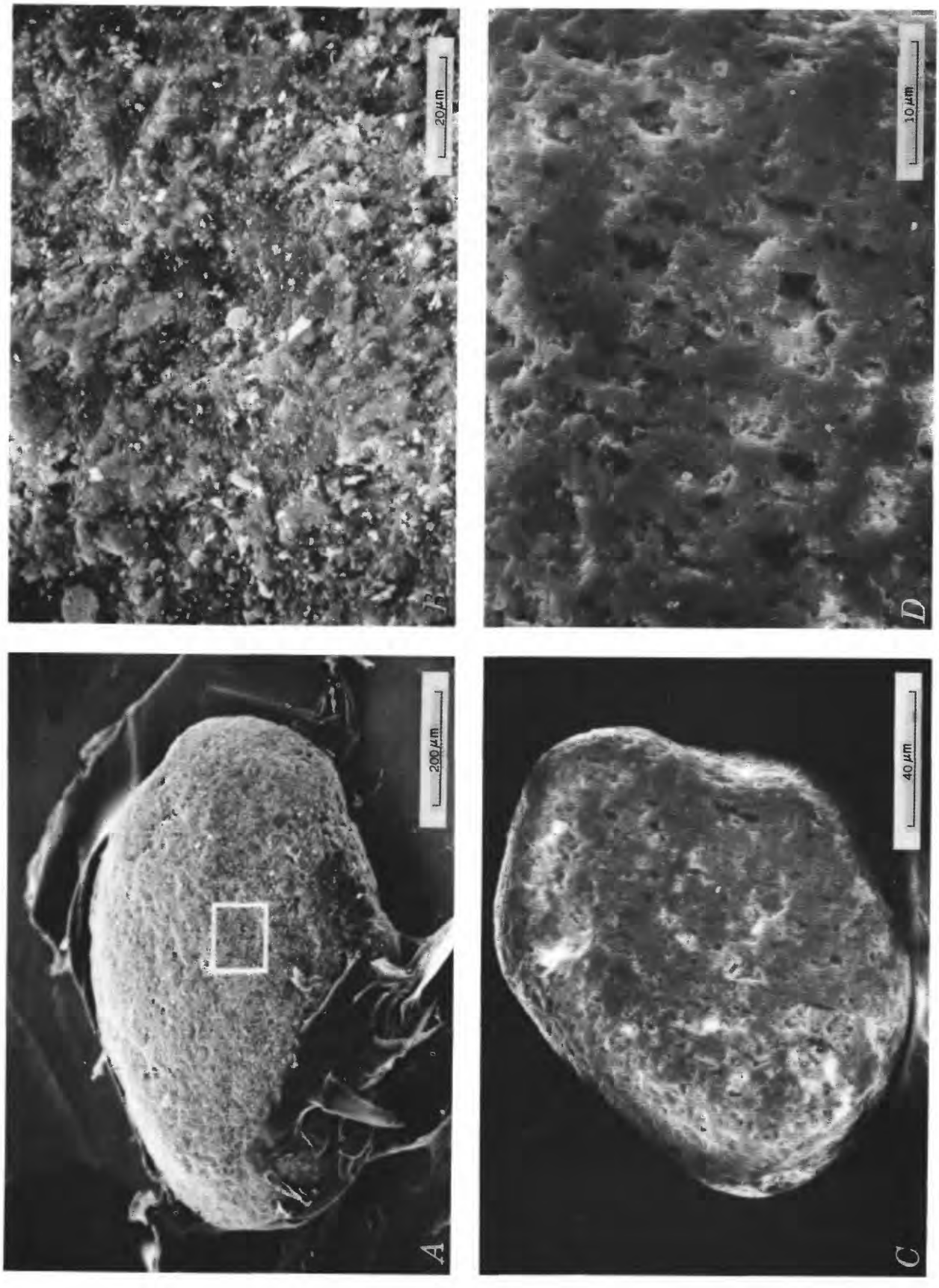

FIGURE 25.—Scanning electron micrographs of dark monazite. *A*, *B*, grain from France; *C*, *D*, grain from Bangladesh. Dusty material in *B* includes Fe-chlorite and sericite; dark areas, silica inclusions. Box in *A*, area of *B*.

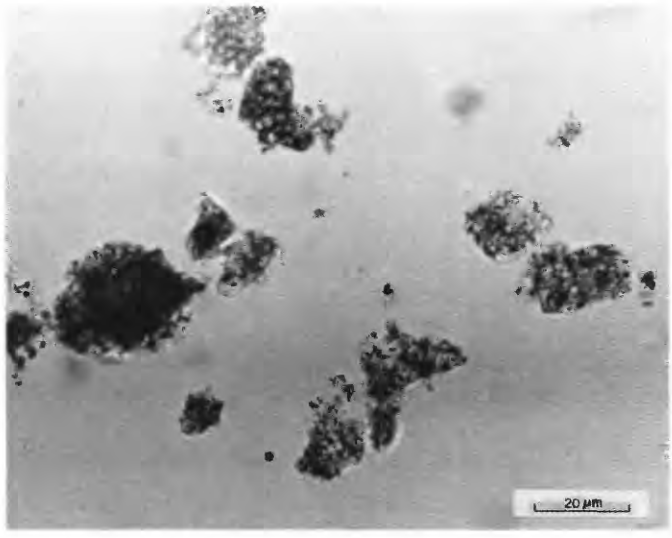

FIGURE 26.—Photomicrograph of Eu-rich dark monazite showing turbidity due to numerous submicrometer-sized inclusions. Crushed grain is mounted in liquid with 1.73 refractive index; many fragments lie on the best cleavage (001) and yield off-center Bxa figures.

range; and these appeared otherwise to be similar to those in the 0.7–0.8 A range. A roughly inverse relation was noted between the abundances of dark and of yellow monazite in these separations—where dark monazite is abundant, yellow monazite is scarce or absent. Other minerals that are common in Alaskan dark monazite fractions made by magnetic separator include ilmenite-leucoxene, almandine, colored zircon, chromite, pyrite, gold, epidote, and materials that resemble dark monazite: hematite, rutile, and rounded fine-grained sedimentary rock fragments. The magnetic susceptibility of yellow monazite has been shown to vary systematically with the chemical composition and may be related to the paramagnetism of the rare-earth elements (Mertie, 1953, p. 5). The most magnetic grains contain the least lanthanum and cerium and the most neodymium, samarium, and yttrium (Richartz, 1961, p. 54–56).

RADIOACTIVITY

The net radioactivity of dark monazite from Alaska, Taiwan, and Zaire measured on a scaler alpha-counter, is generally one to three times the background count.

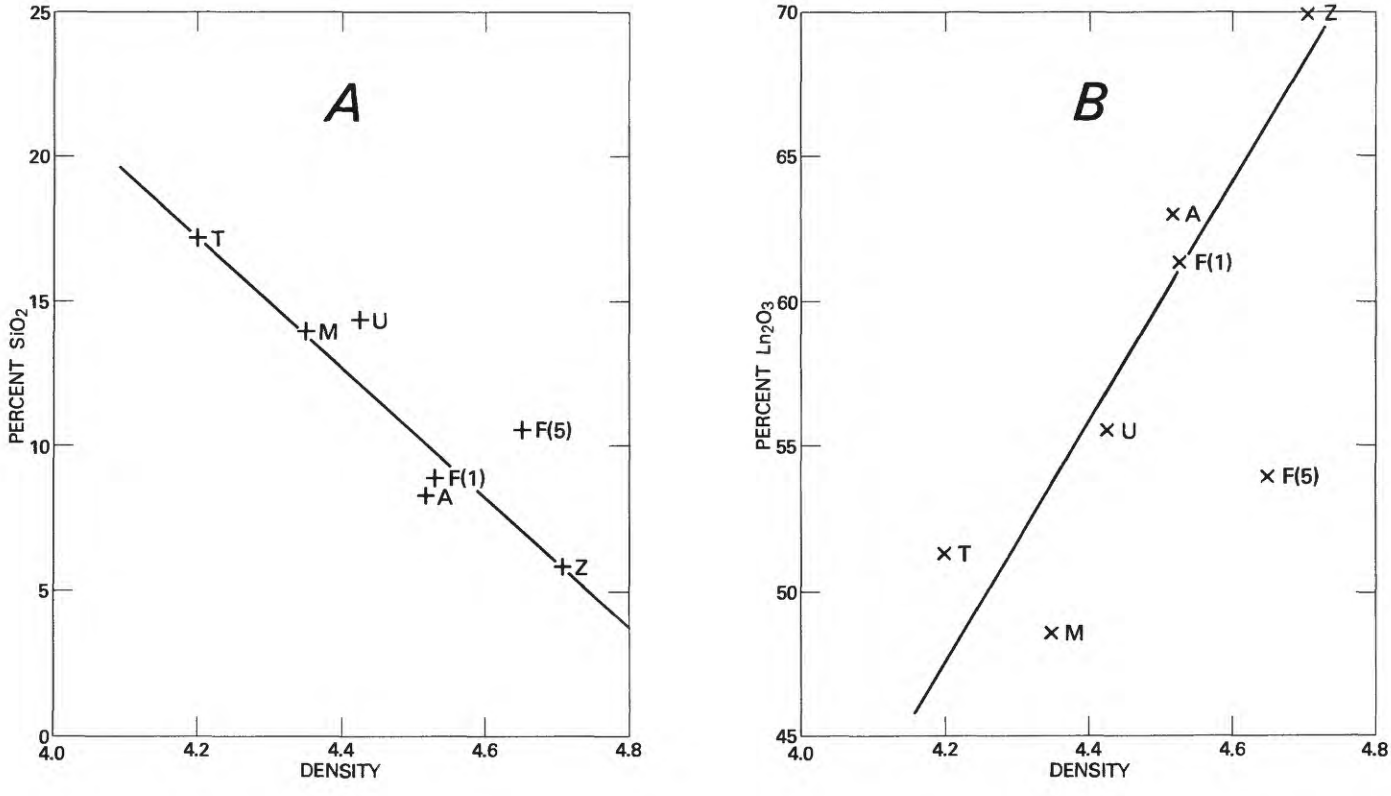

FIGURE 27.—Density of dark monazite versus *A*, percent SiO_2, and *B*, percent Ln_2O_3 (ΣLa_2O_3 to Gd_2O_3). Data from tables 2, 7, and 8. A, Alaska (11); T, Taiwan (4); Z, Zaire (5); U, U.S.S.R. (2); M, Montana (1); F, France (5) from the literature, and (1) from this report. Numbers in parentheses indicate the number of samples for each area.

This compares with the radioactivity of yellow monazite containing 6.4–8.4 percent ThO_2, which ranges from 12 to 17 times the background count. Following is a summary of the results determined from calibration curves drawn from analyzed samples:

Locality and Field No.		Radioactivity net counts per 10 minutes	ThO_2 (in percent) Equivalent ThO_2	Analyzed ThO_2
		Dark monazite		
Alaska	56	87	2.90	3.2
	2411	25	.84	.79
	2418	36	1.20	.82
Taiwan	RO-4B	13	.44	.58
	RO-4C	6	.21	.59
	RO-4D	10	.34	.58
Zaire	A58/50	9	.31	1.0
	A70/50	19	.66	.85
	A121/51	17	.58	.75
	A122/51	10	.34	.68
	D1C/71	21	.71	.65
		Yellow monazite		
Liberia	RO-142E	183	6.0	6.4
	RO-217G	248	8.1	8.4

From these data it seems that detection by radioactivity of any deposit with less than 100 percent dark monazite would not be feasible.

OPTICAL PROPERTIES

Refractive indices of dark monazite from Alaska, Montana, Taiwan, and Zaire were determined in white light using the technique of Emmons and Gates (1948, p. 615). The results were remarkably similar among themselves and similar to those reported for French and Siberian dark monazite, despite the confusion of false Becke lines due to the numerous micro-inclusions and the diverse orientations of monazite aggregates. The optic axial angle (2V) was estimated by comparison with the 2V obtained directly for a yellow monazite using a spindle stage according to the technique of Wilcox (1959). The interference figure for dark monazite is always too diffuse to permit determining the 2V directly, as can be done for yellow monazite, but most grains show estimated positive angles from slightly larger than 0° to about 10°. In most grains, the acute bisectrix (Bxa) was near the edge of the microscope field. This accords well with the interpretation that these grains rest on the 001 cleavage, for the Bxa (Z) lies about 8°–11° from the pole to this plane (Tröger, 1952, p. 35). Thin multiple twinning parallel to (100) was seen in only one dark monazite grain from Montana.

X-RAY DATA

X-ray diffraction patterns for dark monazite from Alaska and elsewhere are similar to those for yellow monazite (table 3). Differences in chemical composition between the two types of monazite that could yield recognizable differences in the X-ray patterns are apparently too small to do so. Peaks for chlorite and sericite on the diffractograms have appeared where these minerals coat the grains examined, and a few peaks were attributed to quartz and rutile. However, decrease of Th from about 7 percent in yellow monazite

TABLE 3.—*X-ray data for dark monazite and yellow monazite*

[dnm^{-1}, interplanar spacing in 0.1 nanometer; I, relative intensity, 10 strongest]

Dark monazite				Yellow monazite	
Reference--	This report	This report		Molloy (1959)[2]	This report[3]
Area-------	Alaska	Ex-Alaska[1]			
Samples----	9	9		10	11
	dnm^{-1}	(I)	dnm^{-1} (I)	dnm^{-1} (I)	dnm^{-1} (I)
	5.21		5.20	5.22	5.22
				5.17	
	4.82		4.81	4.81	4.82
	4.69		4.68	4.68	4.69
	4.19		4.18	4.18	4.18
	4.11		4.09	4.10	4.11
				3.85	
				3.53	
	3.51		3.51	3.51	3.51
				3.46	
	3.31	(8)	3.30 (8)	3.29 (7)	3.30 (6)
				3.13	
	3.10	(10)	3.10 (10)	3.08 (10)	3.10 (10)
	2.99		2.98	2.98	2.99
	2.87	(6)	2.87 (6)	2.87 (5)	2.88 (5)
				2.82	
				2.79	
				2.71	
				2.67	
	2.60		2.60	2.61	2.61
				2.58	
	2.45		2.44	2.44	2.45
				2.41	2.41
	2.19		2.19	2.17	2.19
			2.149		2.149
	2.145		2.140		
	2.130		2.132	2.13	2.130
				2.11	
				2.09	
				1.98	
	1.969		1.969	1.97	1.971
				1.95	1.964
			1.900	1.91	1.899
	1.876		1.876	1.88	1.872
	1.866		1.869	1.86	1.863
				1.80	1.802
	1.765		1.762	1.77	1.766
	1.742			1.75	1.743
			1.738	1.73	
				1.72	
	1.695		1.693	1.69	1.695
				1.65	
				1.61	
					1.607
			1.598	1.59	
	1.542		1.541	1.55	
	1.538				1.537
	1.535		1.532		

[1] Ex-Alaskan samples include: Taiwan, 2; Zaire, 2; E. Siberia, 1; and Montana, 4.

[2] Molloy's samples are from United States, 7; Norway, 1; Brazil, 1; and U.S.S.R., 1.

[3] Yellow monazites include: Liberia, 7; South Africa, 1; U.S.S.R., 1; and United States, 2.

to less than 1 percent in dark monazite and increase of Eu to about 0.2–0.7 percent in dark monazite did not appear as recognizable features.

In table 3 the X-ray diffraction data of nine samples of dark monazite from Alaska are averaged for comparison with the average of nine other samples of dark monazite from locations outside Alaska, including eight analyzed in this investigation and one analysis from the literature. These values of dark monazite are compared with the average for 10 yellow monazites reported by Molloy (1959, p. 514–515), and the average for 11 yellow monazites compiled for this paper. In table 4 the cell dimensions and volumes are computed for four dark monazites and are compared with those for five yellow monazites. The mineral is monoclinic, and the average angle β computed for dark monazite is 103°2.863′; the average for yellow monazite is 103°38.183′. The averages and standard deviations indicate overlap of values between the two sets, and like the data on d-spacings, support the contention of similarity of X-ray patterns for the two varieties of monazite. Factor analysis and analysis of variance have not been done for these data. These statistical techniques might reveal subtle differences in X-ray patterns that the present examination has missed.

TABLE 4.—*Cell parameters for dark monazite and yellow monazite*

[a, b, c, crystal axes; nm^{-1}, 0.1 nanometer; Vol., cell volume]

Sample No. (area)	a(nm^{-1})	b(nm^{-1})	c(nm^{-1})	Vol.(nm^{-1})^3
Dark monazite				
2417---------- (Alaska)	6.794	7.016	6.469	299.8
2418A---------- (Alaska)	6.808	7.025	6.478	301.1
RO-4C---------- (Taiwan)	6.780	7.009	6.461	298.4
DIC/71---------- (Zaire)	6.796	7.013	6.506	301.8
Average------	6.795	7.016	6.479	300.3
s[1]----------	.011	.007	.020	1.5
Yellow monazite				
Magnet Cove[2]--- (Arkansas)	6.816	6.991	6.444	298.0
2418D---------- (Alaska)	6.796	7.012	6.476	299.9
1[2]---------- (Taiwan)	6.735	7.006	6.474	296.9
RO-148A---------- (Liberia)	6.808	7.023	6.490	301.6
RO-217G---------- (Liberia)	6.781	7.012	6.517	301.4
Average-----	6.787	7.009	6.480	299.6
s----------	.032	.012	.027	2.1

[1]Standard deviation.

[2]Cell parameters computed from data of Matzko and Overstreet, 1977, p. 24.

CHEMICAL COMPOSITION

The sparsity of dark monazite in the concentrates from Alaska and Montana necessitated that special methods of spectrochemical analysis be developed to meet the small sizes of the handpicked samples: they weighed from 10 to 100 mg. Larger samples were available for analysis from Taiwan and Zaire, but the controlling factor for the analytical work was the weight of the material from Alaska and Montana. Of 64 concentrates from Alaska that contained dark monazite, only 11 yielded enough material for analysis. Of 12 concentrates from Montana with dark monazite, only 1 had sufficient grains that could be handpicked from the appropriate magnetic fraction of the heavy minerals.

ANALYTICAL PROCEDURES

The main method of analysis was spectrochemical, but instrumental neutron activation analysis was employed on several samples as a check on the spectrographic procedure. Water was determined by the loss-on-ignition method. Because carbon had been detected by simple optical and chemical tests of a qualitative character, a quantitative test for carbon in six samples was made by a commercial laboratory.

SPECTROGRAPHIC ANALYSIS

The dark monazite samples were analyzed by optical emission spectroscopy using a Jarrell-Ash 3.4 m Ebert-mounted spectrograph. The oxides determined are shown in table 5, and include oxides of the first seven

TABLE 5.—*Wavelengths of elements and concentrations of standard compounds used for analysis, in percent*

Oxides	Wavelength (nm)	Analyzed standard 1	2	3	4	5
[1]La_2O_3------	289.31	8.8	13.5	16.7	18.7	14.6
[1]Ce_2O_3------	283.09	14.7	22.5	27.9	31.2	24.4
Pr_2O_3-------	316.82	2.9	1.7	.87	.35	6.8
Nd_2O_3-------	325.92	10.0	6.0	3.0	.36	15.0
Sm_2O_3-------	315.25	2.0	1.2	.60	.24	5.0
Eu_2O_3-------	290.67	1.0	.6	.30	.12	---
Gd_2O_3-------	280.97	1.0	.6	.30	.12	---
Y_2O_3--------	320.03	1.0	.6	.30	.12	---
[1]P_2O_5-------	255.49	12.2	18.5	23.1	25.9	20.4
ThO_2--------	277.08	8.0	4.8	2.40	0.96	---
SiO_2--------	298.76	15.0	9.0	4.5	1.8	---
TiO_2--------	288.41	3.0	1.8	.90	.36	---
Al_2O_3-------	266.04	5.0	3.0	1.50	.60	---
Fe_2O_3-------	295.73	5.0	3.0	1.50	.60	---
CaO---------	315.89	1.0	.6	.30	.12	---
MgO---------	277.98	1.0	.6	.30	.12	---

[1]Calculated from the matrix material. Sc - 298.07 nm line used for internal standard.

[2]Leaders (---), not reported.

naturally occurring elements of the lanthanide series, the most abundant group of REE in dark monazite, plus Y.

The lanthanide series consists of 15 elements.

Atomic No. (Z)	Name and symbol	Remarks
57	Lanthanum (La)------	Major in monazite.
58	Cerium (Ce)---------	Do.
59	Praseodymium (Pr)---	Do.
60	Neodymium (Nd)------	Do.
61	Promethium (Pm)-----	Artificial.
62	Samarium (Sm)-------	Abundant in monazite.
63	Europium (Eu)-------	Minor in monazite.
64	Gadolinium (Gd)-----	Abundant in monazite.
65	Terbium (Tb)--------	Minor to absent in monazite.
66	Dysprosium (Dy)-----	Do.
67	Holmium (Ho)--------	Do.
68	Erbium (Er)---------	Do.
69	Thulium (Tm)--------	Do.
70	Ytterbium (Yt)------	Do.
71	Lutetium (Lu)-------	Do.

In monazite, elements 65 through 71 (Tb to Lu) generally comprise less than 1 percent of the REE content. See further discussion of the lanthanides in section, "Geochemistry."

A series of standards were made by mixing spectrographically pure compounds of interest in a matrix (35 percent CeO_2, 20 percent La_2O_3, and 45 percent $NH_4H_2PO_4$) to cover concentration ranges expected to occur in Eu-rich dark monazite.

Due to the sparsity of the mineral in the original stream-sediment concentrates, 10–15 mg of the mineral per concentrate were handpicked for analysis from concentrates with sufficient dark monazite. The samples were ground to a fine powder and mixed 1:4 with graphite containing 1 percent Sc_2O_3 as an internal standard. Three to five ASTM S-13 type electrodes were charged with 15 mg of the above mixture for replicate analyses. The samples were burned to completion during a 70-second exposure, using a 13-A D-C arc discharge. A 15-percent-transmission quartz filter was placed in the optical path. The first-order spectra were recorded on Kodak Spectrum-Analysis No. 1 glass plates, and the concentrations were determined by standard quantitative emission spectrographic procedures.

NEUTRON ACTIVATION ANALYSIS

To confirm the accuracy of in-house SQA (spectrographic quantitative analysis) of dark monazite, samples of this mineral were tested by an alternate method, instrumental NAA (neutron activation analysis), by P. A. Baedecker, U.S. Geological Survey. Aliquots of approximately 5 mg of each monazite sample were irradiated in the National Bureau of Standards reactor for 10 minutes at a flux of 6×10^{13} neutrons cm^{-1} s^{-1}. Flux monitors were prepared by pipetting aliquots of a mixed rare-earth element flux monitor solution into polyethylene vials and evaporating to dryness. A multi-element standard sample HMS-1 (Baedecker and others, 1977) was also used as a flux monitor. The samples were counted on a high-resolution Ge(Li) detector and a planar intrinsic Ge detector 2 weeks following irradiation and again on both detectors after a 2-month decay period. Data processing was carried out on an IBM 370 computer using the SPECTRA3 program (Baedecker, 1976). The estimated precision (one standard deviation on a single determination) of the results, based on counting statistics, is (in percent): Th 8, La 5, Ce 2, Nd 3, Sm 2, Eu 2, and Gd 15.

Because several rare-earth isotopes have very large cross sections for thermal neutron capture, it was anticipated that the analysis of monazite samples would be subject to serious self-shielding problems. Six samples of RO-4D (beach sand concentrate from Taiwan) were prepared which ranged in weight from 2.5 to 20 mg. Three samples weighing 2.5, 5, and 7.5 mg had comparable specific activities, indicating no serious self-shielding problems. Samples heavier than 8 mg showed a decrease in specific activity with increasing sample size, and indicated a self-shielding effect. The agreement between the NAA data and that obtained via emission spectroscopy and the agreement between replicates for samples of less than 8 mg suggest that the maximum error due to self-shielding for 5-mg samples is approximately 5 percent.

Following is a comparison of the results (SQA) reported as weight percent oxides, and the differences, in percent, of the values reported with respect to the results of NAA [100 (SQA-NAA)/NAA]:

Sample No.--	RO-4D			56			2418		
	SQA	NAA	Diff.	SQA	NAA	Diff.	SQA	NAA	Diff.
La	11.0	11.4	-3.5	14.0	14.2	-1.4	12.0	13.7	-12.4
Ce	26.0	26.2	-0.8	26.0	24.1	+7.9	26.0	27.1	-4.1
Nd	13.0	12.2	+6.6	14.0	12.7	+10.2	13.0	12.4	+4.8
Sm	1.7	1.67	+1.8	2.2	1.8	+22.2	1.6	1.39	+15.1
Eu	.26	.31	-16.1	.39	.43	-9.3	.25	.30	-16.7
Gd	.90	.90	0	1.3	1.28	+1.6	.90	.83	+8.4
Th	.58	.55	+5.5	3.2	2.8	+14.3	.82	.85	-3.5

Of 21 pairs, 7 show differences of 10 percent or more, but these are not significant considering the low values of most of the 7 pairs. This comparison enables us to view the results of SQA of as little as 5 mg of dark monazite with considerable confidence.

OTHER PROCEDURES

The amount of water in dark monazite from Alaska, Taiwan, and Zaire was determined by the senior author using the loss-on-ignition method. High-purity samples from Alaska and Zaire ranged between 16 and 106 mg; and from abundant concentrates from Taiwan, the samples selected weighed 1,000 mg. All were heated an hour at a time at 105°C to constant weight. Then the samples were heated for 1½ hr at 650°C in a muffle furnace, cooled, weighed, and the loss in weight was computed as H_2O+.

Amorphous carbon in dark monazite from Alaska, Taiwan, and Zaire was determined in Rinehart Laboratories, Inc., Arvada, Colo., by the standard Pregl method (Steyermark, 1961, p. 221–275). The sample is heated to redness in oxygen in a combustion apparatus, and CO_2 is absorbed by sodium hydroxide on asbestos (Ascarite). The Ascarite is weighed before and after the combustion, and carbon is computed from the gain in weight.

RESULTS

Spectrochemical analyses of 11 samples of dark monazite from Alaska are given in table 6 and may be compared with similar analyses of 20 samples of dark monazite from other areas (tables 7 and 8). No other analyses of dark monazites were found in the literature. Only the oxides of the first seven naturally occurring elements in the lanthanide series are given, plus Y_2O_3, because this group generally comprises 99 to 100 percent of the REE present in monazites of all types from all sources (Fleischer and Altschuler, 1969, and Michael Fleischer, written commun., 1969). Considering the minute sample (10–15 mg) which we chose as a standard for spectrochemical analysis, the totals of the analyses of samples from Taiwan, Zaire, and Alaska and Montana, U.S.A., ranging from 92.65 to 109.12 percent, are reasonable values that may, with caution, be used.

Also shown for comparison are the totals of the lanthanide oxides (Ln_2O_3) and the values for La+Ce+Pr (Σ) and La/Nd using atomic percentages according to Murata and others (1957), p. 148); and Fleischer (1965, p. 764). Minor elements detected in seven dark monazites from Alaska by SQA showed the following magnitudes, in ppm: Ba 100–500, Cr 200–2,000, Cu 50, Pb 20–70, and Sn 150. In addition, selected samples analyzed for carbon in 1975 gave the following data, in percent:

[Analyst: A. W. Stone, Rinehart Laboratories, Inc., Arvada, Colo.]

Sample No.	Area	Carbon
506	Alaska	0.65
1446	--do--	.33
2418	--do--	.22
2432	--do--	1.22
RO-4C	Taiwan	.35
D1C/71	Zaire-	.31

As an index of the uranium content of dark monazites, delayed-neutron analysis of selected samples showed the following results:

[Analysts: H. T. Millard, Jr., C. M. Ellis, and C. McFee, U.S. Geological Survey]

Sample No.	Area	U (ppm)
2418	Alaska	28.70
RO-4D	Taiwan	260.07

DISCUSSION

REVIEW OF COMPOSITION OF MONAZITE

Yellow monazite is essentially an anhydrous phosphate of the light REE plus Th, and a thorough understanding of its composition is required in order to characterize any of its varieties. Older analyses usually give CeO_2 or Ce_2O_3 and lump the rest of the lanthanides as Ln_2O_3 (Palache and others, 1951, p. 694). As analytical methods developed from gravimetric to spectrographic, X-ray fluorescence, and neutron-activation procedures, the REE were reported as individual oxides (usually as RE_2O_3, but also as CeO_2 and Pr_6O_{11}), and lately as atomic percentages of the metals. For this discussion, use is made primarily of the oxides as reported, and atomic percentages are cited where these are the only form reported in the literature.

The general formula of monazite is ABO_4, where A=REE, Th, Fe, Al, Ca, and Mg; and B=P and Si. REO (excluding Y_2O_3) in monazite range from 28 percent of the total oxides in the cheralite variety from India (Bowie and Horne, 1953) to 74 percent in a monazite from Katanga (Palache and others, 1951, p. 694, anal. 10), but except for these extremes the average (La to $Gd)_2O_3$ in 100 yellow monazites from all rock types is about 59 percent. The same oxides in 31 dark monazites average a little more than 60 percent. Y_2O_3 is about

TABLE 6.—*Analyses of Eu-rich dark monazite from Alaska, in percent*

[Analyst: E. L. Mosier. $\bar{X}$, average; s, standard deviation; leaders (—), not reported. Ln_2O_3, total of La_2O_3 to Gd_2O_3; Σ, sum of La+Ce+Pr atomic percentages, where La through Gd=100 percent; La/Nd, ratio of atomic percentages]

Sample No.--	47	56	74	183	256	506	1325	1446	2411	2418	2432	-	
Quad.-------	Ophir	Ruby	Livengood	Livengood	Eagle	Teller	Talkeetna	Livengood	Tanana	Tanana	Tanana	X	s
La_2O_3	15	14	13.3	12.5	12.5	12.5	13.7	14	14	12	15.4	13.54	1.09
Ce_2O_3	30	26	29	27	30	30	29	32	28	26	32	29.00	2.10
Pr_2O_3	2.7	3.1	3.4	3.1	3.6	3.5	3.3	4.1	2.9	3.1	3.9	3.34	.42
Nd_2O_3	10	14	13.0	13	15.5	15.5	14	18	12	13	16	14.00	2.18
Sm_2O_3	1.4	2.2	2.2	2.0	2.2	2.1	1.9	2.1	1.4	1.6	2.0	1.92	.31
Eu_2O_3	.24	.39	.36	.25	.35	.32	.36	.36	.22	.25	.29	.31	.06
Gd_2O_3	.70	1.3	1.0	.85	.87	.98	.95	1.3	.8	.9	1.1	.98	.19
Y_2O_3	.35	.65	.51	.44	.34	.36	.49	.56	.51	.52	.49	.47	.095
P_2O_5	20	24	21	23	22	20	23	25	23	20	25	22.36	1.91
ThO_2	---	3.2	.70	.70	.60	.60	.83	.70	.79	.82	.70	.88	.80
SiO_2	10.8	2.1	5.5	5.2	14.4	12.3	5.3	7.1	8.4	12	8.7	8.35	3.74
TiO_2	.46	.71	.41	.36	.46	.46	.76	.50	.45	2.0	.69	.66	.46
Al_2O_3	1.9	.72	1.9	1.9	3.1	1.4	1.4	1.2	1.0	6.0	1.3	1.98	1.47
Fe_2O_3	1.4	1.6	1.4	1.7	2.5	2.2	.89	1.1	.59	2.4	.97	1.77	1.00
CaO	.32	.49	.20	.32	.20	.21	.32	.30	---	.30	.40	.28	.13
MgO	.24	---	.22	.33	.24	.18	.21	.25	---	.65	.18	.23	.17
H_2O	---	1.46	---	---	---	---	---	---	.64	.71	---	.94	---
Total-----	95.51	95.92	94.10	92.65	108.86	102.61	96.41	108.57	94.70	102.25	109.12	101.01	6.43
Ln_2O_3	60.04	60.99	62.26	58.70	65.02	64.90	63.21	71.86	59.32	56.85	70.69	63.09	4.90
Σ	80.1	71.6	74.2	73.4	71.7	71.7	73.6	70.6	76.4	73.1	73.4	73.6	2.66
La/Nd	1.56	1.04	1.06	1.00	.84	.84	1.02	.81	1.21	.96	1.00	1.03	.38

TABLE 7.—*Analyses of Eu-rich dark monazite from Taiwan, Zaire, France,*

[Analyst for samples from Taiwan, Zaire, France (RO-38F), and Peru: E. L. Mosier. Leaders (—), not reported; ≈, about equal to; Tr, trace; Ln_2O_3, total of

Country--	Taiwan				Zaire					France					
Area------	Southwestern beaches				Kivu					Riviera Area			Riviera Gras		
References--	This report			K. L. Soong, (written commun., 1978)	This report					Donnot and others (1973)					This report
Sample No.	RO-4B	RO-4C	RO-4D		A48/50A	A70/50A	A121/51	A122/51	DIC/71	1	2	3	4	5	RO-38F
La_2O_3-----	11	11	11	7.52	12	10	7	15	14	9.4	9.1	7.8	8.0	7.9	11
Ce_2O_3-----	24	25	26	22.65	30	31	27	32	31	25.3	24.2	22.1	22.8	22.9	27
Pr_2O_3-----	2.5	2.7	2.7	2.49	3.9	4.4	4.3	3.8	4.1	3.2	3.2	3.0	3.1	3.2	3.2
Nd_2O_3-----	11	13	13	8.43	18	21	22	17	17	14.0	13.4	12.8	13.1	13.6	16
Sm_2O_3-----	1.4	1.7	1.7	1.95	3.2	4.6	5.4	2.7	2.5	3.1	2.8	2.7	2.9	2.9	24
Eu_2O_3-----	.20	.25	.26	.16	.45	.58	.68	.36	.35	≈.5	≈.5	≈.5	≈.5	.5	37
Gd_2O_3-----	.72	.92	.90	1.04	1.0	1.5	1.8	1.1	1.0	3.1	2.9	1.5	1.6	1.7	1.4
Y_2O_3------	.46	.51	.53	.50	.57	.64	.60	.60	.60	.4	.4	.9	.9	.9	.51
P_2O_5------	20	20	20	22.6	23	24	23	24	23	23.0	23.4	18.9	19.5	19.4	22
ThO_2--------	.58	.59	.58	1.3	1.0	.85	.75	.68	.65	---	---	---	---	---	.53
SiO_2--------	16	14	14	25.0	7.1	6.4	5.2	6.6	3.6	8.2	7.6	13.3	11.7	12.2	8.9
TiO_2--------	.42	.47	.47	1.5	.61	.76	.70	.65	.60	---	---	---	---	---	.51
Al_2O_3-------	1.7	1.6	1.6	1.3	1.3	1.2	.96	1.4	1.2	3.4	3.2	4.6	4.2	4.6	3.8
Fe_2O_3-------	1.1	1.0	.8	1.0	.69	.80	.49	.69	.39	3.6	.35	3.9	2.9	2.6	2.4
CaO---------	.53	.47	.46	.64	.28	.27	.25	---	---	---	---	---	---	---	.52
MgO---------	.32	.30	.30	.66	.12	.11	---	---	---	---	---	---	---	---	.37
H_2O---------	.78	1.43	1.62	---	.70	.99	1.24	.92	.92	---	---	---	---	---	
Total---	92.71	94.94	95.94	98.74[1]	103.92	109.10	101.37	107.50	100.91	97.2	94.2	≈92.0	≈91.2	≈92.4	100.91
Ln_2O_3-------	50.82	54.57	55.56	44.24	67.55	72.08	68.18	71.96	69.95	58.6	56.1	50.4	52.0	52.7	61.4
--------	74.6	71.8	72.3	74.7	68.9	62.6	57.3	71.5	71.1	65.8	66.2	66.3	66.2	65.6	68.1
La/Nd-------	1.04	.88	.88	.93	.73	.49	.33	.92	.86	.70	.71	.63	.63	.60	.71

[1]Plus 0.035 percent MnO_2; 0.04 percent Pb; and 0.66 percent ZrO_2.
[2]Plus 0.3 percent Dy_2O_3.
[3]Plus 0.17 percent Ho_2O_3.

1.6 percent in most yellow monazites, and averages less than 0.6 percent in dark monazites. ThO_2 ranges up to 31.5 percent but averages about 7 percent in yellow monazites; in dark monazites it rarely exceeds 1 percent. As an index of the amount of Eu in all monazites, we note that of 642 analyses from all sources (Michael Fleischer, written commun., 1982), only 149 (including 11 identifiable Eu-rich dark monazites) show 0.1 atomic percent or more of Eu. This is greater than the amount of Eu_2O_3 in commercial yellow monazite—0.06–0.07 percent—from data by Jolly (1976, p. 894, table 5). Among the 11 dark monazites in Fleischer's tables of analyses, the atomic percentages of Eu range from 0.3 to 1.7, and average 0.8 percent.

In a study of yellow monazites, Murata and others (1953) showed considerable variation in the proportions of every element except Pr, but the variations were systematic. As La and Ce increased, Nd, Sm, Gd, and Y decreased; and the following rules were generally true:

1. The sum of the atomic percentages of La and Nd is 42±2.

2. The atomic percentage of Pr is approximately constant at 5±1.

3. The sum of Ce, Sm, Gd, and Y is 53±3 atomic percent.

The antipathetic relations are attributed to fractional precipitation whereby there is gradational increase in precipitation of REE with decreasing ionic radius. To this precept, the following factors should be added: the starting abundances of the REE, and the pH and temperature of fluids that affect the solubilities of simple and complex REE compounds (Taylor, 1972, p. 1027; Carron and others, 1958, p. 271–273).

DARK MONAZITE AND YELLOW MONAZITE

The average composition of dark monazite in eight different areas is shown in table 8. Table 9 presents the weighted-average values for 31 selected analyses of dark monazite and gives the average abundances of the same oxides in 64 analyses of yellow monazite. These figures show the chemical differences between dark and yellow monazites: dark monazite contains greater amounts of Eu_2O_3, SiO_2, TiO_2, Al_2O_3, Fe_2O_3, MgO, and H_2O; and less Y_2O_3, ThO_2, P_2O_5, and CaO than does

U.S.S.R., Peru, and Spain, in percent

[La_2O_3 to Gd_2O_3; Σ, sum of La+Ce+Pr atomic percentages, where La to Gd=100 percent; La/Nd, ratio of atomic percentages]

U.S.S.R.				Peru	
E. Siberia	S. Yenisei	Siberia	Timan Ridge	Rio San Juan	Rio Morro Grande
Kosterin and others (1962)	Zemel (1936)	Li and Grebennikova (1962)	Serdyuchenko and Kochetkov (1974)		This report
				RO-54D	RO-54E
10.0	7.07	11.9	9.59	12	12
18.2	30.40	2.71	25.95	27.5	29
5.0	1.13	4.43	2.71	3.3	3.35
14.3	9.04	15.18	13.25	13.5	13.5
3.2	6.22	3.64	1.80	2.15	2.05
1.0	.85	---	.17	.37	.37
3.7	1.13	2.06	.90	1.25	1.2
---	.51	---	=1.80	.57	.52
23.80	23.63	24.50	28.	21.5	21
.001	.26	.67	1.5	.5	.5
15.80	12.92	8.60	4.42	14	13
---	.88	---	.89	.71	.71
---	1.16	1.75	---	2.0	1.7
3.11	4.32	2.20	1.23	1.35	1.2
---	.52	.55	---	.22	.18
---	.28	.45	Tr	.17	.23
1.25	---	---	2.9	---	---
99.36[2]	100.32[3]	98.64[4]	95.10[5]	101.09	99.31
55.40	55.84	59.92	54.36	60.07	61.47
61.2	70.3	66.2	71.2	72.1	73.0
.73	.81	.81	.75	.93	.93

[4]Plus 0.24 percent Dy_2O_3; 0.53 percent Er_2O_3, and 0.55 percent organic material.
[5]Plus 0.23 percent Dy_2O_3.

TABLE 8.—*Comparison of analyses of Eu-rich dark monazite, in percent*

[Leaders (–), not reported. NA, not applicable; $\bar{X}$, average; s, standard deviation]

Locality-------	Alaska		Montana	Taiwan		Zaire		France[1]		U.S.S.R.[2]		Spain[3]	Peru	
No. of samples-	11		1	4		5		6		4		1	2	
	$\bar{X}$	s	$\bar{X}$	$\bar{X}$	s	$\bar{X}$	s	$\bar{X}$	s	$\bar{X}$	s		$\bar{X}$	s
La_2O_3--------	13.54	1.09	11	10.13	1.74	11.60	3.21	8.87	1.24	9.64	1.99	10.55	12.00	.00
Ce_2O_3--------	29.00	2.10	21	24.41	1.43	30.20	1.92	24.05	1.84	24.32	5.15	23.43	28.25	1.06
Pr_2O_3--------	3.34	.42	2.6	2.60	.12	4.10	.25	3.15	.08	3.32	1.75	1.05	3.33	.04
Nd_2O_3--------	14.00	2.18	11	11.36	2.17	19.00	2.35	13.82	1.15	12.94	2.72	1.17	13.50	.00
Sm_2O_3--------	1.92	.31	1.7	1.69	.23	3.68	1.26	2.80	.24	3.72	1.85	1.62	2.10	.07
Eu_2O_3--------	.31	.06	.24	.22	.05	.48	.14	.48	.05	.51	.49	.14	.37	.00
Gd_2O_3--------	.98	.19	1.1	.90	.13	1.28	.36	2.03	.76	1.95	1.27	2.08	1.23	.04
Y_2O_3---------	.47	.10	1.2	.50	.03	.60	.02	.67	.26	.58	.85	.47	.55	.04
P_2O_5---------	22.36	1.91	20	20.65	1.30	23.40	.05	21.03	2.00	24.98	2.05	28.85	21.25	.35
ThO_2---------	.88	.80	.57	.76	.36	.79	.14	[4].53	NA	.61	.66	.32	.50	.00
SiO_2---------	8.35	3.74	14	17.25	5.25	5.78	1.40	10.32	2.38	10.44	4.98	13.80	13.50	.71
TiO_2---------	.66	.46	1	.72	.52	.66	.07	[4].51	NA	.44	.51	---	.71	.00
Al_2O_3--------	1.98	1.47	4.4	1.55	.17	1.21	.16	3.97	.60	.73	.87	4.70	1.85	.21
Fe_2O_3--------	1.77	1.00	7.5	.98	.12	.61	.17	3.15	.60	2.72	1.32	1.50	1.28	.11
CaO----------	.28	.13	1.1	.53	.83	.16	.15	---	NA	.27	.31	---	.20	.03
MgO----------	.23	.17	.42	.40	.18	.05	.06	---	NA	.18	.22	---	.20	.04
H_2O----------	[5].94	.46	---	[5]1.28	.44	.88	.19	---	NA	1.04	1.37	---	---	NA
Total----	101.01		98.83	95.93		104.48		95.38		[6]98.39		89.68	100.82	

[1] From data by Donnot and others (1973); and this study.

[2] From data by Zemel (1936); Kosterin and others (1962); Li and Grebennikova (1962); and Serdyuchenko and Kochetkov (1974).

[3] From data by Vaquero (1979).

[4] One analysis.

[5] Average of three samples.

[6] Plus 0.19 Dy_2O_3, 0.04 Ho_2O_3, 0.13 Er_2O_3, and 0.14 organic matter.

yellow monazite. The greater content of Eu and the lesser amount of Th compared to yellow monazite are characteristic features of dark monazite that are interpreted to be inherent because of the mode of origin. Li and Grebennikova (1962) observed that in dark monazite La and Ce are less, and Nd and Sm are greater, than in yellow monazite. Theoretically, SiO_2 and the oxides that follow in the tables should be nil in monazite. However, SiO_2 is found to substitute for PO_4 in the monazite structure, and a case for considerable substitution is made by Nekrasov (1972), who described a greenish-yellow monazite with 13.2 percent SiO_2 and named it silicomonazite. In dark monazites, SiO_2 and the oxides that follow in tables 6–9 are due to the many inclusions that are an obvious and characteristic feature of this variety of monazite. Considering the variability of the inclusions from place to place, it is remarkable how uniform in composition these monazites are worldwide, as indicated by the small to moderate standard deviations, s, of each of the averages in table 8.

It is appropriate here to note the average composition, in atomic percent, of La to Gd in yellow monazites from different rock types, according to unpublished data of Michael Fleischer (written commun., 1969):

	Granitic rocks, 158	Granitic pegmatites, 114	Alkalic rocks and carbonatites, 21	Gneisses and schists, 45	Average of 338 samples
La	24.1	21.0	30.0	24.6	24.9
Ce	47.6	44.9	50.7	42.5	46.4
Pr	5.3	5.6	4.5	8.4	6.0
Nd	17.4	19.7	12.1	20.0	17.3
Sm	2.7	5.0	1.2	2.1	2.8
Eu	.05	.03	.01	.02	.03
Gd	1.7	2.8	.5	2.1	1.8
Total---	98.85	99.03	99.01	99.72	99.23

TABLE 9.—*Average compositions of dark and yellow monazite in percent*

[Number in parentheses indicates the number of values used to calculate the average. Remainder includes small amounts of BaO, F, K_2O, Na_2O, PbO, SO_3, U_3O_8, and $(Y)_2O_3$; Ln_2O_3, total of La_2O_3 to Gd_2O_3]

	Dark monazite	Yellow monazite[1]
No. of samples--	31	64
La_2O_3----------	11.51	13.25
Ce_2O_3----------	27.18	26.90
Pr_2O_3----------	3.28	3.11
Nd_2O_3----------	14.29	11.71
Sm_2O_3----------	2.36	2.72
Eu_2O_3----------	.36	.05
Gd_2O_3----------	1.25	1.27
Y_2O_3----------	.61	1.58
ThO_2----------	.81 (25)	7.15
P_2O_5----------	22.07	26.00 (11)
SiO_2----------	9.90	1.70 (26)
TiO_2----------	.69 (25)	.005 (40)
Al_2O_3----------	2.27	.17 (40)
Fe_2O_3----------	1.89	.57 (40)
CaO----------	.33 (24)	1.98 (40)
MgO----------	.23 (24)	.01 (40)
H_2O+ ----------	1.16 (12)	.11 (40)
Remainder-------		.42 (37)
Total-------	100.19	98.71
Ln_2O_3----------	60.23	59.01

[1]Data for yellow monazites from Flinter, Butler, and Harral (1963); Heinrich, Borup, and Levinson (1960); Holt (1965), Jaffe (1955); Lee and Bastron (1967); Marchenko (1967); Rosenblum (1974b), Serdyuchenko and others (1967); and this report.

Multiplication of each figure by 0.6 will yield the approximate oxide weight percent.

Minor elements (less than 1 percent) reported in yellow monazites, other than the heavy REE, include Al, C, Ca, Fe, Mg, Mn, Nb, Pb, Sn, Ta, and U (Palache and others, 1951, p. 694). Minor elements found in Alaskan dark monazites other than those shown in table 6 include Ba, C, Cr, Cu, Hg, Pb, Sn, and U, none exceeding 2,700 ppm—most are 200 ppm or less. Elsewhere, minor elements detected in dark monazite include Ba, Be, Dy, Er, Ho, Mn, Na, Pb, Sc, Sn, Sr, U, V, and Zr; but not all in a single sample.

One complication in comparing data in table 9 is that the composition of yellow monazite is known to vary complexly but systematically with the nature of the igneous host rock. Monazites from alkalic rocks and carbonatites are enriched in light lanthanides, whereas those from granitic rocks and pegmatites are generally richer in the heavier lanthanides and Y (Fleischer and Altschuler, 1969). Also, two studies of REE in accessory and major minerals from an intrusive granitic rock that ranges from quartz monzonite to granodiorite showed a direct relation between the light REE content and the tenor of CaO in the whole rock (Lee and Bastron, 1967; Cain, 1974). A vein-type monazite is reported markedly enriched in Ce and poorer than average in Nd, Sm, and Th (Marchenko, 1967, p. 144). Other vein-type monazites with low Th content are described (Gordon, 1944; Rose and others, 1958). Little is known of the effects of metamorphism on the distribution of REE in yellow monazites, but a statement was made that the REE contents of metasedimentary rocks do not change as a function of metamorphic grade (Cullers and others, 1974).

A better comparison of dark and yellow monazites than the worldwide averages in table 9 might be a pair of analyses for the two varieties from a single location, but few such pairs are available. In table 10 the results of analyses of dark and yellow monazites in one concentrate from Alaska are shown, and a similar pair from Taiwan are likewise compared. The same relations among the oxides cited for table 9 are evident. In table 10, however, the sum of $(La\text{-to-}Gd)_2O_3$ in the dark monazites is less than in the yellow monazites. Thorium again is much less; and elements found in the many inclusions—Si, Ti, Al, Fe, and Mg—are greater. Similar relations of rare-earth oxides and ThO_2 between dark and yellow monazites in Taiwan are tabulated by Chen, Li, and Wu (1973, p. 71).

Several noteworthy examples are recorded in the literature of yellow monazites with unusual Eu, and (or) low Th. Three clear, deep-canary-yellow monazites from alluvial deposits in Malaysia contain 0.13–0.6 percent Eu_2O_3. The one with the greatest Eu content also had the least ThO_2 (2.00 percent) and the least SiO_2 (0.60 percent), and it showed a pale salmon tinge apparently superposed on the clear deep-yellow color (Flinter and others, 1963, p. 1211, 1215). That unusually high Eu is not necessarily associated with low Th in monazite is demonstrated by 11 yellow monazites from Liberia with an average 0.11 percent Eu_2O_3 and 7.2 percent ThO_2 (Rosenblum, 1974b, p. 691); and reddish-brown monazite from Aldan, eastern U.S.S.R., with 0.50 percent Eu_2O_3 and 14.90 percent ThO_2 (Zemel', 1936).

On the other hand, low Th in monazite is cited with low to high Eu content. Flesh-pink monazite crystals as much as 1 cm across in tin veins at Llallagua, Bolivia, contain no Th or Eu but, like the low-Th/high Eu monazite from Malaysia, are associated with cassiterite (Gordon, 1939, 1944). A monazite from Belorussia, U.S.S.R., contains 0.11 percent ThO_2, has about 0.07 percent Eu_2O_3, is pale greenish yellow, and is thought to be of

TABLE 10.—*Comparison of compositions of dark and yellow monazites from Alaska and Taiwan, in percent*

[Analyst: E. L. Mosier, U.S. Geological Survey. Leaders (—), not reported; NA, not applicable; <, less than shown; Ln_2O_3, total of La_2O_3 to Gd_2O_3; Σ, sum of La+Ce+Pr atomic percentages, where La to Gd=100 percent; La/Nd, ratio of atomic percentages. R, reported; P, prorated]

	Alaska				Taiwan			
Sample---	1325A		1325B		RO-4D		RO-4DY	
Color----	Dark		Yellow		Dark		Yellow	
Oxide----	R	P	R	P	R	P	R	P
La_2O_3	13.7	14.21	14.0	14.72	11	11.47	16	15.15
Ce_2O_3	29	30.08	29	30.48	24	27.10	30	28.40
Pr_2O_3	3.3	3.42	3.2	3.36	2.7	2.81	3.2	3.03
Nd_2O_3	14	14.52	15	15.77	13	13.55	16	15.15
Sm_2O_3	1.9	1.97	2.4	2.52	1.7	1.77	1.9	1.80
Eu_2O_3	.36	.37	---	NA	.26	.27	.08	.08
Gd_2O_3	.95	.99	1.3	1.37	.90	.94	1.0	.95
Y_2O_3	.49	.51	1.6	1.68	.53	.55	1.0	1.95
ThO_2	.83	.86	3.2	3.36	.58	.61	6.0	5.68
P_2O_5	23	23.86	22	23.12	20	20.85	26	24.61
SiO_2	5.3	5.50	2.3	2.42	14	14.59	1.6	1.52
TiO_2	.76	.79	---	NA	.47	.49	<.40	<.38
Al_2O_3	1.4	1.45	---	NA	1.6	1.67	<.50	<.47
Fe_2O_3	.89	.92	.52	.55	.82	.85	<.35	<.33
CaO	.32	.33	.51	.54	.46	.48	1.5	1.42
MgO	.21	.22	.11	.12	.30	.31	<.10	<.95
H_2O	---	NA	---	NA	1.62	1.69	---	NA
Total---	96.41	100.00	95.14	100.01	95.94	100.00	<105.63	<100.87
Ln_2O_3	63.21	65.56	64.9	68.22	55.56	57.91	68.18	64.56
Σ	73.6		72.1		72.3		73.0	
La/Nd	1.02		.97		.88		1.04	

metasedimentary origin (Serdyuchenko and others, 1967). Six pinkish-yellow monazites from the southern Urals have no ThO_2 and about 0.1–0.5 percent Eu_2O_3, and six yellow monazites from the Pamir Range contain about 1.8–3.6 percent ThO_2 and 0.1–0.4 percent Eu_2O_3 (Komov and others, 1974). A pneumatolytic white to red and brown-red monazite in the northern Caucasus contains about 2.39 percent ThO_2 and 0.06 percent Eu_2O_3 (Ploshko, 1961). Earthy monazite from a vein in carbonatite at Magnet Cove, Ark., U.S.A., contains no detectable Th, and the low content of Th as well as of Y is thought to be characteristic of monazites from alkalic rocks (Rose and others, 1958, p. 996). Abnormally low ThO_2 (0.08 percent) is recorded for pistachio-green and colorless monazites from a carbonatite at Kangankunde Hill, Malawi, and the Eu_2O_3 content is 0.05 percent (Holt, 1965). A high Th content in monazites is directly related to high-grade conditions of temperature and pressure during magmatic or metamorphic crystallization (Overstreet, 1967, table 2; Overstreet and others, 1969). The greatest amounts of ThO_2 in monazite (29.45–31.50 percent) are found in the cheralite variety, a sparse accessory mineral in a kaolinized pegmatite dike (Bowie and Horne, 1953, p. 95).

A brief discussion of carbon in monazites was included in the section on color. The dark color of dark monazite is mostly due to extremely minute particles of amorphous carbon distributed randomly. Other than as fine inclusions, carbon apparently takes no part in the chemical nature of monazite.

Attempts to relate chemistry to physical properties of dark monazites have yielded few positive results. An estimate of the relation between the density of dark monazite and its tenor in SiO_2 and the total lanthanide-oxides is shown in figure 27. As expected, the first is an inverse relation and the second is direct. Similarly, a direct relation exists between density and Th content, and inverse relations are noted between Th and Si, between Eu and Si, and between total lanthanides and Si. In another study, Overstreet, Warr, and White (1970) showed that the grain size of yellow monazites from North Carolina and South Carolina is related to the

tenors of Th and U; the percentages of these elements are greater for +40-mesh monazite than for −40-mesh material.

GEOCHEMISTRY

NATURE OF THE LANTHANIDES

The chemical nature of the lanthanides, and their abundances and relative distributions in cosmological and terrestrial materials, including chondrites, ocean waters, marine sediments, rocks, and minerals, are summarized here from discussions in Rankama and Sahama (1950), Herrmann (1970), Philpotts and Schnetzler (1971), and Taylor (1972), as well as other sources. This summary provides a geochemical background against which the abundances of the REE in dark monazite can be evaluated for an interpretation of the origin of this variety of monazite.

The REE include the 15 elements in Group 3, Series 8 of the periodic table (Green, 1959, table 2) from La (Z=57) to Lu (Z=71) plus Y (Z=39), which is commonly associated with the heavier REE. Promethium (Z=61) is not normally found in nature, for it has no stable isotopes; it exists only as a product of nuclear reactions. Several elements have more than one isotope, some radioactive, but isotopic compositions of REE in dark versus yellow monazites are not available. The usual oxidation state for the REE is 3+; the only other oxidation states important in geological processes are Ce^{4+} and Eu^{2+}.

Rankama and Sahama (1950, p. 510) pointed out that the name rare-earth metals, which was first applied to members of this group of elements, is no longer consistent with their real abundance. Inspection of their table 2 (p. 39–40) on abundance of the elements shows the REE in igneous rocks to be more abundant, for example, than bismuth, cadmium, gold, mercury, silver, and all of the platinum-group metals. Natural processes tend to fractionate the lanthanides into light and heavy groups in different minerals. The light group, from La to Gd, is called the cerium group, named after the element which is usually the most abundant; and the heavy group, from Tb to Lu and including Y, is called the yttrium group. Monazite is a Ce-group mineral, and xenotime is a good example of a Y-group mineral.

The regular decrease in ionic radius of the trivalent ion from La to Lu is known as the lanthanide contraction, which allows the heavier REE to be similar in ionic radius to much lighter elements (such as Y). The ionic radii of the trivalent lanthanides also depend on the coordination number, and for plotting data on REE distributions here, use is made of the ionic radii for coordination number 6, according to Whittaker and Muntus (1970).

GEOCHEMICAL ABUNDANCES OF THE RARE-EARTH ELEMENTS

CHONDRITES

The abundance of REE in chondrites (stony meteorites) is taken as a standard against which all other materials may be measured for comparison of the REE contents, as well as the abundances of the other elements (Schmitt and others, 1964; Haskin and others, 1966, 1968; Haskin and Korotev, 1973). The choice of an extraterrestrial material with abundances presumed to represent primordial abundances in the universe seems best as a basis for comparison of REE in minerals with REE in other minerals or rocks. Moreover, use of a chondrite as a standard introduces no bias in favor of one mineral or rock type or locality. Masuda, Nakamura, and Tanaka (1973), Nakamura (1974), Masuda (1975) and Evensen, Hamilton, and O'Nions (1978) have shown a variation in REE content among different chondrites, but these variations are negligible compared to the variations among different specimens of even a single mineral species. In this study, the REE abundances in chondrites (total REE=5.42 ppm) shown by Herrmann (1970, p. C–5, table 39) are used to compute CNR (chondrite-normalized ratios) for each REE.

SEAWATER AND ROCKS

Absolute abundances and relative distributions of REE in terrestrial materials are dependent on paragenesis. In seawater, the REE concentration at a depth of 4,000 m is four times greater than in surface water (which contains 0.1 ppm REE); and relative to REE in chondrites, seawater, recent phosphorite, and manganese nodules show marked depletion of the heavy REE (Goldberg and others, 1963). Cerium abundance in seawater is depleted in comparison with adjacent REE; but Eu abundance in seawater is normal, relative to the other REE, despite a general depletion in crustal rocks and REE minerals, which are the ultimate sources of REE in the ocean. The literature contains articles on precipitation of REE in Holocene sediments directly from seawater, proved by matching REE patterns (Piper and Graef, 1974); on depletion of light REE in other Holocene sediments (Wildeman and Haskin, 1965); and on fractionation of heavy REE into clays rich in bone phosphate, and light REE into Fe-Mn concretions (Volkov and Fomina, 1973). The totals of the REE

in eight recent ocean sediments from the Atlantic and Pacific Oceans average about 168 ppm (Wildeman and Haskin, 1965).

Discussions on REE in clay minerals from weathered and eroded source rocks indicate lower light-REE/heavy-REE ratios in marine versus continental deposits. These lower ratios in marine deposits are attributed to the greater solubility and to the greater stability of aqueous complexes of heavy REE relative to those of the light REE (Balashov and others, 1964; Ronov and others, 1967). Accordingly, the heavy REE are carried into marine basins by natural waters more readily than the light REE, with the bulk of the REE being left in the clay minerals forming on the continents (Cullers and others, 1975). Clay minerals contain a considerable reserve of mobile REE (estimated at 20 to 95 percent of the total REE in the rocks) that is capable of migrating during diagenesis (Balashov and Girin, 1969). Evidence from concretions indicates that in the course of diagenesis the composition of the mobile REE changes towards relative enrichment in the heavier lanthanides (Girin and others, 1970). However, the insoluble residues of these concretions are enriched in the light lanthanides and are deficient in the intermediate lanthanides.

In older sediments, the REE abundances compared to the chondritic REE abundances show a relative depletion of the heavy REE or enrichment of the lighter ones (Taylor, 1972). Precambrian sediments have the same REE abundances (except for greater Eu) that were reported for a composite of Paleozoic shales (total =194 ppm), which indicates that the relative abundances of REE at the Earth's surface have remained constant over the past 3 billion years (Wildeman and Haskin, 1973, p. 436). However, in a report on Australian Proterozoic to Triassic sedimentary rocks, Nance and Taylor (1976) indicated that although REE relative abundances are unchanged, the average absolute content of REE increases in the order limestone, sandstone, graywacke, ocean sediment, shale; and the absolute REE content of shales ranges from about 60 to 410 ppm (Haskin, Wildeman, and others, 1966, p. 6103). The average REE content of shales is in the range of 200 to 280 ppm (Haskin and others, 1968; Balashov and others, 1964). Phosphatic carbonaceous shales commonly have higher REE content than nonphosphatic carbonaceous shales, and contents may reach several hundred parts per million (Sozinov and others, 1977).

In igneous rocks, the REE abundance in more than 500 granitic rocks ranges from 220 to 315 ppm, and the REE content of a composite of 213 continental basalts is 175 ppm (Haskin, Wildeman, and others, 1966, p. 6103). Oceanic peridotites are enriched in light REE relative to chondrites, while tholeiitic basalts are enriched in the heavier REE (Balashov and others, 1970). Data from African and Russian kimberlites indicate that they contain 10 to 100 times more REE than the enclosing alkalic and normal ultramafic rocks, that a well-defined correlation (+0.834) exists between CaO and REE content, and that the REE composition is cerian (Ilupin and others, 1974). Alkalic rocks and carbonatites generally are enriched in the lighter REE, as well as having greater abundances—up to 0.75 percent (Flanagan, 1976, p. 108, 171; Vlasov, 1966, v. 1, p. 234, v. 3, p. 209, 219; Balashov and Pozharitskaya, 1968, p. 274; Michael Fleischer, written commun., 1969), but siliceous rocks including the calc-alkaline series and their pegmatites are relatively enriched in the heavier REE (Fleischer and Altschuler, 1969). Archean volcanic rocks and sediments derived therefrom have REE abundance and distribution patterns similar to those of modern volcanic rocks (Nance and Taylor, 1977; O'Nions and Pankhurst, 1978).

Fractionation of REE generally occurs in deeper, more slowly cooled parts of an igneous mass, but the evidence is not so clear for REE fractionation under metamorphic conditions, for the literature is sparse on REE abundances in metamorphic rocks. Haskin and others (1968, p. 895, table 2) showed that the averages for REE in metamorphosed North American shales are close to those for unmetamorphosed North American shales. Similarly, Bliskovskiy, Mineyev, and Kholodov (1969, p. 1059) indicated that metamorphism has little effect on the REE content of phosporites in the Karatau area, U.S.S.R.; metamorphosed phosphorites have only slightly higher REE content than the unmetamorphosed phosporites of the same region. A reference to REE content of metasomatites indicated that in alkalic terrane in the Urals, the REE were carried by plutonic alkaline solutions, and their concentrations increased regularly toward the end of the processes as the grade of metasomatism increased (Yes'kova and Yefimov, 1972). However, evidence from metasomatic zones in amphibolites in Nova Scotia showed that these zones have retained the REE chemistry of the host (Muecke and Sarkar, 1977). The high grade conditions of temperature and pressure involved in granitization of sediments apparently lead to loss of light REE, and magmatic differentiation produces accumulation of heavy REE (Tikhomirova, 1971).

The REE in crustal rocks have fractionated, compared to the distribution of REE in meteoritic materials and mantle rocks. The heavier REE in crustal rocks are preferentially concentrated in the dark rock-forming minerals, and the lighter lanthanides are more concentrated in the light-colored minerals (Balashov, 1972). The essential chemical factors in the fractionation process are temperature and pH, but the degree of alkalinity

plays an important role (Balashov and others, 1969). Fractionation of the REE results from the greater ability of the heavier REE to form transportable complexes as the ionic radius becomes smaller and the elements become less basic (Fomina, 1966; Vinogradov and others, 1960). However, Carron and others (1958) showed that the solubilities of REE in several systems are not regular from La to Lu. Eu^{2+} apparently shows a preferential substitution for K^+ in feldspars (Taylor, 1965, p. 162). That potassium plays a greater role than sodium in fractionation of REE is supported by leaching experiments up to 450°C (Sin'kova and Turanskaya, 1968). A positive correlation with Na_2O and a negative correlation with CaO for total REE in metasomatized alkaline ultramafic rocks have been cited (Rass, 1972).

In granitic rocks that intruded calcareous sediments in Nevada, U.S.A., the degree of fractionation of rare earths varies directly with the CaO content of the granitic rocks so that Ce+La+Pr are concentrated in Ce-group minerals present in rocks with higher CaO contents (Lee and Bastron, 1967). In the same area, a later study of REE distribution yielded an interpretation opposite to that expected from a differentiated intrusive: the light REE are associated with high CaO rocks, and the heavy REE are concentrated in the residual melt and crystallize in low-CaO rocks (Cain, 1974). Bearing on this, Adams (1969) pointed out that minerals in which REE have high coordination numbers (10–12) are Ce-group species, and those with low coordination numbers, such as 6, are Y-group materials. He cited a theory proposed by Khomyakov (1963) to explain the variations in REE assemblages found in isomorphous replacement of Ca: in 6-coordination, Ca has an ionic radius comparable to Y-group REE, but in 12-coordination it has a radius equal to that of Pr and, therefore, would be replaced preferentially by the light REE.

ROCK-FORMING MINERALS

The REE distribution in minerals is usually normalized against the REE abundances in the host rock or a standard like the average chondrite or the average of 40 North American shales, and the ratios are plotted on a logarithmic ordinate versus the atomic number or ionic radius for the abscissa. The ratio obtained by normalizing against the REE content of the host rock (or the matrix, in a porphyritic rock) is called the partition coefficient, and the curve plotted by joining the points from La to Lu is generally slightly bowed upward in the midsection for mafic minerals (pyroxenes, amphiboles, and micas). For feldspars, this curve is generally horizontal or bowed downward in the middle. A small downward deflection for the Eu in mafic minerals indicates a depletion, whereas a large upward deflection for Eu in feldspars indicates an enrichment (Haskin and Korotev, 1973; Nagasawa and Schnetzler, 1971; Paster and others, 1974; Schnetzler and Philpotts, 1970; and Wildeman and Condie, 1973). Some evidence indicates that potash feldspars are relatively more enriched in Eu than are plagioclases (Mason, 1972; and Schnetzler and Philpotts, 1970). Accessory minerals, including apatite, allanite, monazite, and zircon, show the same partition-coefficient curves as the mafic minerals, with various depletions for Eu (Haskin and Korotev, 1973; Wildeman and Condie, 1973).

The REE distributions in micas from some Precambrian igneous and metamorphic rocks apparently differ from those in other igneous and sedimentary rocks by showing equivocal Eu anomalies in SNR (shale-normalized-ratio) curves (Roaldset, 1975). The curves for biotites are essentially horizontal or rise slightly toward the Lu end. Eu (relative to neighboring Sm and Gd) shows a negative anomaly in biotite from one granite, a positive anomaly in biotite from another granite, and no anomaly from mylonitic gneiss (Roaldset, 1975, figs. 4 and 5). Clearly, further analyses of REE in biotite from igneous rocks of differing ages and rock types are needed to assess the role of the REE therein. To help fill this need for analyses, seven biotite concentrates from Western United States were submitted for REE analyses. The results are presented in the section, "Preferred mode of origin," and CNR plots are compared to those of dark monazite.

MONAZITE

The REE distribution in monazite when plotted on rectilinear graph paper with abundance as the ordinate and atomic numbers as the abscissa shows a rapidly decreasing sawtooth pattern from Ce to Gd (Rankama and Sahama, 1950, p. 520). The lanthanide series is a good example of the rule of Oddo and Harkins on elemental abundances, which states that elements with odd atomic numbers are, as a rule, less abundant than their even-numbered neighbors, in cosmic as well as terrestrial materials (Rankama and Sahama, 1950, p. 511). The rule reflects the greater stability of nuclei with even numbers of protons and neutrons compared to nuclei with odd numbers. This rule applies equally to dark monazite as well as yellow monazite, for the gross patterns of REE distribution of the two varieties are similar. They differ in details that do not upset the rule of Oddo and Harkins (see table 9).

Yellow monazite has been shown in the literature to form through igneous and regional metamorphic processes, the latter involving metasomatism, which make

detrital monazite unstable in the lower grades of metamorphism, but this monazite is stable in the environments of the amphibolite and granulite facies (Overstreet, 1967, p. 17). Yellow monazite occurs as a minor accessory mineral in magmatic rocks ranging in composition from diorite to muscovite granite; in associated pegmatite, greisen, and vein quartz; and in alkalic rocks including nepheline syenite and carbonatite. Monazite has been recorded in quartz veins ranging from low-temperature fissure fillings to hypothermal tin- and tungsten-bearing veins and alteration zones. Low-thorium varieties of monazite are found in cassiterite-bearing veins in Bolivia (Gordon, 1939, 1944). The source of monazite in metasedimentary rocks is interpreted to be REE, thorium, and phosphorus dispersed among clays, micas, and apatites in the unmetamorphosed sediments; and the amount of thorium in monazite from metasedimentary rocks was found to increase as the grade of metamorphism increased (Overstreet, 1967, p. 18–20).

Dark monazite with low Th and high Eu was thought to originate by several processes including diagenesis involving precipitation of REE from seawater, derivation from diagenetic rhabdophane, and as an accessory mineral of cassiterite-bearing granites (Overstreet, 1971; Matzko and Overstreet, 1977); but none of these concepts has general application. We accept the idea that the REE pattern in this distinctive variety of monazite is inherited from the REE distribution in a precursor mineral, rock, or environment. This presumption enables us to narrow the likely sources to fine-grained sedimentary rocks, especially carbonaceous and phosphatic shales.

Statistical treatment of analyses of minerals (and rocks) containing REE is used to point up interesting relations between two elements or groups of elements (Murata and others, 1953, 1957; Fleischer, 1965). For minerals containing the light lanthanides (Ce-group), the ratio of atomic percentages of La/Nd is plotted against Σ, the sum of the atomic percentages for La+Ce+Pr, to show fractionation of the Ce-group among different minerals and, for monazites, the fractionation of the Ce-group according to the source of the monazite among different rocks (Fleischer, 1965, p. 765, fig. 8). The values for Σ and La/Nd are shown for all analyzed samples of dark monazite (tables 6 and 7). These values are based on $(La\text{-to-}Gd)_2O_3=100$ percent, and the atomic percentages are computed therefrom for comparison with similar values in the literature.

Fleischer's diagram showing La/Nd versus Σ for monazites from different sources (Fleischer, 1965, p. 769, fig. 12) is expanded here (fig. 28) by the addition of points representing 32 dark monazites (including one partial analysis) from five countries, the averages of 40 North American shales, 22 phosphorites, 40 miscellaneous gneisses, 3 granitic gneisses, 5 schists; and 4 averages for chondrites. The log-normal distribution of these points is apparent in figure 29 where the points for the monazites lie on or close to a straight line on log-normal graph paper. The densest cluster of points for Eu-rich dark monazite from Alaska and Taiwan is near the average of 40 North American shales, but the average for 22 phosphorites lies well outside this group. In both diagrams a rather small cluster of points can be noted for the French data, whereas the groups of dark monazites from Alaska and Zaire each have considerable spread with only a small overlap near the average for the North American shales.

PRESENTATION OF DATA ON RARE-EARTH ELEMENTS

Presentation of REE data has been discussed by Haskin, Frey, and others (1966). They showed that tabulation of analytical results into Ce-group (La to Gd) and Y-group (Tb to Lu and Y) is the simplest technique, but detailed variations are lumped, and fractionations within a group may be masked by this treatment. Variation in the ratio of two elements has been used, but such ratios ignore other REE in the group. Summing the values for the REE and determining the percentages that each REE contributes offers little advantage over the raw analytical data. Normalization of all REE values to the value of one member of the series to emphasize the relative distributions suffers from the fact that elements chosen for normalization (La and Nd) are usually fractionated, and that two closely related REE patterns may yield normalized distributions which appear to be different. Another technique is to report the ratio of each element to one of its adjacent elements.

Graphical displays readily show information that is concealed in tabular data. This is not so for simple plots of REE abundances versus atomic number or ionic radius, because the sawtooth plot of REE abundances in many minerals may disguise subtle relations in the REE distributions. However, this problem has been overcome by the use of separate plots for even-Z and odd-Z elements (Semenov and Barinskiy, 1958; Adams, 1969). The most successful procedure for comparing all the data for two or more REE distributions on a single graph is the Masuda-Coryell plot (Masuda, 1962; Coryell and others, 1963; Haskin and Gehl, 1962). The sawtooth effect is removed by dividing each distribution, element by element, by the REE abundances in the average chondrite. In recent literature, the CNR for each element has been plotted as the ordinate on a logarithmic scale against the atomic number as the

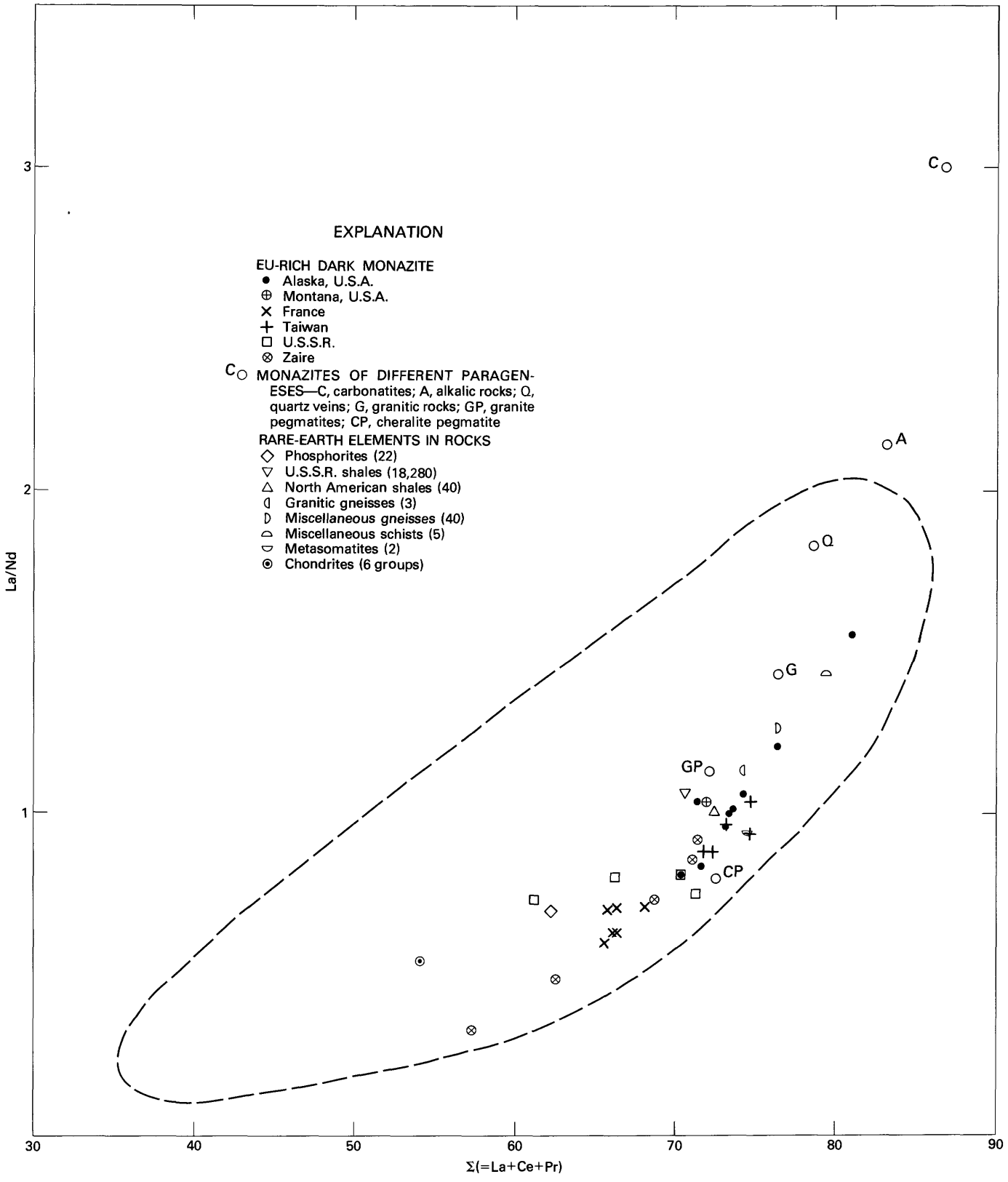

FIGURE 28.—Rare-earth element relations, in atomic percent, for Eu-rich dark monazite from several countries, and for averages of several rock types and chondrites; plotted on the same base as figure 12 of Fleischer (1965, p. 769). The dashed line shows the field for various plutonic and sedimentary rocks. Atomic percents are based on La to Gd=100.

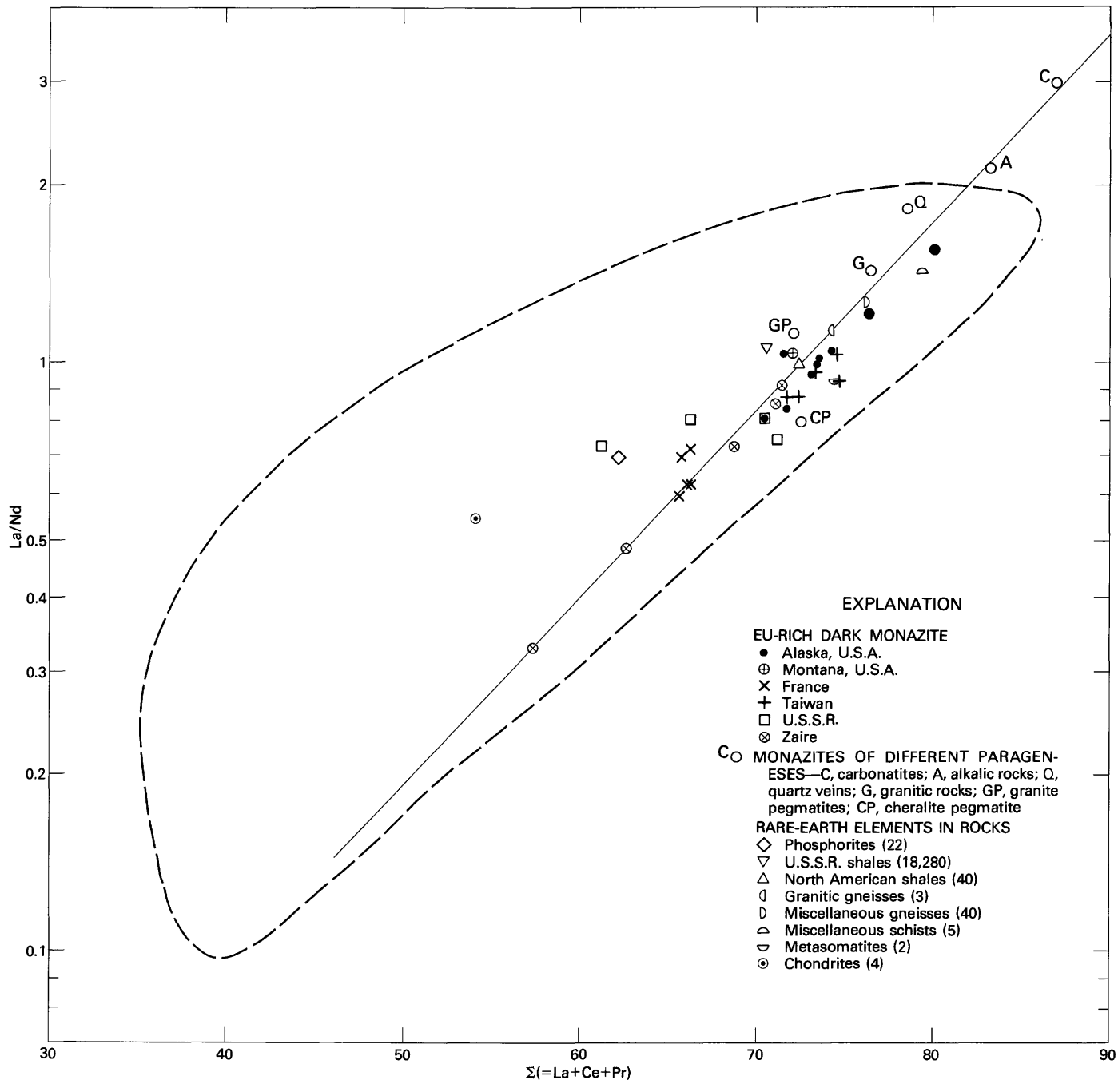

FIGURE 29.—Data of figure 28 plotted on log-normal graph paper. Elements are in atomic percentages. Straight line represents best fit for distribution of points.

abscissa. In this report, the CNR is computed from the atomic percent for each REE (with La to Gd=100 percent) divided by the atomic percent of REE in chondrites, and the abscissa represents the ionic radius for each REE. If the REE distributions in a mineral and in the average chondrite are identical, all ratios are the same and a horizontal line results. Differences appear as curves or sloped lines, and slightly different REE distributions will appear as similar curves.

CNR curves for monazites from granitic and metamorphic rocks are compared with CNR curves for Eu-rich dark monazites from six different areas, with CNR curves for biotites, and with CNR distributions in shales and phosphorites in figure 30. Similar information using the REE abundances in 36 ES (European shales) as the normalizing values is shown in figure 31. CNR curves for three of the four Russian dark monazites are not shown, for they are inconsistent among

themselves as well as departing markedly from the close family of curves for dark monazites from the six areas cited. Similarly, the CNR curve for a nodular dark monazite from Spain is not shown, because this curve does not resemble those for dark monazites nor those for yellow monazites. Compared to REE distributions in yellow monazites from igneous and metamorphic sources, the REE distributions in dark monazites show a more concise pattern in both figures. The plot of CNR for dark monazite is similar to that of the shales, but SNR for dark monazite in figure 31 show a strong divergence from the horizontal line representing the 36 European shales from Nd to Gd. That a part of this divergence may be due to the European shales standard is apparent in figure 31*B*, where SNR values for Sm to Gd in shales from the U.S.A. and U.S.S.R., and in recent ocean sediments are seen to diverge from the horizontal line for European shales in complementary fashion to those of the dark monazites.

CNR plots are shown in figure 32 for other sedimentary rocks, seawater, and rhabdophane, a mineral that French and Russian investigators propose as the precursor to dark monazite. SNR plots are shown in figure 33 for the same items. The igneous, metamorphic, and sedimentary rocks and seawater cited in figures 30–33 are possible sources of the REE in dark monazite, and each is discussed in the section, "Genesis."

Despite the divergences of the SNR for the heavy REE in dark monazites and sedimentary rocks from the line showing the average for 36 European shales in figures 31 and 33, the similarity between REE distributions in dark monazites and in shales, graywackes, and sandstones is more than just coincidence and, as shown in the section, "Genesis," the REE distribution found in dark monazite most likely is inherited from sedimentary materials. The curves of figures 30 and 31 support the idea that a phosphatic shale would supply the REE distribution for dark monazites with little or no metasomatic enrichment or depletion of individual REE. Such enrichments and depletions apparently occur at increased temperatures and pressures, aided by well-charged fluids of magmatic and high-grade metamorphic environments. However, present evidence points to the formation of dark monazite under low-grade metamorphic conditions, mostly thermal.

GENESIS

CONSISTENT PROPERTIES OF DARK MONAZITE

Six worldwide consistent features of Eu-rich, Th-poor dark monazite must be accommodated in any general explanation of genesis. These features are:

1. A dark color that is mainly due to minute particles of amorphous carbon. Where carbon is sparse, translucence is due to ever-present fine rods and sagenitic needles of rutile; to other inclusions; and to microcrystallinity or cryptocrystallinity.
2. Spherical to ellipsoidal forms of grains of dark monazite that may encompass a monocrystal, an aggregate of discrete microcrystals, or a mass of cryptocrystalline monazite with wavy extinctions. Some grains may show radial-fibrous or radial-dentate structure (Donnot and others, 1973, p. 12, fig. 3), annular structure (fig. 22), irregular neoblastic forms (fig. 19), or monazite microcrystals enclosed in a matrix of monazite (Matzko and Overstreet, 1977, p. 32).
3. Large inclusions that are sparse to abundant and consist of sericite, muscovite, biotite, chlorite, quartz, chalcedony(?), rutile, anatase, feldspars, Fe-hydroxides, and lesser amounts of other silicate and oxide minerals.
4. Eu that ranges between 0.2 and 1.0 percent, about 4 to 20 times more than in yellow monazites.
5. Th that is generally less than 1.0 percent, one-seventh or less than the average tenor in yellow monazites.
6. A distribution of REE that is unlike the distributions reported for monazites of igneous or high-rank metamorphic origin, but resembles the distribution of REE in shale and phosphorite (figs. 28–31).

In addition, the following constraints upon the source materials and the process of formation need to be observed:

1. The source rock must supply the phosphate ion, amorphous carbon, Th, and Ti consistent with their tenors in dark monazite. These tenors are commonly found in carbonaceous and silty shales.
2. A thermal rise to about 250°C, with or without pressure, is required. The source of the thermal rise is most likely from intrusive granitic rocks (breached or unbreached by erosion), and less likely from low-grade regional metamorphism.

PREVIOUS PROPOSALS OF ORIGIN

Five possible modes of origin for dark monazites were reviewed by Overstreet (1971) and Matzko and Overstreet (1977); but most of them fail to accommodate all six of the aforementioned consistent features observed in dark monazites. The possible origins include:

1. A primary accessory mineral in igneous rocks,
2. A combined sedimentary and metamorphic origin based on conversion of rhabdophane,
3. A contact-metamorphic mineral,
4. An authigenic sedimentary mineral, and
5. A product of weathering of detrital monazite of igneous origin.

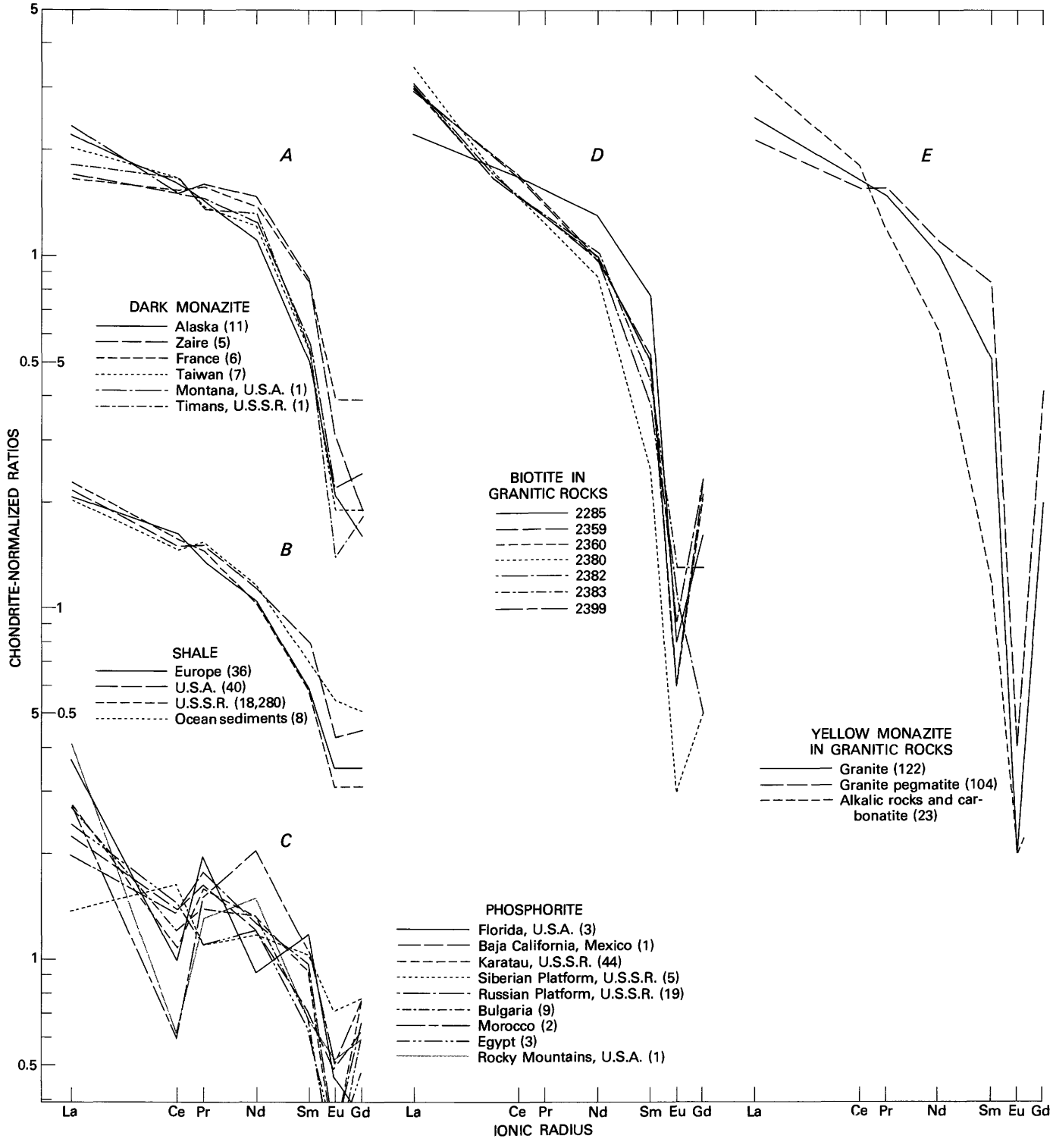

FIGURE 30.—Chondrite-normalized ratios for La to Gd in Eu-rich dark monazites, in yellow monazites from igneous and metamorphic rocks, in biotites from igneous rocks, and in sedimentary rocks. REE abundances in chondrites according to Herrmann (1970); abscissa is REE ionic radius from Whittaker and Muntus (1970); numbers in parentheses, total samples.

A, Ratios for Eu-rich monazites from Alaska, Zaire, Taiwan, Montana, U.S.A. (this report); France (data from Donnot and others, 1973); and Timans U.S.S.R. (Serdyuchenko and Kochetkov, 1974).

B, Ratios for shales and ocean sediments (Haskin and others, 1968; Ronov and others, 1972; Wildeman and Haskin, 1965).

C, Ratios for phosphorites (Alexiev and Arnaudov, 1965; Altschuler and others, 1967; Goldberg and others, 1963; Bliskovskiy and others, 1969; Semenov and others, 1962).

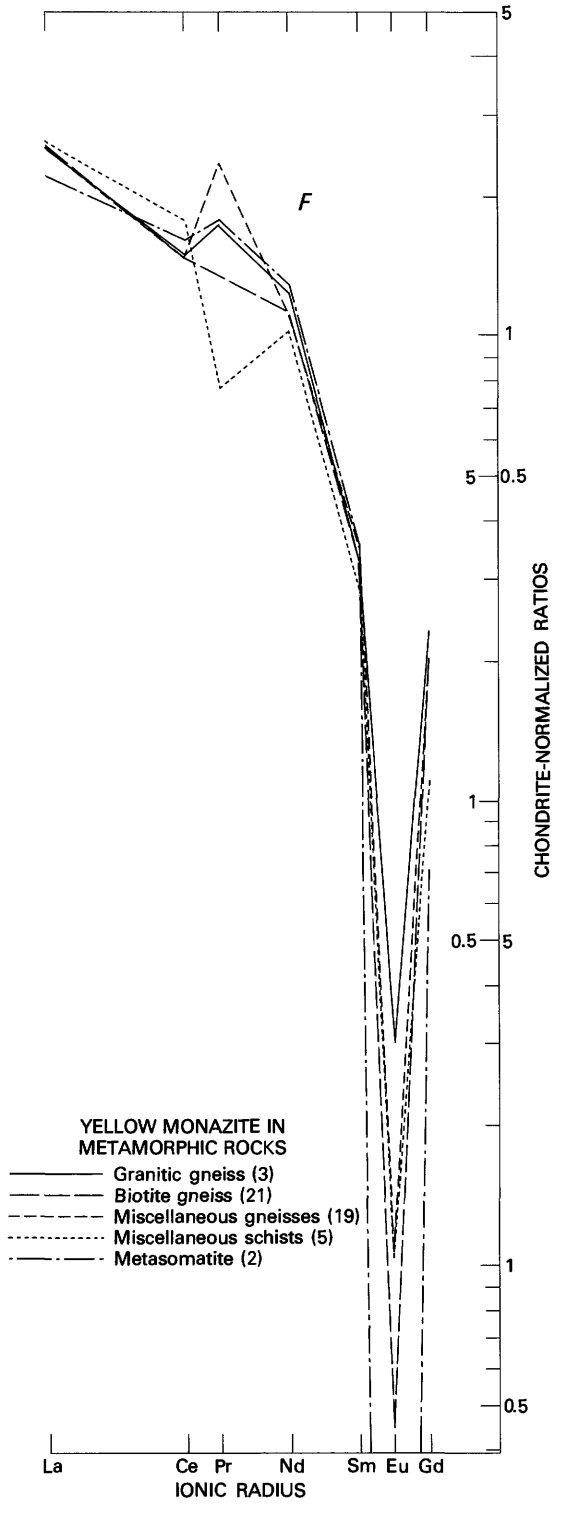

D, Ratios for unaltered biotites from igneous rocks from Idaho, Nevada, Colorado, and Arizona, U.S.A.; data from analyses by P. A. Baedecker, U.S. Geological Survey. Numbers, laboratory references.

E, Ratios for monazites from igneous rocks (Fleischer and Altschuler, 1969).

F, Ratios for monazites from metamorphic rocks; data from Michael Fleischer (written commun., 1969).

Two additional modes of origin for dark monazite have been noted: metasomatic enrichment of REE, as proposed by Li and Grebennikova (1962), and hydrothermal alteration of yellow monazite, as proposed by Soong (1978).

PRIMARY ACCESSORY MINERAL IN IGNEOUS ROCKS

Matzko and Overstreet (1977) rejected an igneous origin for Eu-rich, Th-poor dark monazite in Taiwan on the basis of field relations, physical properties, and chemical composition. The CNR and SNR plots in our figures 30 and 31 lend support for the rejection of this mode of origin on the basis of chemistry, not only for the dark monazite from Taiwan, but also for Eu-rich, Th-poor dark monazites elsewhere.

CONVERSION OF AUTHIGENIC RHABDOPHANE

The combined sedimentary and metamorphic origin, reviewed by Overstreet (1971) and Matzko and Overstreet (1977), whereby sedimentary oolites of rhabdophane, a hydrous Ce-group phosphate, are converted into dark monazite during regional metamorphism (Kosterin and others, 1962; Donnot and others, 1973; Altmann and others, 1970), is here considered inappropriate for several reasons, including chemical composition, form, and temperature of conversion.

The REE distribution in rhabdophanes is entirely different from that in dark monazites. This compositional inconsistency in REE distribution prevents an acceptance of rhabdophane as a precursor mineral. CNR plots for rhabdophanes (fig. 32) prove that their REE distributions are indeed different from those of dark monazite; moreover, the REE distributions in rhabdophanes have no consistent pattern among themselves. REE distributions of 16 rhabdophanes, plotted as La/Nd vs. Σ (figs. 34, 35), and compared with similar data for monazites (figs. 28, 29), show seven rhabdophane points that lie beyond the monazites from alkalic rocks and carbonatites, and have unusual La/Nd ratios of greater than 3. One rhabdophane has a low value for Σ of 36.5 percent. In figure 35, several rhabdophane points lie well off the straight log-normal distribution line that fits most monazite points.

Most dark monazites worldwide are pelletlike, not oolitic; and rhabdophane is absent from all the pellets examined. Rhabdophane, where found with monazite, is a secondary mineral formed by hydration of the monazite (Adams, 1968; Serdyuchenko and others, 1967), instead of being the precursor mineral.

Rhabdophane has been converted into monazite by

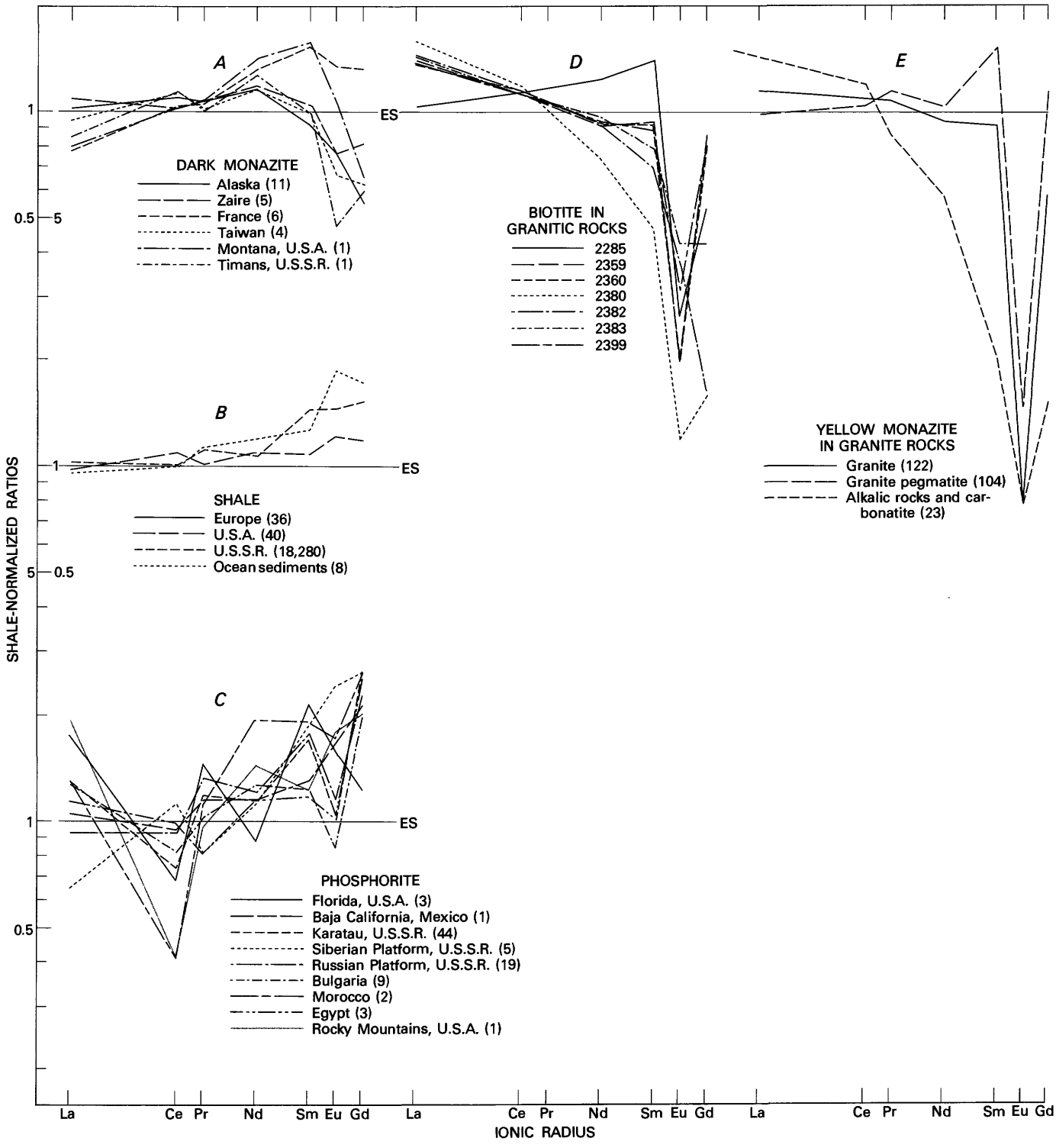

FIGURE 31.—Shale-normalized ratios for La to Gd in Eu-rich dark monazites, in yellow monazites from igneous and metamorphic rocks, in biotites from igneous rocks, and in sedimentary rocks. REE abundance in 36 European shales (ES) according to Herrmann (1970); abscissa is REE ionic radius from Whittaker and Muntus (1970). Numbers in parentheses, total samples.

A, Ratios for Eu-rich monazites from Alaska, Zaire, Taiwan, Montana, U.S.A. (this report); France (data from Donnot and others, 1973); and Timans, U.S.S.R. (Serdyuchenko and Kochetkov, 1974).

B, Ratios for shales and ocean sediments (Haskin and others, 1968; Ronov and others, 1972; Wildeman and Haskin, 1965).

C, Ratios for phosphorites (Alexiev and Arnaudov, 1965; Altschuler and others, 1967; Goldberg and others, 1963; Bliskovskiy and others, 1969; Semenov and others, 1962).

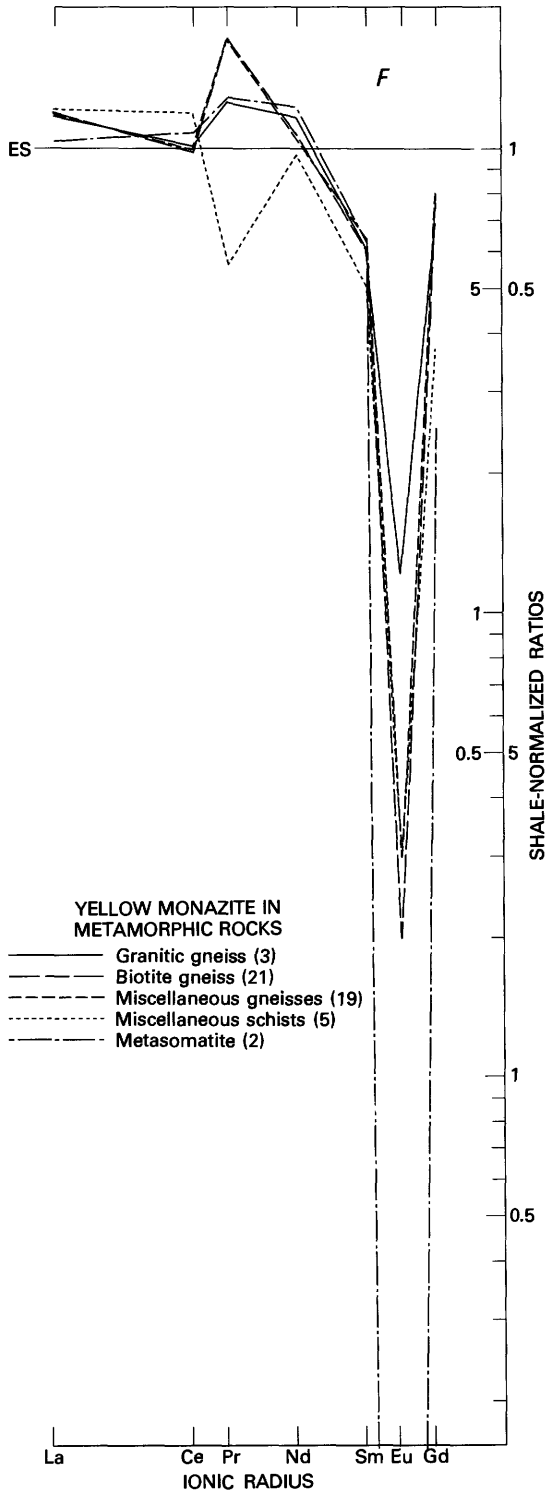

D, Ratios for unaltered biotites from igneous rocks from Idaho, Nevada, Colorado, and Arizona, U.S.A.; data from analyses by P. A. Baedecker, U.S. Geological Survey. Numbers, laboratory references.

E, Ratios for monazites from igneous rocks (Fleischer and Altschuler, 1969).

F, Ratios for monazites from metamorphic rocks; data from Michael Fleischer (written commun., 1969).

heating at 300°C for 5 days in a crucible containing water (Carron and others, 1958, p. 273). Dark monazite from eastern Siberia was found to lose water upon heating to 400°C (Kosterin and others, 1962, p. 26). Therefore, these authors regarded 400°C as the temperature at which metamorphic conversion of rhabdophane (hydrous) to monazite (anhydrous) began, and they interpreted the dark monazite to be a product of metamorphism. In France, the reflectivity of carbonaceous material in dark-monazite-bearing phyllitic shales was used to show that the temperature of regional metamorphism at which the Eu-rich dark monazite of Bretagne formed from supposedly preexisting sedimentary oolites of rhabdophane was greater than 200°C but less than 300°C (Donnot and others, 1973, p. 11). The iron-sulfide mineral, greigite, which is included in grains of dark monazite from Taiwan, is unstable above 295°C, and therefore the greigite-bearing dark monazite must have formed below that temperature (Matzko and Overstreet, 1977, p. 28). Although several of these estimated temperatures of formation of dark monazite are near the temperature at which rhabdophane has been experimentally converted to monazite, the data on preexisting rhabdophane that is converted into dark monazite through metamorphism is regarded here as insufficient to explain the origin of Eu-rich, Th-poor dark monazite.

CONTACT-METAMORPHIC MINERAL

The origin of Eu-rich and Th-poor dark monazite as a contact-metamorphic mineral in the thermal aureole of cassiterite-bearing granites was first proposed by J. J. Altmann, Bureau de Recherches Géologiques et Minières, France, in 1970 (Overstreet, 1971). In the Oulmès, Morocco area, investigators cited the source of Eu-bearing gray monazite to be the contact-metamorphic aureole around the granite of Oulmès (el Aissaoui and Devismes, 1977). However, they did not explicitly state that this variety of monazite originated by contact metamorphism; this implication is left to the reader. A contact-metamorphic origin for dark monazite in Taiwan was thought to be unlikely by Matzko and Overstreet (1977, p. 29), because dark monazites of possible contact metamorphic origin in Zaire and the Malagasy Republic are associated with tin, but tin minerals are not found with dark monazite on the western beaches of Taiwan. Also, certain minerals that indicate contact metamorphism are lacking in the beach deposits of Taiwan. However, we feel that the contact-metamorphic mode of origin of dark monazite in Taiwan should not be rejected on the basis of negative evidence.

If the association of dark monazite and tin can be

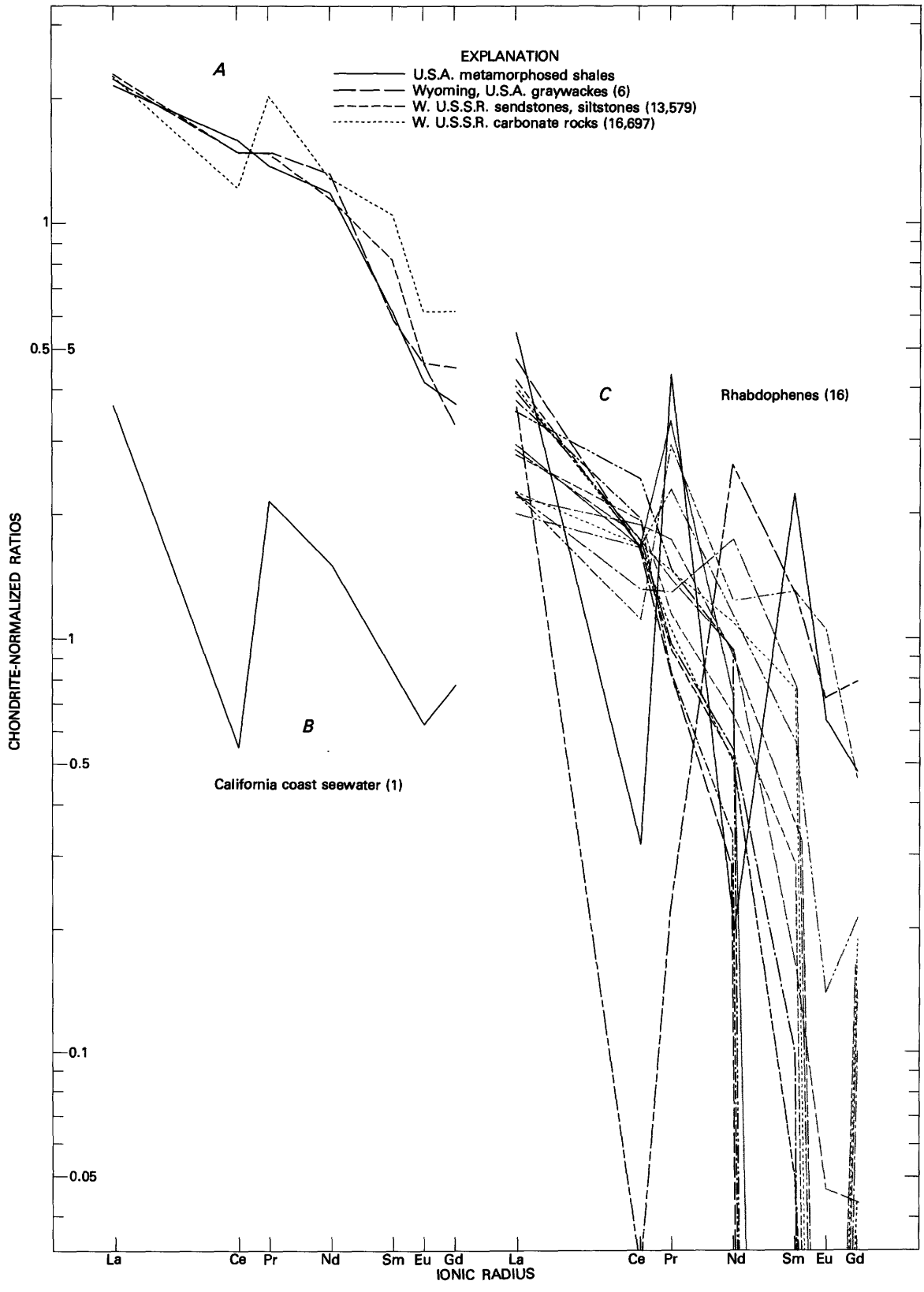
EXPLANATION
U.S.A. metamorphosed shales
Wyoming, U.S.A. graywackes (6)
W. U.S.S.R. sendstones, siltstones (13,579)
W. U.S.S.R. carbonate rocks (16,697)
A
B
C
California coast seewater (1)
Rhabdophenes (16)
CHONDRITE-NORMALIZED RATIOS
1
0.5
5
1
0.5
0.1
0.05
La
Ce
Pr
Nd
Sm
Eu
Gd
La
Ce
Pr
Nd
Sm
Eu
Gd
IONIC RADIUS

discarded as part of the concept of origin by contact metamorphism, then this concept has the possibility of satisfying all the characteristics of dark monazite listed above. The association, Eu and Sn, was first noted by Phan (1967), who cited Eu-rich monazites in cassiterite placers in eastern Siberia and Malaysia. This concept was next recited by Serre-Ratsimandisa (1970, p. 160), who noted coincident geochemical anomalies for Eu and Sn in the southern part of the Malagasy Republic and mentioned the presence of thousands of tons of Eu-bearing dark monazite localized in a contact-metamorphic halo around deposits of cassiterite in Zaire. However, in the Malagasy Republic, the largest cassiterite occurrence is located outside the area where Eu and Sn anomalies were found (Serre-Ratsimandisa, 1970, p. 160). Furthermore, tin mineralization is unknown in a number of places where Eu-rich dark monazite was found, including Taiwan, some areas in Alaska, Montana, northern Pakistan, the beach at Cox's Bazar in Bangladesh, and the Timan, South Yenisei, and northern Verkhoyan'e districts in the U.S.S.R. Therefore, the association of cassiterite with dark monazite must be regarded as a fortuitous one caused by the mingling in placers of detrital grains of heavy resistant minerals from several sources. A tabulation of minerals associated with dark monazite worldwide shows an equal association with gold and somewhat lesser associations with scheelite, chromite, and silver and copper minerals.

In areas such as Alaska, Montana, Peru, Siberia, northern Pakistan, France, Spain, Zaire, Malagasy Republic, and Morocco, published geologic maps disclosed granitic intrusive rocks near the sites of alluvial deposits containing dark monazite. Except for the lack of regionally metamorphosed rocks near the dark monazite localities in Montana, the geologic maps of these areas also revealed nearby metasedimentary rocks. Thus, the arguments in favor of a mode of origin of dark monazite by contact metamorphism or by (low-grade) regional metamorphism might still be regarded as equivocal.

The most convincing argument in favor of contact metamorphism rather than regional metamorphism as a mode of origin is based on the expectable distribution of dark monazite. If regional metamorphism were the process, then the mineral would have a wide distribution and would be rather common in low-grade metamorphic terranes. If the mineral forms in contact aureoles, then the distribution should be restricted to these generally thin zones. A literature search confirms present observations that dark monazite is indeed sparsely distributed and apparently requires a specific set of conditions to form. These conditions must include: (1) presence of a REE-bearing carbonaceous shale, and (2) baking by the heat of a granitic intrusive rock at temperatures as high as 300°C.

AUTHIGENIC SEDIMENTARY MINERAL

An authigenic sedimentary origin for the pelletlike black monazite on the beaches and offshore bars of southwestern Taiwan was first proposed by the senior author in 1958, based on field observations. This mode of origin was reviewed by Overstreet (1971, p. 38) and Matzko and Overstreet (1977, p 29–30), who cited physical features that favor an authigenic sedimentary origin:

1. The grains are cemented aggregates lacking the typical radial or concentric structures of oolites.
2. Two generations of monazite are present in single pellets; the earlier forms large particles (20 μm) and the later forms the matrix (2 μm).
3. The mineral composition is quite variable from pellet to pellet because of the amount and kinds of inclusions.
4. Monazite in the pellets can enclose and be partially protected by projections of detrital grains of igneous origin.
5. Nongraphitic carbon and greigite are present.
6. Hardness is low.
7. Microcrystallinity characterizes some monazite and quartz.

Chemical evidence cited by Matzko and Overstreet (1977, p. 31) that supports the concept of an authigenic sedimentary origin for black monazite in southwestern Taiwan includes the following:

FIGURE 32(facing page).—Chondrite-normalized ratios for La to Gd in sedimentary rocks, seawater, and rhabdophanes. REE abundance in chrondrites according to Herrmann (1970); abscissa is REE ionic radius from Whittaker and Muntus (1970). Numbers in parentheses, total samples. Line patterns for rhabdophanes represent individual samples. *A*, Ratios for metamorphosed shales (Haskin and others, 1968), graywackes (Wildeman and Condie, 1973), sandstones, siltstones, and carbonate rocks (Ronov and others, 1972). *B*, Ratios for seawater (Goldberg and others, 1963). *C*, Ratios for rhabdophanes from U.S.S.R., U.S.A., and Greenland (Michael Fleischer, written commun., 1963, 1976; Vlasov, 1966, v. 2, p. 295; Mitchell, 1965; Dumler and others, 1970).

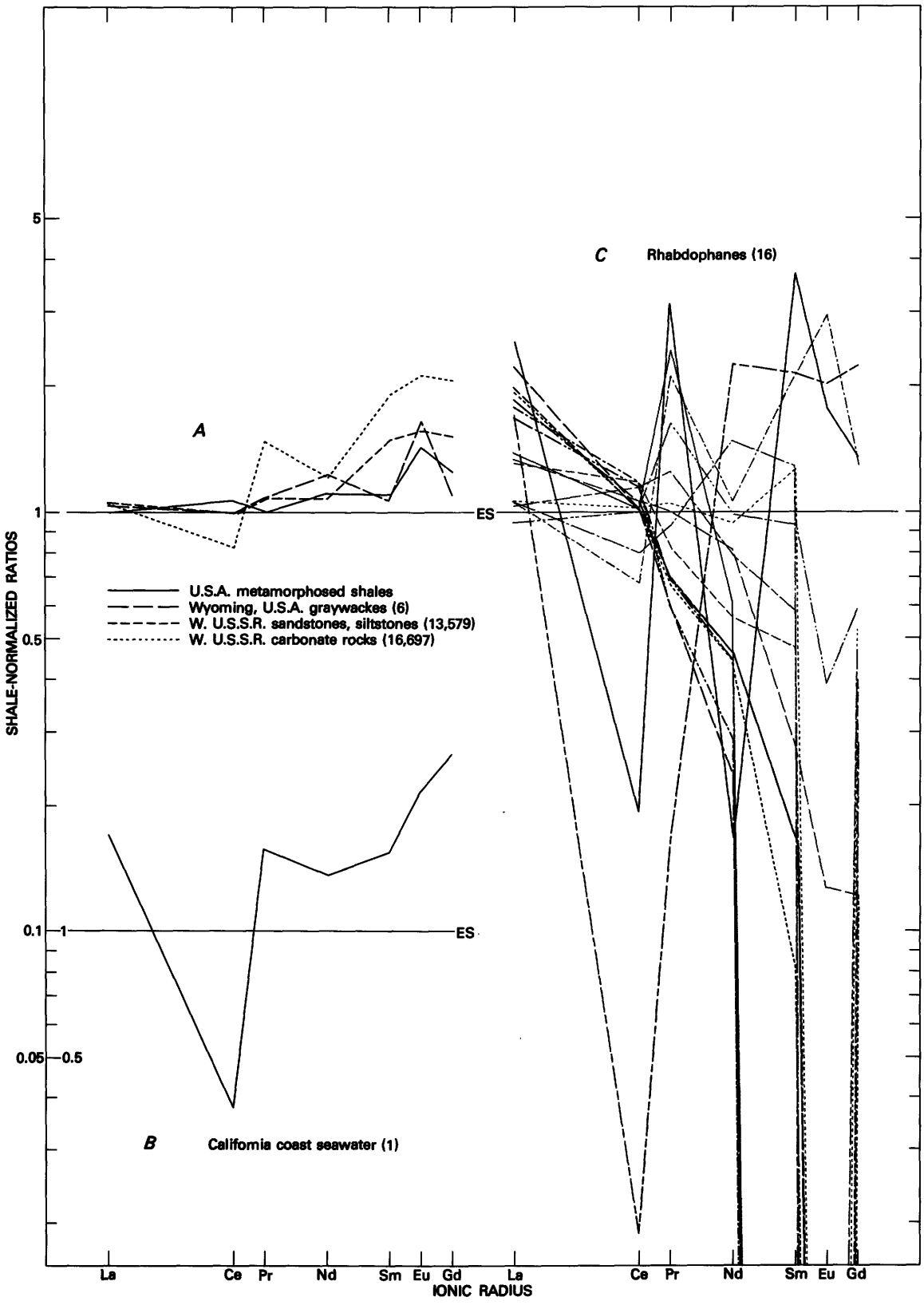
SHALE-NORMALIZED RATIOS
5
1
0.5
0.1
0.05
A
B
C
Rhabdophanes (16)
ES
1
0.5
U.S.A. metamorphosed shales
Wyoming, U.S.A. graywackes (6)
W. U.S.S.R. sandstones, siltstones (13,579)
W. U.S.S.R. carbonate rocks (16,697)
California coast seawater (1)
La
Ce
Pr
Nd
Sm
Eu
Gd
IONIC RADIUS

1. All the black pelletlike monazite is lower in thorium, a characteristic of monazite formed at low pressure and temperature (Overstreet, 1967, table 2).
2. Cerium and thorium are removed from monazite by weathering.
3. The high content of SiO_2 for monazite pellets is due to inclusions of quartz and other silica-bearing minerals.
4. Low contents of Mg, Na, and Ca are due to overgrowths on monazite and inclusions in the dark pellets of authigenic and detrital silicate minerals.
5. The fairly high percentage of TiO_2 (1.7 percent) in the dark monazite is mainly due to inclusions of rutile and anatase.
6. Some of the opaque material in the dark pelletlike monazite consists of authigenic iron sulfides, including greigite and pyrite.

An example of possible authigenic monazite in thin carbon-banded siltite in Precambrian metasedimentary rocks of northern Idaho and Montana and southeastern British Columbia is described by Huebschman (1973, p. 692). Clusters of tiny monazite crystals are concentrated in dark-gray carbon-rich bands less than 1 mm thick, but they show optical unison, indicating that they crystallized during metamorphism. An interpretation of recrystallized monazite of authigenic origin is acceptable for this example; otherwise, introduction of metasomatic fluids and deposition along the carbonaceous bands would be required.

In the present study, evidence in support of an authigenic origin of Eu-rich dark monazite has not been recognized in any of the detrital deposits that contain this variety of monazite. If this mode of origin were valid, then this unusual variety of monazite would be common and more abundant than is presently known in sedimentary terranes. Hence, an authigenic origin is unlikely.

WEATHERING PRODUCT OF DETRITAL MONAZITE OF IGNEOUS ORIGIN

A mode of origin discussed by Matzko and Overstreet (1977, p. 30–32) for the dark monazite in Taiwan is a combination of weathering and diagenetic growth processes. Weathering of at least two sources of REE is required to supply the REE distribution found in this dark monazite. Diagenesis in low-temperature conditions of a near-surface environment (not specified) is supported by textural features of Taiwanese dark monazite (Vinogradov and others, 1960), and by the synthesis of a monoclinic REE-phosphate isotructural with monazite that was produced in aqueous solution held at 97°C for 1 year (Carron and others, 1958, p. 273). A marine environment is thought by Matzko and Overstreet (1977, p. 33) to be unlikely for the precipitation of dark monazite, because dark monazite has a high content of Ce, and Ce is normally less abundant than La or Nd in seawater. This interpretation is another instance where presumption is made that the REE distribution in dark monazite must reflect the REE distribution of the source material(s). Such presumptions must be considered valid working hypotheses until proven erroneous.

METASOMATIC ENRICHMENT

The formation of dark monazite by metasomatic processes would involve the transfer of REE as complexes with $CO_3^=$, $SO_4^=$, and F^- from granitic rocks into the enclosing country rocks (Kosterin, 1959; Li and Grebennikova, 1962). Easily soluble complex fluorides of the $REFeF_6$ type, aided by pneumatolytic solutions, are suggested as the agents responsible for the formation of low-Th monazite in central Asia and the Far East. Inasmuch as Th is less mobile than the REE, this low mobility would cause the metasomatic monazite to contain small amounts of Th. A low-Th monazite from the North Caucasus, U.S.S.R., is cited as a metasomatic mineral formed in a pneumatolytic process, mainly by replacement of allanite and apatite (Ploshko, 1961). Ploshko indicated (1961, p. 73) that the material for monazite was provided by the rare earths and phosphorus extracted from orthite (=allanite) and apatite, and possibly from new additions of these elements brought in by later solutions.

The process is more complex than any of the other modes and would involve transfer of considerable REE and P into contact-metamorphic zones to provide large sources of dark monazite. Conversely, metasomatic depletion of heavy REE might yield sparse deposits of dark monazite with the observed REE distributions. The geologic data on the Alaskan occurrences of Eu-rich

FIGURE 33(facing page).—Shale-normalized ratios for La to Gd in sedimentary rocks, seawater, and rhabdophanes. REE abundances in 36 European shales (ES) according to Herrmann (1970); abscissa is REE ionic radius from Whittaker and Muntus (1970). Numbers in parentheses, total samples. Line patterns for rhabdophanes represent individual samples. *A*, Ratios for metamorphosed shales (Haskin and others, 1968), graywackes (Wildeman and Condie, 1973), sandstones, siltstones, and carbonate rocks (Ronov and others, 1972). *B*, Ratios for seawater (Goldberg and others, 1963). *C*, Ratios for rhabdophanes from U.S.S.R., U.S.A., and Greenland (Michael Fleischer, written commun., 1963, 1976; Vlasov, 1966, v. 2, p. 295; Mitchell, 1965; Dumler and others, 1970).

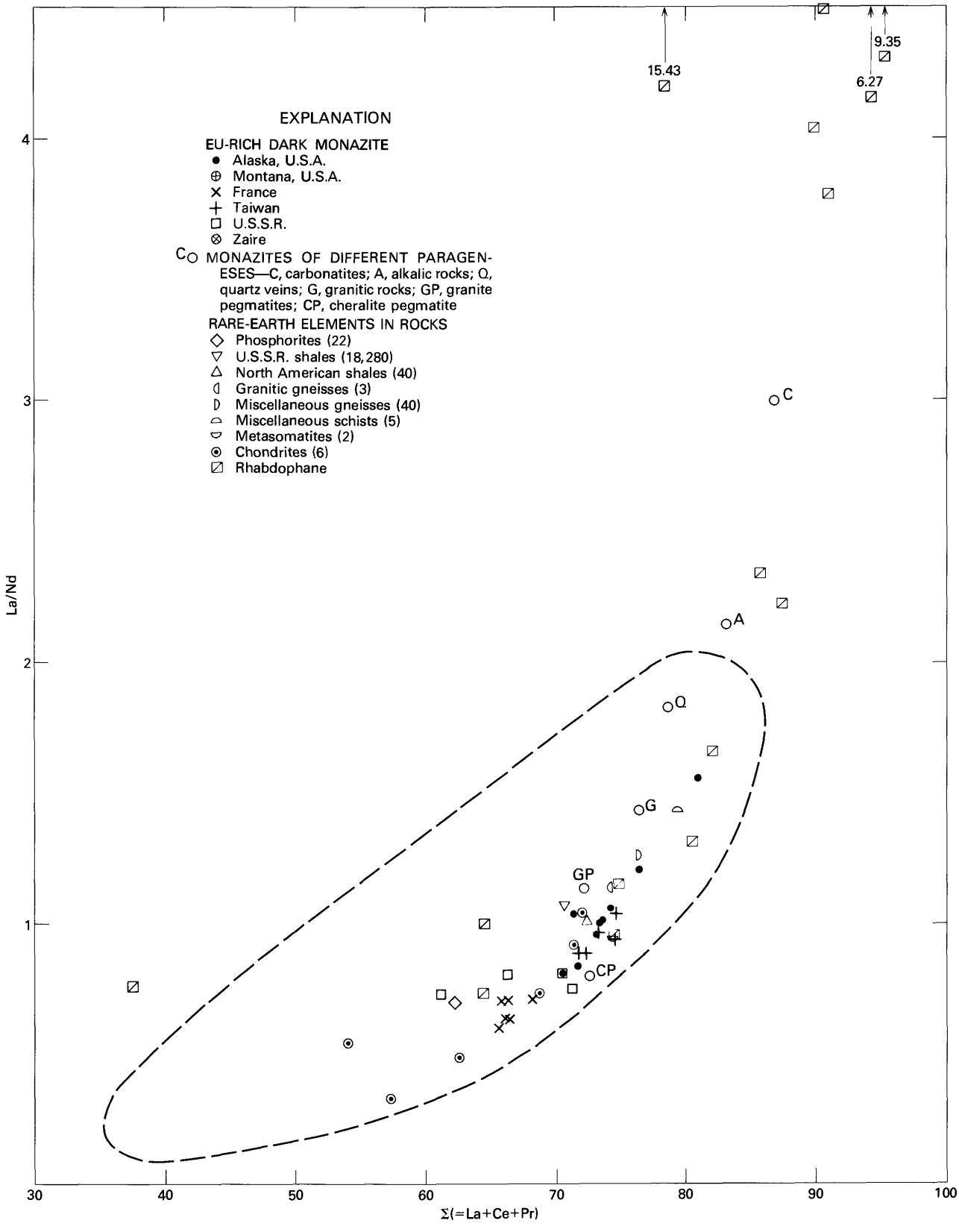

FIGURE 34.—Rare-earth element relations, in atomic percent, for 16 rhabdophanes from U.S.S.R., United States, and Greenland plotted on the data of figure 28. The dashed line shows the field for various plutonic and sedimentary rocks.

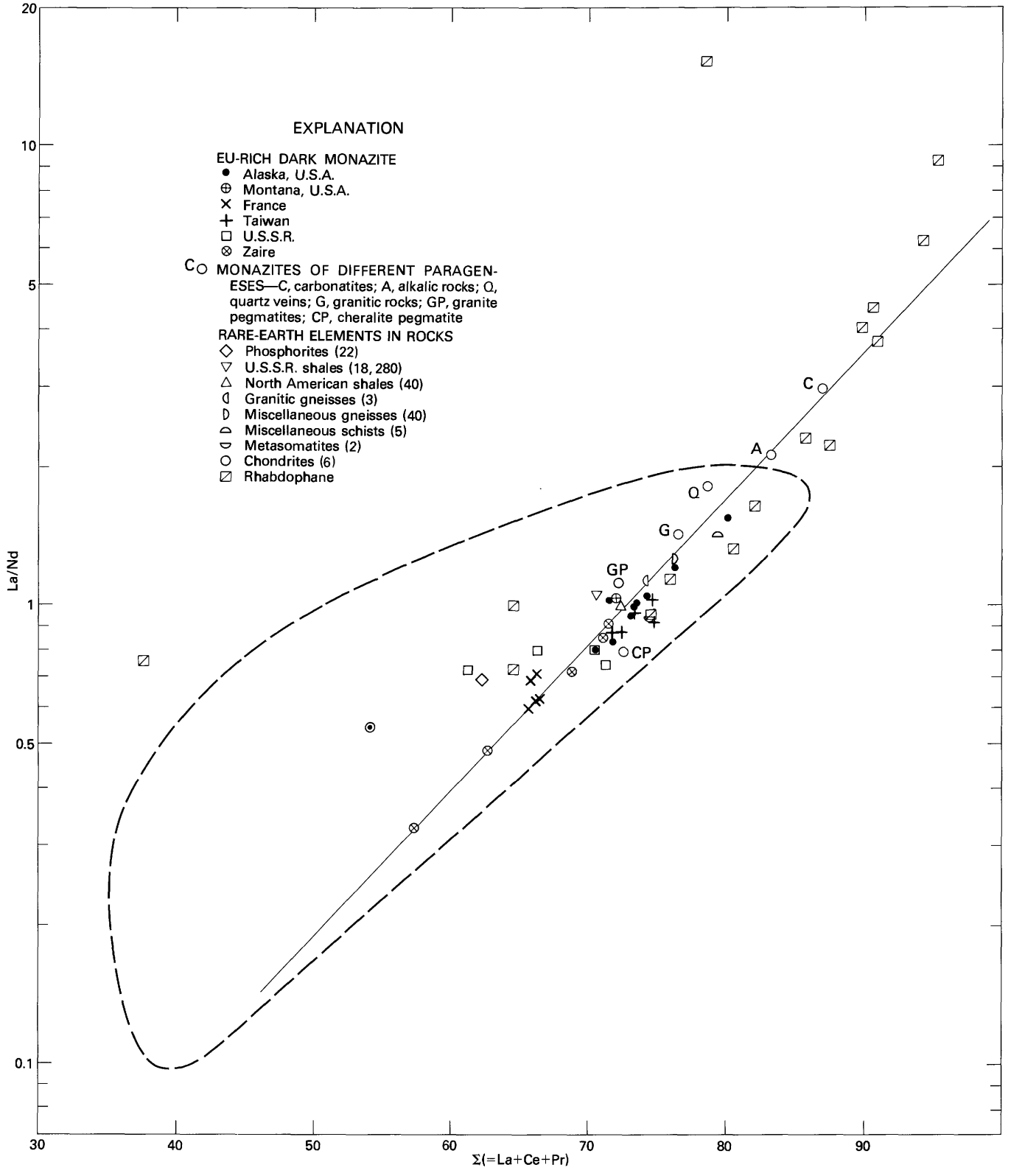

FIGURE 35.—Data of figure 34 plotted on log-normal graph paper. The elements are in atomic percentages. The straight line represents a best fit for the distribution of points.

dark monazite do not permit either acceptance or rejection of this mode of origin. However, a difficulty in accepting metasomatic enrichment is the consistency in physical and chemical properties of dark monazite, throughout Alaska as well as worldwide. This consistency is less likely as a result of metasomatic enrichment than if a widespread rock with consistent composition was metamorphosed to yield dark monazite.

HYDROTHERMAL ALTERATION

Based mainly on textural relations of some corroded cores of yellow monazite enclosed in dark monazite pellets, Soong (1978) proposed hydrothermal alteration of the yellow monazite to produce the dark monazite host-mineral. He suggested that Th would decrease during hydrothermal attack, for it is not stable in monazite that forms under the low temperatures compatible with deposition of greigite, which very likely is deposited after alteration. As supporting evidence, he cited (1) optical continuity obtains in the well-crystallized core and the surrounding cryptocrystalline monazite, (2) enclosed minerals other than monazite and quartz are rare, (3) the quartz inclusions show undulatory extinction typical of hydrothermal vein quartz, and (4) the Ce/La ratios of black and yellow monazites are similar enough to support the concept that black monazite is an alteration product of yellow monazite.

We have demonstrated (fig. 30) that the REE distributions of dark and yellow monazites are dissimilar; therefore, these varieties are unrelated, if the premise of inherited REE distributions is true. Worldwide production by hydrothermal alteration of dark monazite with the restricted REE distributions shown in figure 30 would be fortuitous and less likely than derivation from a worldwide source rock with a common chemistry.

PREFERRED MODE OF ORIGIN

The mode of origin favored here is thermal metamorphism in the outer parts of contact aureoles around granitic rocks that intruded carbonaceous shales. These shales were the sources of the REE (as shown by figs. 28–31) and phosphate ion, and their REE distributions were inherited by the neoblasts of dark monazite that formed in phyllitic rocks formed from shales. The inclusions of amorphous carbon, of rutile rods and needles from degraded biotites in the shales (Harker, 1939, p. 160, fig. 69B), and of various large, apparently detrital grains are interpreted here as having been trapped in rapidly growing neoblasts of dark monazite. The amount of REE represented by dark monazite is undoubtedly a large part of the REE available in the unmetamorphosed clay minerals of the shale, but a considerable amount of the REE is present in other minerals such as biotite, apatite, and chlorite.

To learn the REE distribution in biotite, which largely contributes to the formation of shales, seven unaltered biotite samples from five calcalkaline igneous masses ranging from two-mica granite to biotite granodiorite, and ranging in age from 24 to 1,150 m.y. (million years) were submitted for neutron activation analysis. The results shown in table 11 and figures 30 and 31 indicate that the REE distributions in biotites are indeed like those in dark monazites, except for slightly greater amounts of La and lesser amounts of Eu and Gd. The striking similarity between REE distributions in biotites and in yellow monazites from granitic rocks confirms that the REE distribution in the biotites is due mainly to the REE in tiny included yellow monazites. The dissimilarity between REE distributions in igneous biotites and shales is due to the difference in composition between biotite before being chemically weathered and the final product that is incorporated in the shale.

If our surmise is correct that the REE distribution in dark monazite was inherited from that in shale which received its REE distribution from that in biotite, then the differences between these distributions needs further comment. The approach to chondrite composition, reflected by the flattening of the slope of the distribution curves from biotite to shale, may be an instance of the REE distribution tending toward a steady state (cosmic abundances) as the mineral phase of greater entropy (biotite) is disintegrated and the decomposition products are distributed throughout the depositing mud that eventually turns to shale. During the mild heat of formation of dark monazite, a reversal in this trend toward the chondritic distribution produces the REE distribution in dark monazite that appears to be intermediate between those of shale and biotite. We infer that among Ce-group-rich minerals and rocks, as the heat of formation (enthalpy) increases, the amounts of Sm, Eu, and Gd decrease relative to the lighter REE. Inspection of the CNR in the several sets of REE distribution (figs. 30 and 32) shows that the ratio for Ce is almost constant at 1.7 and acts as an inflection point around which La generally increases or decreases inversely with the heavier REE.

The importance of metasomatic enrichment from the granitic intrusive rocks cannot be assessed from present data, but it is probably slight. The problem of the two light-colored rinds shown by the dark monazites from Zaire (fig. 22) might be resolved by assuming that periods of hydrothermal alteration followed two distinct periods of neoblastic growth. It is tempting to invoke introduction of new materials by metasomatic solu-

TABLE 11.—*Rare-earth elements in biotite from igneous rocks, in ppm.*

[Analyst: P. A. Baedecker, U.S. Geological Survey. <, less than shown; Σ, sum of La+Ce+Pr atomic percentages, where La to Gd=100 percent; La/Nd, ratio of atomic percentages]

Sample No.	D2285B	D2359B	D2360B	D2380B	D2382B	D2383B	D2399B
Area	Idaho	Idaho	Idaho	Nevada	Colorado	Colorado	Arizona
Rock type	Granite	Granodiorite	Granodiorite	welded tuff	Quartz monazite	Quartz monazite	Quartz monazite
Age (m.y.)	1150	67	68	24	41	40	24
La	359.7	103.0	106.3	746.3	1397.0	697.7	405.3
Ce	799.7	169.0	181.3	1119.7	2270.3	1111.3	672.7
Nd	394.3	62.0	66.3	316.7	830.0	441.0	256.0
Sm	77.7	11.1	11.5	34.9	108.2	62.7	42.1
Eu	2.85	.44	.50	1.65	11.7	6.63	2.94
Gd	24.8	7.60	<.74	9.83	22.0	28.2	30.3
Tb	6.49	.98	1.00	1.56	4.48	2.98	4.22
Tm	1.98	<.61	<.67	<.64	<1.11	<1.00	1.98
Yb	11.2	1.43	1.20	2.20	3.93	3.40	11.1
Lu	1.48	.22	.23	.41	.59	.49	1.62
La to Gd[1]	1657.	353.	373.	2229.	4635.	2348.	1409.
	70.9	77.8	79.1	84.2	79.7	77.8	77.3
La/Nd	.95	1.73	1.67	2.45	1.75	1.64	1.64

[1]Totals are averages of 3 analyses for each sample; Pr not reported due to inferences in instrumental neutron activation analysis.

tions, with Eu enrichment resulting from hydrothermal destruction of Eu-bearing feldspars, for the second episode of growth of those dark monazites. Evidence for low temperature of formation includes the presence in the dark monazite of amorphous carbon, chlorite, and greigite (in Taiwanese dark monazite). Indirect evidence is the lack of dark monazite in concentrates panned at localities close to a granitic contact in Montana in contrast to the presence of dark monazite in concentrates panned 3–6 km downstream from a contact between granite and phosphatic shale.

Geologic data from the investigation of many panned concentrates in Alaska where Eu-rich monazite was identified support an origin by contact metamorphism of carbonaceous shales by silicic to intermediate stocks. The most common intrusive rock is biotite granite, and the stocks are interpreted to be cupolas of granitic batholiths. In areas where intrusive granitic rocks are more than 5 km from shaly to phyllitic source rocks, a subjacent granitic mass must be inferred. Host rocks for the Eu-rich monazite are spotted phyllites in which dark elliptical spots are monazite neoblasts (fig. 20). The original rocks are carbonaceous shales or shaly members of phosphorites with REE content presumed to be comparable to rocks of the Phosphoria Formation in the west-central region of the North American continent (Gulbrandsen, 1966, 1975; Maughan, 1975, 1976).

Steps in the formation of the dark Eu-rich monazite are interpreted to be:

1. Deposition and lithification of clay- and silt-size carbonaceous, biotitic sediments. REE content of these sediments most likely occurs in the phyllosilicates as adsorbed ions, whereas the phosphate ion is generally bound up in phosphate minerals like carbonate fluorapatite.

2. Metamorphic conditions of low grade (with temperatures 200°C to 300°C) mobilized the REE sufficiently to combine with phosphate ions released from the breakdown of phosphate minerals to form monazite nuclei in the carbonaceous host rock. During this mobilization, fractionation of the light REE plus a small depletion of Eu and Gd changed the REE ratios slightly from those of the unmetamorphosed sediments to those of the resulting dark monazite. Much of the REE apparently remains in the rock, because the quantity of dark monazite produced is small compared to the volume of the source rock. Moderate to rapid growth of the monazite resulted in the mineral enclosing other minerals of the host rock: minute carbon specks, neoblastic rutile rods and needles, and generally larger grains of opal, chalcedony, quartz, micas, chlorites, sphene, zircon, and minor amounts of other oxide and silicate minerals. Initial growth was amoeboid as indicated by micro-, poly-, and cryptocrystalline internal textures, and irregular shapes of dark monazite spots (fig. 19). Later growth was uniform enough to produce radial and annular structures and spherical shapes. Directed pressures flattened and elongated most grains and wrapped micaceous minerals of the phyllitic host rock around these grains (figs. 18–20), and apparently rotated some from their positions of initial growth (Donnot and others, 1973, p. 13).

3. Weathering and erosion released the monazite from the host rocks, and concentrations in modern

stream and beach placers sufficient to constitute commercial deposits are only recently being recognized. Apparently concentrations of monazite in the host rocks are insufficient to enable mining at the source (Donnot and others, 1973, p. 13).

CONCLUSIONS AND IMPLICATIONS

Based on the foregoing discussions of the several occurrences in Alaska of Eu-rich dark monazite, as well as elsewhere in the world, the following conclusions are drawn:

1. Dark monazite is a source of REE, especially Eu; and where it forms sufficiently large deposits, it may be mined for these elements, as in Bretagne, France. Marginal and (or) commercial deposits are known in the beaches of southwestern Taiwan, and in the Kivu district of eastern Zaire. The commercial possibilities of deposits in Siberian localities are not known. The presence of dark monazite at many localities in Alaska indicates that minable deposits may be discovered there.

2. Biotite granite is the most common igneous rock associated with in-place occurrences as well as placer deposits of dark monazite. The most common host rocks are weakly metamorphosed shales and argillites. The process here thought to be dominant in the formation of dark monazite is contact metamorphism, but low-grade regional metamorphism also may be a factor. Contact-metamorphic deposits tend to occupy small areas on the borders of granitic intrusives, whereas regional-metamorphic deposits would be more widespread. The restricted areas of dark-monazite placers favor contact metamorphism as the source of the thermal energy required to form the mineral.

3. Dark monazite is characterized by a gray to black pelletlike form; high-Eu and low-Th contents; and numerous inclusions, mostly microfine amorphous carbon, very fine rutile rods, and lesser quantities of silt-size detrital grains.

4. REE distributions in dark monazite are similar to those of sedimentary rocks including shales, graywackes, limestones, and phosphorites. They are dissimilar to REE distributions in yellow monazites from igneous and high-grade metamorphic rocks. Compared to dark monazites, almost all yellow monazites are Eu-poor and Th-rich.

5. The relation La/Nd versus Σ for all types of monazite is apparently log-normal, but the reason for log-normal distribution rather than any other distribution is unclear. As the ionic radius decreases in size from light to heavy REE, the abundances of odd-numbered and even-numbered series of REE decrease in a log-normal mode for monazite. Inspection of data on 642 monazites (Michael Fleischer, unpub. data, 1982) shows that La and Ce are complementary, proving a complete substitution between them, with the greatest dispersion of abundances in the high-Σ range.

6. REE distributions in dark monazite are dissimilar to the REE distribution in seawater. Under the premise that REE distributions are inherited, origins by precipitation from seawater or under diagenetic conditions are unlikely.

7. The "Eu-Sn affinity" is fortuitous. Dark monazite, with density=4.5 (worldwide average) is expected to accumulate with other resistant heavy minerals. These minerals (with D) include garnet (3.3–4.3), sphene (3.4–3.6), allanite (3.5–4.2), staurolite (3.65–3.77), rutile (4.18–4.25), chromite (4.3–4.6), xenotime (4.45–4.59), zircon (4.7), ilmenite (4.5–5.0), yellow monazite (5.0–5.3), magnetite (5.18), hematite (5.2–5.3), scheelite (6.0), cassiterite (7.0), cinnabar (8.1), and gold (15.6–19.3). All of these are found with dark monazite in Alaska, but there is no evidence that any are genetically related to this variety of monazite. However, the intrusive granite which was the source of the heat that caused the dark monazite to form may contain some of these minerals.

8. Dark monazite has not been recognized due to its "rolled-shale" appearance. It has been overlooked in most places, and misidentified as "cerite" in the Kivu district of Zaire (Magnée, 1958). This mineral is probably more common than is currently known. The descriptions given here show that simple optical-mineralogical tests will permit its identification, and will reveal many other occurrences in assemblages of detrital minerals elsewhere in the world.

Certain geologic implications are apparent from the foregoing conclusions:

1. The presence of dark monazite in stream concentrates may be used as a guide to contact-metamorphic zones in previously unexplored areas. This implication is based on many dark-monazite contact-zone associations in Alaska; and the successful prediction and discovery of dark monazite in Montana, U.S.A., in southeastern Peru, and southwest of Bangkok, Thailand, downstream from contact zones in fine-grained sedimentary terranes.

2. Dark monazite may be used as a guide to phosphate layers. The Phosphoria Formation in Montana upstream from dark monazite occurrences is being mined for fertilizer raw material.

3. Dark monazite may be used as a geothermometer with an upper limit of 295°C. This is the stability limit of greigite, which was identified in Taiwanese dark monazite. Possibly this limit may have application by oil geologists in their search for oil-bearing rocks.

REFERENCES CITED

Adams, J. W., 1968, Rhabdophane from a rare-earth occurrence, Valley County, Idaho, *in* Geological Survey research 1968: U.S. Geological Survey Professional Paper 600-B, p. B48-B51.

_____1969, Distribution of lanthanides in minerals, *in* Geological Survey research 1969: U.S. Geological Survey Professional Paper 650-C, p. C38-C44.

Ahlfeld, Federico, and Branisa, Leonardo, 1960, Geología de Bolivia: Instituto Boliviano Petroleo, La Paz, 245 p.

Alexiev, E., and Arnaudov, V., 1965, Rare earths, uranium, and thorium in certain Bulgarian phosphorites: Trudovye V'rkhu Geologiyata na B'ulgariya, v. 5, p. 69-78 [in Bulgarian].

Altmann, J., Radelli, L., and Serre-Ratsimandisa, R., 1970, Rare earths of monazites and geology of southern Madagascar: Seminar on Geochemical Prospecting Methods and Techniques, Second, Proceedings, U.N. Economic Commission on Asia and the Far East, Mineral Resources Development Series no. 38, p. 115-126.

Altschuler, Z. S., Berman, Sol, and Cuttitta, Frank, 1967, Rare earths in phosphorite—Geochemistry and potential recovery, *in* Geological Survey research 1967: U.S. Geological Survey Professional Paper 575-B, 9 p.

Baedecker, P. A., 1976, SPECTRA—Computer reduction of gamma-ray spectroscopic data for neutron activation analysis, *in* Taylor, R. E., ed., Advances in Obsidian Glass Studies: Park Ridge, New Jersey, Noyes Press, p. 334-349.

Baedecker, P. A., Rowe, J. J., and Steinnes, E., 1977, Application of epithermal neutron activation in multielement analysis of silicate rocks employing both coaxial Ge(Li) and low energy photon detector systems: Journal Radioanalytical Chemistry, v. 40, p. 115-146.

Bakr, M. A., and Jackson, R. O., 1964, Geological map of Pakistan: Pakistan Geological Survey, scale 1:2,000,000, 1 sheet.

Balashov, Yu. A., 1972, Partition of rare-earth elements during fractional crystallization of magmatic melts: Geochemistry International, v. 9, p. 320-335.

Balashov, Yu. A., Dmitriev, L. V., and Sharas'kin, A. Ya., 1970, Distribution of the rare earths and yttrium in the bedrock of the ocean floor: Geochemistry International, v. 7, p. 456-468.

Balashov, Yu. A., and Girin, Yu. P., 1969, On the reserve of mobile rare-earth elements in sedimentary rocks: Geochemistry International, v. 6, p. 649-659.

Balashov, Yu. A., Kekeliya, M. A., and Nadareyshvili, D. G., 1969, Effect of alkali content on fractionation of the rare earths in rocks of gabbroid intrusives: Geochemistry International, v. 6, p. 476-486.

Balashov, Yu. A., and Pozharitskaya, L. K., 1968, Factors governing the behavior of rare-earth elements in the carbonatite process: Geochemistry International, v. 5, p. 271-288.

Balashov, Yu. A., Ronov, A. B., Migdisov, A. A., and Turanskaya, N. V., 1964, The effect of climate and facies environment of the rare earths during sedimentation: Geochemistry International, v. 1, p. 951-969.

Ballén, J. G., 1969, Mapa geológico de la República del Ecuador: Servicio Nacional de Geología y Minería, scale 1:1,000,000, 2 sheets.

Besaire, Henri, 1969, Carte géologique-Tanarive (sheet 5): Madagascar Service Géologique, scale 1:500,000, 8 sheets.

Bliskovskiy, V. Z., Mineyev, D. A., and Kholodov, V. N., 1969, Accessory lanthanides in phosphorites: Geochemistry International, v. 6, p. 1055-1069.

Bowie, S. H. U., and Horne, J. E. T., 1953, Cheralite, a new mineral of the monazite group: Mineralogical Magazine, v. 30, p. 93-99.

Cain, Doug, 1974, The determination and interpretation of rare earth abundances in hybrid granitoid rocks of the southern Snake Range, Nevada: Colorado School of Mines M.Sc. thesis, 94 p.

Carron, M. K., Naeser, C. R., Rose, H. J., Jr., and Hildebrand, F. A., 1958, Fractional precipitation of rare earths with phosphoric acid: U.S. Geological Survey Bulletin 1036-N, p. N253-275.

Cass, J. T., 1959, Reconnaissance geologic map of the Ruby quadrangle, Alaska: U.S. Geological Survey Miscellaneous Geologic Investigations Map I-289, scale 1:250,000, 1 sheet.

Chapman, R. M., Weber, F. R., and Tabor, Bond, 1971, Preliminary geologic map of the Livengood quadrangle, Alaska: U.S. Geological Survey Open-File Report, scale 1:250,000, 2 sheets.

Chapman, R. M., Yeend, W. E., Brosgé, W. P., and Reiser, H. N., 1975, Preliminary geologic map of the Tanana and northeast part of the Kantishna River quadrangles, Alaska: U.S. Geological Survey Open-File Report 75-337, scale 1:250,000, 1 sheet.

Chen, M. C., Li, K., T., and Wu, K., C., 1973, A study of black monazite in Taiwan heavy sand: [Taiwan] Mining and Metallurgy, v. 17, no. 3, p. 61-72.

Chen, P. Y., 1953, Heavy mineral deposits of western Taiwan: Taiwan Geological Survey Bulletin, no. 4, p. 13-21.

Clark, A. L., and Cobb, E. H., 1970, Metallic mineral resources map of the Talkeetna quadrangle, Alaska: U.S. Geological Survey Open file report, 5 p., map scale 1:250,000, 1 sheet.

_____1972, Metallic mineral resources map of the Talkeetna quadrangle, Alaska: U.S. Geological Survey Miscellaneous Field Studies Map MF-369, scale 1:250,000, 1 sheet.

Cobb, E. H., 1972a, Metallic mineral resources map of the Tanana quadrangle, Alaska: U.S. Geological Survey Miscellaneous Field Studies Map MF-371, scale 1:250,000, 1 sheet.

_____1972b, Metallic mineral resources map of the Livengood quadrangle, Alaska: U.S. Geological Survey Miscellaneous Field Studies Map MF-413, scale 1:250,000, 2 sheets.

_____1972c, Metallic mineral resource map of the Fairbanks quadrangle, Alaska: U.S. Geological Survey Miscellaneous Field Studies Map MF-410, scale 1:250,000, 1 sheet.

_____1972d, Metallic mineral resources map of the Ruby quadrangle, Alaska: U.S. Geological Survey Miscellaneous Field Studies Map MF-405, scale 1:250,000, 1 sheet.

_____1972e, Metallic mineral resources map of the Ophir quadrangle, Alaska: U.S. Geological Survey Miscellaneous Field Studies Map MF-367, scale 1:250,000, 1 sheet.

_____1972f, Metallic mineral resources map of the Mt. Michelson quadrangle, Alaska: U.S. Geological Survey Miscellaneous Field Studies Map MF-462, scale 1:250,000, 1 sheet.

_____1972g, Metallic mineral resources map of the Circle quadrangle, Alaska: U.S. Geological Survey Miscellaneous Field Studies Map MF-391, scale 1:250,000, 1 sheet.

_____1972h, Metallic mineral resources map of the Eagle quadrangle, Alaska: U.S. Geological Survey Miscellaneous Field Studies Map MF-393, scale 1:250,000, 1 sheet.

_____1972i, Metallic mineral resources map of the Bendeleben quadrangle, Alaska: U.S. Geological Survey Miscellaneous Field Studies Map MF-417, scale 1:250,000, 1 sheet.

_____1972j, Metallic mineral resources map of the Nome quadrangle, Alaska: U.S. Geological Survey Miscellaneous Field Studies Map MF-463, scale 1:250,000, 2 sheets.

_____1972k, Metallic mineral resources map of the Solomon quadrangle, Alaska: U.S. Geological Survey Miscellaneous Field Studies Map MF-445, scale: 1:250,000, 1 sheet.

Cobb, E. H., and Sainsbury, C. L., 1972, Metallic mineral resources map of the Teller quadrangle, Alaska: U.S. Geological Survey Miscellaneous Field Studies Map MF-426, scale 1:250,000, 1 sheet.

Coryell, C. D., Chase, J. W., and Winchester, J. W., 1963, A procedure for geochemical interpretation of terrestrial rare-earth abundance patterns: Journal of Geophysical Research, v. 68, no. 2, p. 559–566.

Cullers, R. L., Chaudhuri, Sambhudas, Arnold, Bill, Lee, Moon, and Wolf, C. W., Jr., 1975, Rare earth distributions in clay minerals and in the clay-sized fraction of the Lower Permian Havensville and Eskridge shales of Kansas and Oklahoma: Geochimica et Cosmochimica Acta, v. 39, p. 1691–1703.

Cullers, R. L., Yeh, L.-T., Chaudhuri, Sambhudas, and Guidotti, C. V., 1974, Rare earth elements in Silurian pelitic schists from N.W. Maine: Geochimica et Cosmochimica Acta, v. 38, no. 3, p. 389–400.

Davies, W. E., 1972, The Tintina trench and its reflection in the structure of the Circle area, Yukon-Tanana upland, Alaska: Tectonics—Tectonique, Section 3, International Geological Congress, no. 24, p. 211–216.

Deer, W. A., Howie, R. A., and Zussman, J., 1966, An introduction to the rock-forming minerals: New York, John Wiley, 528 p.

Donnot, M., Guigues, J., Lulzac, Y., Magnien, A., Parfenoff, A., and Picot, P., 1973, Un nouveau type de gisement d'europium:—la monazite grise à europium en nodules dans les schistes paléozoiques de Bretagne: Mineralium Deposita, v. 8, p. 7–18.

Dostal, J., and Capedri, S., 1979, Rare earth elements in high-grade metamorphic rocks from the western Alps: Lithos, v. 12, no. 1, p. 41–49.

Dumler, F. L., Skornyakova, K. P., and Shul'ga, G. G., 1970, Lanthanum rhabdophane in the weathered mantle on limestones; a new type of rare earth mineralization: International Geology Review, v. 12, no. 9, p. 1140–1145.

Eakin, H. M., 1913, A geologic reconnaissance of a part of the Rampart quadrangle, Alaska: U.S. Geological Survey Bulletin 535, 38 p.

el Aissaoui, Mohamed, and Devismes, Pierre, 1977, Monazite grise à europium de la région d'Oulmès (Maroc central): Notes service géologique Maroc, v. 38, no. 268, p. 237–239.

Ellsworth, H. V., 1932, Monazite colored by carbon from Dickens Township, Nipissing district, Ontario: American Mineralogist, v. 17, no. 1, p. 19–28.

Emmons, R. C., and Gates, R. M., 1948, The use of Becke line colors in refractive index determination: American Mineralogist, v. 33, nos. 9–10, p. 612–618.

Evensen, N. M., Hamilton, P. J., and O'Nions, R. K., 1978, Rare-earth abundances in chondritic meteorites: Geochimica et Cosmochimica Acta, v. 42, p. 1199–1212.

Fadeev, V. A., 1959, On elevated concentrations of rare earths in rocks of northern Verkhoyanya: Instituta Geologii Arktiki, Informatsionniy Byulleten' 13, p. 54–57 [in Russian].

Flanagan, F. J., 1976, Descriptions and analyses of eight new U.S. Geological Survey rock standards: U.S. Geological Survey Professional Paper 840, 192 p.

Fleischer, Michael, 1965, Some aspects of the geochemistry of yttrium and the lanthanides: Geochimica et Cosmochimica Acta, v. 29, no. 7, p. 755–772.

Fleischer, Michael, and Altschuler, Z. S., 1969, The relationship of the rare-earth composition of minerals to geological environment: Geochimica et Cosmochimica Acta, v. 33, no. 6, p. 725–732.

Flinter, B. H., Butler, J. R., and Harral, G. M., 1963, A study of alluvial monazite from Malaya: American Mineralogist, v. 48, nos. 11–12, p. 1210–1226.

Fomina, L. S., 1966, Accumulation and redistribution of rare earth elements during formation of iron-manganese concretions in the ocean: Doklady Academy Science U.S.S.R., Earth Science Section, v. 170, p. 221–224.

Foster, H. L., 1970, Reconnaissance geologic map of the Tanacross quadrangle, Alaska: U.S. Geological Survey Miscellaneous Geologic Investigations Map I–593, scale 1:250,000, 1 sheet.

———1976, Geologic map of the Eagle quadrangle, Alaska: U.S. Geological Survey Miscellaneous Geologic Investigations Map I–922, scale 1:250,000, 1 sheet.

Foster, H. L., Weber, F. R., and Forbes, R. B., and Brabb, E. E., 1973, Regional Geology of Yukon-Tanana Upland, Alaska, *in* Arctic Geology: American Association of Petroleum Geologists Memoir 19, p. 388–395.

Gary, Margaret, McAfee, Robert, Jr., and Wolf, C. L., eds., 1972, Glossary of geology: American Geological Institute, 858 p., appendix A1–A52.

Girin, Yu. P., Balashov, Yu. A., and Bratishko, R. K. H., 1970, Redistribution of rare earths during diagenesis of humid sediments: Geochemistry International, v. 7, p. 438–452.

Goguel, Jean, 1968, Carte géologique de la France: Service de la Carte Géologique de la France, scale 1:1,000,000, 2 sheets.

Goldberg, E. D., Koide, Minoru, Schmitt, R. A., and Smith, R. H., 1963, Rare-earth distributions in the marine environment: Journal of Geophysical Research, v. 68, no. 14, p. 4209–4217.

Gordon, S. G., 1939, Thorium-free monazite from Llallagua, Bolivia: Notulae Naturae, Academy of Natural Sciences of Philadelphia, no. 2, 7 p.

———1944, The mineralogy of the tin mines of Cerro de Llallagua, Bolivia: Proceedings of the Academy of Natural Sciences of Philadelphia, v. 96, p. 279–359.

Green, Jack, 1959, Geochemical table of the elements for 1959: Geological Society of America Bulletin, v. 70, no. 9, p. 1127–1183.

Guigues, Jean, and Devismes, Pierre, 1969, La prospection minière à la batée dans le massif Armoricain: Bureau Recherches Géologiques Minières, Memoir 71, 171 p.

Gulbrandsen, R. A., 1966, Chemical composition of phosphorites of the Phosphoria Formation: Geochimica et Coschimica Acta, v. 30, no. 8, p. 769–778.

———1975, Analytical data on the Phosphoria Formation, western United States: U.S. Geological Survey Open-file Report 75–554, 45 p.

Harker, Alfred, 1939, Metamorphism—a study of the transformations of rock masses: New York, E. P. Dutton, 362 p.

Haskin, L. A., Frey, F. A., Schmitt, R. A., and Smith, R. H., 1966, Meteoritic, solar, and terrestrial rare-earth distributions, *in* Ahrens, L. H., and others, eds., Physics and chemistry of the Earth: London and New York, Pergamon Press, v. 7, p. 167–321.

Haskin, L. A., and Gehl, M. A., 1962, The rare-earth distribution in sediments: Journal of Geophysical Research, v. 67, no. 6, p. 2537–2541.

Haskin, L. A., Haskin, M. A., Frey, F. A., and Wildeman, T. R., 1968, Relative and absolute terrestrial abundances of the rare earths, *in* Ahrens, L. H., ed., Origin and distribution of the elements: Oxford, Pergamon Press, p. 889–912.

Haskin, L. A., and Korotev, R. L., 1973, Determination of rare earths in geological samples and raw materials, *in* Analysis and application of rare earth materials: NATO Advanced Study Institute, Kjeller, Norway, p.183–211.

Haskin, L. A., Wildeman, T. R., Frey, F. A., Collins, K. A., Keedy, C. R., and Haskin, M. A., 1966, Rare earths in sediments: Journal of Geophysical Research, v. 71, no. 24, p. 6091–6105.

Hawley, C. C., and Clark, A. L., 1973, Geology and mineral deposits of the Chulitna-Yentna mineral belt, Alaska: U.S. Geological Survey Professional Paper 758–A, 10 p.

Heinrich, E. W., Borup, R. A., and Levinson, A. A., 1960, Relationships between geology and composition of some pegmatitic monazites: Geochimica et Cosmochimica Acta, v. 19, no. 3, p. 222–231.

Herrmann, A. G., 1970, Yttrium, and the Lanthanides, chapters 39, 57–71 *in* Wedepohl, K. H., and others, eds., Handbook of Geochemistry: Berlin, Springer-Verlag.

Ho, C. S., 1975, An introduction to the geology of Taiwan—Explanatory text of the geologic map of Taiwan: Taipei, Ministry of Economic Affairs, 153 p. [English text].

Ho, C. S., and Lee, C. N., 1963, Economic minerals of Taiwan: Geological Survey of Taiwan, 495 p.

Holt, D. N., 1965, The Kangankunde Hill rare-earth prospect: Malawi Geological Survey Department, Bulletin 20, 130 p.

Huang, S. C., 1958, The heavy sand deposits in the coastal region between Tainan and Pintung: (Taiwan) Mineral Survey Team Annual Report, 1957–58, Ministry of Economic Affairs, Republic of China, Taipei, Taiwan, p. 63–78 [in Chinese, summary in English].

Huebschman, R. P., 1973, Correlation of fine carbonaceous bands across a Precambrian stagnant basin: Journal of Sedimentary Petrology, v. 43, no. 3, p. 688–699.

Iimori, Takeo, 1941, The black monazite occurring in northeast Korea: Tokyo Institute Physics and Chemistry Research Bulletin, v. 20, no. 12, p. 1052–1054 [in Japanese].

Ilupin, I. P., Varshal, G. M., Pavlutskaya, V. I., and Kalenchuk, G. E., 1974, Rare earth elements in Yakutian kimberlites: Geochemistry International, v. 11, no. 1, p. 106–110.

Instituto de Geología y Minería, 1975, Mapa geológico del Peru: Ministerio de Energía y Minas, Lima, scale 1:1,000,000, 4 sheets.

Izrailev, L. M., and Solov'eva, N. A., 1975, Accessory authigenic monazite in the upper Paleozoic deposits of northern Verkhoyan'e, *in* Aerogeological Expedition no. 3, All-Union Aerogeological Trust, Moscow, Lithology and Mineral Resources: v. 9, no. 5, p. 624–628.

Jaffe, H. W., 1955, Precambrian monazite and zircon from the Mountain Pass rare-earth district, San Bernardino County, California: Geological Society of America Bulletin, v. 66, no. 10, p. 1247–1256.

Jolly, J. H., 1976, Rare-earth elements and yttrium: U.S. Bureau of Mines Bulletin 667, p. 889–904.

Khomyakov, A. P., 1963, Relation between content and composition of rare earths in minerals: Geochemistry 1963, v. 2, p. 125–132.

Komov, I. L., Melnikova, E. M., and Kokarev, G. N., 1974, Some typomorphic features of accessory monazite from hydrothermal quartz veins and altered rocks of the Pamirs and Urals: Trudy Mineralogicheskogo Muzeya A. E. Fersmana, Akademiya Nauk S.S.S.R., v. 23, p. 87–93 [in Russian].

Kosterin, A. V., 1959, The possible modes of transport of the rare earths by hydrothermal solutions: Geochemistry 1959, no. 4, p. 381–387.

Kosterin, A. V., Alekhina, K. N., and Kizura, V. E., 1962, Monazite of an unusual origin: Academy Science U.S.S.R., Reports of the Far Eastern Branch of the Siberian Section, no. 15, p. 23–26 [in Russian].

Krishnan, M. S., 1956, Geology of India and Burma: Madras, Higginbothams (Private) Ltd., 555 p.

Lacomme, André, and Fontan, Francois, 1971, Sur la présence de la monazite dans les Pyrénées: Compte Rendue Académie Paris, Série D, tome 272, p. 1193–1194.

Laurin, A. F., 1969, Geological map of Quebec: Canada Department of Natural Resources, scale 1:1,013,760, 2 sheets.

Lee, D. E., and Bastron, Harry, 1967, Fractionation of rare-earth elements in allanite and monazite as related to geology of the Mt. Wheeler mine area, Nevada: Geochimica et Cosmochimica Acta, v. 31, p. 339–356.

Lepersonne, J., 1974, Carte géologique du Zaire: Zaire Service Géologique, scale 1:2,000,000, 2 sheets.

Li, A. F., and Grebennikova, O. T., 1962, Low-thorium monazite: Academy Science U.S.S.R., Zapisky Vostochno-Sibirskogo, Otdeleniya Mineralogicheskogo Obshchestva, v. 4, p. 155–161 [in Russian].

Magnée, I. de, 1958, L'avenir du thorium congolais: Académie Royale des Sciences Coloniales Bulletin, new series 4, no. 2, p. 457–474 [in French].

Marchenko, E. Ya., 1967, Certain characteristics of accessory monazite from Precambrian crystalline rocks in southeastern Ukrainian S.S.R.: Doklady Academy Science U.S.S.R., Earth Science Section, v. 176, p. 142–145.

Marcos, Alberto, Pérez-Estaún, Andrés, Pulgar, J. A., Bastida, Fernando, and Vargas, Ignacio, 1980, Mapa geológico de España E. 1:50,000 (Becerreá): Instituto Geológico y Minero de España, 2nd ser., 1st ed., 32 p., 1 map sheet.

Marsh, W. R., Sainsbury, C. L., Hamilton, J. C., and Ewing, Rodney, 1972, Tin in panned concentrates, Serpentine River, Seward Peninsula, Alaska: U.S. Geological Survey Open-File Report 536, 7 p.

Mason, Brian, 1972, Minor and trace element distribution in minerals of the Muzzle River Gabbro: New Zealand Journal of Geology and Geophysics, v. 15, no. 3, p. 465–475.

Masuda, Akimasa, 1962, Regularities in variation of relative abundances of lanthanide elements and an attempt to analyze separation-index patterns of some minerals: Nagoya University, Journal Earth Sciences, v. 10, p. 173–187.

_____1975, Abundances of monoisotopic REE, consistent with the Leedey chondrite values: Geochemical Journal (Japan), v. 9, p. 183–184.

Masuda, Akimasa, Nakamura, N., and Tanaka, T., 1973, Fine structures of mutually normalized rare-earth patterns of chondrites: Geochimica et Cosmochimica Acta, v. 37, no. 2, p. 239–248.

Matzko, J. J., and Overstreet, W. C., 1977, Black monazite from Taiwan: Geological Society Taiwan Proceedings no. 20, p. 16–35.

Maughan, E. K., 1975, Organic carbon in shale beds of the Permian Phosphoria Formation of eastern Idaho and adjacent states—a summary report: Wyoming Geological Association Guidebook, Annual Field Conference, 27th, p. 107–115.

_____1976, Organic carbon and selected element distribution in phosphatic shale members of the Permian Phosphoria Formation, eastern Idaho and parts of adjacent states: U.S. Geological Survey Open-File Report 76–577, 92 p.

Mertie, J. B., Jr., 1934, Mineral deposits of the Rampart and Hot Springs districts, Alaska: U.S. Geological Survey Bulletin 844–D, p. 163–226.

_____1936, Mineral deposits of the Ruby-Kuskokwim region, Alaska: U.S. Geological Survey Bulletin 864–C, p. 115–245.

_____1937, The Yukon-Tanana region, Alaska: U.S. Geological Survey Bulletin 872, 276 p.

_____1953, Monazite deposits of the southeastern Atlantic states: U.S. Geological Survey Circular 237, 31 p.

Mertie, J. B., Jr., and Harrington, G. L., 1924, The Ruby-Kuskokwim region, Alaska: U.S. Geological Survey Bulletin 754, 129 p.

Ministry of Economic Affairs, 1974, Geologic map of Taiwan: Taipei, Ministry of Economic Affairs, scale 1:500,000, 1 sheet.

Mitchell, R. S., 1965, Rhabdophane from the Champion pegmatite, Amelia County, Virginia: American Mineralogist, v. 50, nos. 1–2, p. 231–235.

Molloy, M. W., 1959, A comparative study of ten monazites: American Mineralogist, v. 44, p. 510-532.

Muecke, G. K., and Sarkar, Prasanta, 1977, Rare earth mobility during amphibolite-facies metamorphism of White Rock Formation metavolcanics, Nova Scotia: Geological Society of America Abstracts with Programs, v. 9, no. 3, p. 303.

Murata, K. J., Rose, H. J., Jr., and Carron, M. K., 1953, Systematic variation of rare earths in monazite: Geochimica et Cosmochimica Acta, v. 4, p. 292- 300.

Murata, K.J., Rose, H. J. Jr., Carron, M. K., and Glass, J. J., 1957, Systematic variation of rare-earth elements in cerium-earth minerals: Geochimica et Cosmochimica Acta, v. 11, no. 3, p. 141-161.

Nagasawa, Hiroshi, and Schnetzler, C. C., 1971, Partitioning of rare earth, alkali and alkaline earth elements between phenocrysts and acidic igneous magma: Geochimica et Cosmochimica Acta, v. 35, no. 9, p. 953-968.

Nakamura, Noboru, 1974, Determination of REE, Ba, Fe, Mg, Na, and K in carbonaceous and ordinary chondrites: Geochimica et Cosmochimica Acta, v. 38. p. 757-775.

Nalivkin, D. V., 1965, Geologic map of the U.S.S.R.: Ministry of Geology, U.S.S.R., scale 1:2,500,000, 17 sheets [in Russian].

Nance, W. B., and Taylor, S. R., 1976, Rare earth element patterns and crustal evolution—I. Australian post-Archean sedimentary rocks: Geochemica et Cosmochimica Acta. v. 40, p. 1539-1551.

_____1977, Rare earth element patterns and crustal evolution—II. Archean sedimentary rocks from Kalgoorlie, Australia: Geochimica et Cosmochimica Acta, v. 41, p. 225-231.

Nekrasov, I. Ya., 1972, New data on a mineral of the monazite-cheralite-huttonite group: Doklady Academy Science U.S.S.R., Earth Science Section, v. 204, p. 134-136.

O'Nions, R. K., and Pankhurst, R. J., 1978, Early Archean rocks and geochemical evolution of the Earth's crust: Earth and Planetary Science Letters, v. 38, p. 211-236.

Overstreet, W. C., 1967, The geologic occurrence of monazite, U.S. Geological Professional Paper 530, 327 p.

_____1971, Monazite in Taiwan: U.S. Geological Survey Open-File Report, 80 p.

Overstreet, W. C., Warr, J. J., Jr., and White, A. M., 1970, Influence of grain size on percentages of ThO_2 and U_3O_8 in detrital monazite from North Carolina and South Carolina: U.S. Geological Survey Professional Paper 700-D, p. D207-D216.

_____1969, Thorium and uranium in detrital monazite from the Georgia Piedmont: Southeastern Geology, v. 10, no. 2, p. 63-76.

Overstreet, W. C., Hamilton, J. C., Boerngen, J. G., Rosenblum, Sam, Marsh, W. R., and Sainsbury, C. L., 1975, Minor elements in nonmagnetic concentrates from Alaska: U.S. Geological Survey Report GD-74-320, 440 p.; available from U.S. Department of Commerce National Technical Information Service, Springfield, Virginia 22161, as Rept. PB-238989.

Palache, Charles, Berman, Harry, and Frondel, Clifford, 1951, The system of mineralogy (7th ed.): New York, John Wiley, v. 2, 1124 p.

Parfenoff, A., 1963, Découverte de monazite grise en nodules dans les concentrés alluvionnaires de Bretagne: Bureau Recherches Géologiques et Minières, Étude 6086/MPMG inédit.

Paster, T. P., Schauwecker, D. S., and Haskin, L. A., 1974, The behavior of some trace elements during solidification of the Skaergaard layered series: Geochimica et Cosmochimica Acta, v. 38, no. 10, p. 1549-1577.

Péwé, T. L., Wahrhaftig, Clyde, and Weber, F. R., 1966, Geologic map of the Fairbanks quadrangle, Alaska: U.S. Geological Survey Miscellaneous Geologic Investigations Map I-455, scale 1:250,000.

Phan, K. D., 1967, Note sur l'europium et l'yttrium: Bureau Recherches Géologiques et Minières Bulletin 2, p. 82-87.

Philpotts, J. A., and Schnetzler, C. C., 1971, Rare earths, *in* Mason, Brian, ed., Handbook of elemental abundances in meteorites: New York, Gordon and Breach Science Publishers, p. 419-424.

Piper, D. Z., and Graef, P. A., 1974, Gold and rare-earth elements in sediments from the East Pacific Rise: Marine Geology, v. 17, no. 5, p. 287-297.

Ploshko, V. V., 1961, Pneumatolytic monazite of Malaya Laba River (North Caucasus): Izvestiya Akademiya Nauk S.S.S.R., Seriya Geologicheskiy, no. 1, p. 70-75.

Rankama, Kalervo, and Sahama, T. G., 1950, Geochemistry: University of Chicago Press, 912 p.

Rass, I. T., 1972, Behavior of the rare-earth elements and yttrium during magmatic metasomatism of ultramafic rocks: Geochemistry International, v. 9, no. 1, p. 68-78.

Reiser, H. N., Brosgé, W. P., Dutro, J. T., Jr., and Detterman, R. L., 1971, Preliminary geologic map, Mt. Michelson quadrangle, Alaska: U.S. Geological Survey Open-File Map, scale 1:200,000, 2 sheets.

_____1974, Preliminary geologic map of the Demarcation Point quadrangle, Alaska: U.S. Geological Survey Miscellaneous Field Studies Map MF-610, scale 1:200,000, 1 sheet.

Richartz, W., 1961, Über kristallchemische Untersuchungen und magnetische Aufbereitung von Monazit: Fortschrift der Mineralogie, v. 39, no. 1, p. 53-59.

Roaldset, Elen, 1975, Rare earth element distributions in some Precambrian rocks and their phyllosilicates, Numedal, Norway: Geochimica et Cosmochimica Acta, v. 39, no. 4, p. 455-469.

Ronov, A. B., Balashov, Yu. A., and Migdisov, A. A., 1967, Geochemistry of the rare earths in the sedimentary cycle: Geochemistry International, v. 4, p. 1-17.

Ronov, A. B., Balashov, Yu. A., Girin, Yu. P., Bratishko, R. Kh., and Kasakov, G. A., 1972, Trends in rare-earth distribution in the sedimentary shell and in the earth's crust: Geochemistry International, v. 9, p. 987-1016.

Ronov, A. B., Migdisov, A. A., and Lobach-Zhuchenko, S. B., 1977, Regional metamorphism and sediment composition evolution: Geochemistry International, v. 14, p. 90-112.

Rose, H. J., Jr., Blade, L. V., and Ross, Malcom, 1958, Earthy monazite at Magnet Cove, Arkansas: American Mineralogist, v. 43, nos. 9-10, p. 995-997.

Rosenblum, Sam, 1960, Mineral exploration in Taiwan, 1959: The Taiwan Mining Industry, no. 1 & 2, v. 12, p. 1-6.

_____1974a, A mineral separation procedure using hot Clerici solution: U.S. Geological Survey Journal of Research, v. 2, no. 4, p. 479-481.

_____1974b, Analyses and economic potential of monazite in Liberia: U.S. Geological Survey Journal of Research, v. 2, no. 6, p. 689-692.

Rosenblum, Sam, and Mosier, E. L., 1975, Nonmetamict nioboeschynite-(Ce) from Alaska: American Mineralogist, v. 60, nos. 3-4, p. 309-315.

Sainsbury, C. L., 1972, Geologic map of the Teller quadrangle, western Seward Peninsula, Alaska: U.S. Geological Survey Miscellaneous Geologic Investigations Map I-685, scale 1:250,000, 1 sheet.

_____1974, Geologic map of the Bendeleben quadrangle, Seward Peninsula, Alaska: Anchorage, Alaska, The Mapmakers, 31 p.

Sainsbury, C. L., Hudson, Travis, Ewing, Rodney, and Marsh, W. R., 1972, Reconnaissance geologic map of the west half of the Solomon quadrangle, Alaska: U.S. Geological Survey Open-File Report 1796, 10 p., scale 1:250,000, 1 sheet.

Sainsbury, C. L., Hummel, C. L., and Hudson, Travis, 1972, Reconnaissance geologic map of the Nome quadrangle, Seward Peninsula, Alaska: U.S. Geological Survey Open-File Report 1792, 28 p., scale 1:250,000, 1 sheet.

Schmidt, R. G., and Asad, S. A., 1962, Beach placers containing radioactive minerals, Bay of Bengal, East Pakistan: U.S. Geological Survey Professional Paper 450-C, p. 12-14.

_____1963, A reconnaissance survey of radioactive beach sand at Cox's Bazar: Pakistan Geological Survey Interim Report, no. 3, 14 p.

Schmitt, R. A., Smith, R. H., and Olehy, D. A., 1964, Rare-earth, yttrium, and scandium abundances in meteoritic and terrestrial matter-II: Geochimica et Cosmochimica Acta, v. 28, no. 1, p. 67-86.

Schnetzler, C. C., and Philpotts, J. A., 1970, Partition coefficients of rare-earth elements between igneous matrix material and rock-forming mineral phenocrysts-II: Geochimica et Cosmochimica Acta, v. 34, p. 331-340.

Semenov, E. I., and Barinskiy, R. L., 1958, The composition characteristics of the rare earths in minerals: Geochemistry, no. 4, p. 398-419.

Semenov, E. I., Kholodov, V.N., and Barinskiy, R. L., 1962, Rare earths in phosphorites: Geochemistry, no. 5, p. 501-507.

Serdyuchenko, D. P., and Kochetkov, O. S., 1974, Metasedimentary monazite in Riphean schists of the Timans: Doklady Academy Science U.S.S.R., Earth Science Section, v. 218, p. 124-125.

Serdyuchenko, D. P., Pap, A. N., Borkovskaya, V. N., and Bykova, A. V., 1967, A thorium-free monazite from Precambrian gneisses of Belorussia and its genesis: Doklady Academy Science U.S.S.R., Earth Science Section, v. 175, p. 140-142.

Serre-Ratsimandisa, R., 1970, Geochemistry of monazite from Madagascar: Seminar on Geochemical Prospecting Methods and Techniques, Second, Proceedings, U.N. Economic Commission on Asia and the Far East, Mineral Resources Development Series, no. 38, p. 154-161.

Shen, J. T., Li, H. Y., and Chao, T. H., 1958, A practical process for the separation of monazite and associated minerals from low-grade ores, *in* Processing of raw materials: Geneva, United Nations, International Conference Peaceful Uses Atomic Energy, September 1-13, 1958, Proceedings, v. 3, p. 167-169.

Sin'kova, L. A., and Turanskaya, N. V., 1968, Differences between the effects of potassium and sodium on the migration tendencies of rare-earth elements: Geochemistry International, v. 5, p. 481-488.

Soong, K.-L., 1970, Preliminary study on the altered monazite from the beach sand of western Taiwan: Chinese Institute Mining Metallurgical Engineers, Mining Technical Digest, v. 8, no. 2, p. 2-10 [in Chinese].

_____1978, On the genesis of the black monazite from Taiwan: Acta Oceanographica Taiwanica, no. 8, p. 43-62.

Sozinov, N. A., Deryagin, A. A., and Sidorenko, S. A., 1977, Rare earths in carbonaceous rocks: Doklady Academy Science U.S.S.R., Earth Sciences Section, v. 235, p. 192-194.

Steyermark, Al, 1961, Quantitative organic microanalysis: New York, Academic Press, 665 p.

Taylor, S. R., 1965, The application of trace element data to problems in petrology, *in* Physics and chemistry of the earth: Oxford, Pergamon Press, v. 6, p. 133-213.

_____1972, Rare-earths (lanthanide series), *in* The encyclopedia of geochemistry and environmental sciences: Encyclopedia Earth Sciences Series, v. IVA, p. 1020-1029.

Tikhomirova, N. I., 1971, Behavior of rare and trace elements in granitization in the Syrostan-Turgoyak massif, south Ural: Geochemistry International, v. 8, p. 81-89.

Tripp, R. B., Curtin, G. C., Day, G. W., Karlson, R. C., and Marsh, S. P., 1976, Maps showing mineralogical and geochemical data for heavy-mineral concentrates in the Tanacross quadrangle, Alaska: U.S. Geological Survey Miscellaneous Field Studies Map MF-767-O, 2 sheets, scale 1:500,000.

Tröger, W. E., 1952, Tabellen zur optischen Bestimmung der gesteinsbildenden Minerale: Stuttgart, E. Schweizerbartsche Verlagsbuchhandlung, 147 p.

Vaquero, C., 1979, Descubrimiento, por primera vez en España, de una monacita de facies aberrantes portado de Europia: [Spain] Boletín Geológico y Minero, v. xc-iv, p. 374-379.

Vinogradov, V. A., Arskiy, Yu. M., and Mikhailova, A. F., 1960, Geochemistry of rare earths in northern Verkhoyanya: Instituta Geologii Arktiki, Informatsionniy Byulleten 22, p. 21-29 [in Russian].

Vlasov, K. A., ed., 1966, Geochemistry and mineralogy of rare elements and genetic types of their deposits: Jerusalem, Israel Program for Scientific Translations, v. 1, 688 p., v. 2, 945 p., v. 3, 916 p.

Volkov, I. I., and Fomina, L. S., 1973, New data on the geochemistry of the rare earths in the Pacific Ocean sediments: Geochemistry International, v. 10, p. 1178-1187.

Waters, A. E., Jr., 1934, Placer concentrates of the Rampart and Hot Springs districts: U.S. Geological Survey Bulletin 844, p. 227-246.

Wayland, R. G., 1961, Tofty tin belt, Manley Hot Springs district, Alaska: U.S. Geological Survey Bulletin 1058-I, p. 363-414.

Whittaker, E. J. W., and Muntus, R., 1970, Ionic radii for use in geochemistry: Geochimica et Cosmochimica Acta, v. 34, no. 6, p. 945-956.

Wilcox, R. E., 1959, Use of the spindle stage for determination of principal indices of refraction of crystal fragments: American Mineralogist, v. 44, nos. 11-12, p. 1272-1293.

Wildeman, T. R., and Condie, K. C., 1973, Rare earths in Archean graywackes from Wyoming and from the Fig Tree Group, South Africa: Geochimica et Cosmochimica Acta, v. 37, no. 3, p. 439-453.

Wildeman, T. R., and Haskin, L. A., 1965, Rare-earth elements in ocean sediments: Journal of Geophysical Research, v. 70, no. 12, p. 2905-2910.

_____1973, Rare earths in Precambrian sediments: Geochimica et Cosmochimica Acta, v. 37, no. 3, p. 419-438.

Winchell, A. N., and Winchell, Horace, 1951, Description of minerals, Part 2 *of* Elements of optical mineralogy—an introduction to microscopic petrography: New York, John Wiley, 551 p.

Yes'kova, Ye. M., and Yefimov, A. F., 1972, Geochemistry of the rare earths, Sr, and Ba in Ural alkali apoeffusive metasomatites: Geochemistry International, v. 9, p. 845-854.

Zemel', V. K., 1936, Analyses of monazites from gold placers of Aldan and So. Yenisei: Zhurnal Prikladnoi Khimii, v. 9, no. 11, p. 1969-1971 [in Russian].

☆ U.S. GOVERNMENT PRINTING OFFICE: 1983—676-041/28 REGION No. 8